PAULO RENATO DA COSTA MENDES

PREDICTIVE CONTROL FOR ENERGY MANAGEMENT OF RENEWABLE ENERGY BASED MICROGRIDS

FLORIANÓPOLIS
2016

UNIVERSIDADE FEDERAL DE SANTA CATARINA
PROGRAMA DE PÓS-GRADUAÇÃO EM ENGENHARIA DE AUTOMAÇÃO E SISTEMAS

PREDICTIVE CONTROL FOR ENERGY MANAGEMENT OF RENEWABLE ENERGY BASED MICROGRIDS

Tese de doutorado submetida ao Programa de Pós-Graduação em Engenharia de Automação e Sistemas para a obtenção do Grau de Doutor em Engenharia de Automação e Sistemas.

PAULO RENATO DA COSTA MENDES

Florianópolis, Agosto de 2016.

PREDICTIVE CONTROL FOR ENERGY MANAGEMENT OF RENEWABLE ENERGY BASED MICROGRIDS

Paulo Renato da Costa Mendes

'Esta tese de doutorado foi julgada aprovada para a obtenção do título de **Doutor em Engenharia de Automação e Sistemas**, Área de Concentração em *Controle, Automação e Sistemas*, e aprovada em sua forma final pelo **Programa de Pós-Graduação em Engenharia de Automação e Sistemas da Universidade Federal de Santa Catarina**.'

Julio Elias Normey-Rico, Dr.
Orientador

Carlos Bordons Alba, Dr.
Coorientador

Daniel Ferreira Coutinho , Dr.
Coordenador do Programa de Pós-Graduação em Engenharia de Automação e Sistemas

Banca Examinadora:

Julio Elias Normey-Rico, Dr.
Presidente

Ricardo Hiroshi Caldeira Takahashi , Dr.

Aguinaldo Silveira e Silva, Dr.

Jorge Otávio Trierweiler, Dr.

Eduardo Camponogara, Dr.

Rodolfo Cesar Costa Flesch, Dr.

iii

ACKNOWLEDGMENTS

I would like to thanks

My family that always encouraged me and support me at all times.

Resumo da tese de doutorado submetida à Universidade Federal de Santa Catarina como parte dos requisitos para a obtenção do grau de Doutor em Engenharia de Automação e Sistemas.

Controle Preditivo para Gerenciamento de Energia de Micro-redes Baseadas em Energia Renovável

Paulo Renato da Costa Mendes

Agosto/2016

O objetivo deste trabalho é abordar a gestão de energia dos sistemas de geração e armazenamento de energia. Estes sistemas são atualmente uma realidade em países onde é desejada uma diversificação das fontes de energia e uma maior penetração das fontes renováveis. Em particular, o Brasil possui uma matriz energética diversificada com base em recursos hídricos, biomassa (etanol), gás natural e petróleo. Mas, expectativa para o futuro próximo é um aumento da utilização de fontes de energia renováveis, principalmente solar e eólica. Dessa forma, este trabalho ataca um problema econômico atual e importante para o País. Uma rede de energia em grande escala pode ser subdividida em subsistemas chamados micro-redes, que podem ser vistos como um conjunto de geradores despacháveis e/ou não-despacháveis que utilizam energias fósseis e/ou renováveis, armazenadores de energia e consumidores. Uma micro-rede pode operar em modo ilha, conectada com a rede principal e interligada com outras micro-redes. Sabe-se que a operação ideal de cada unidade não garante o perfeito funcionamento global da micro-rede, o que leva a um comportamento inaceitável. Assim, torna-se necessária a coordenação entre todos os elementos da micro-rede. A mesma filosofia deve ser aplicada no problema de micro-redes interligadas. Do ponto de vista da modelagem, os modelos de sistemas de gestão de energia no nível superior têm características híbridas, devido à necessidade de introduzir variáveis binárias, por exemplo, para modelar a dinâmica de armazenamento ou preços diferentes para operações econômicas como compra/venda de energia.

Assim, uma abordagem natural para controlar esses sistemas é a utilização de controle preditivo, o qual já é amplamente utilizado na indústria de processos e pode lidar com problemas híbridos de optimização. Em uma micro-rede operando em modo conectada à rede principal o desafio de controle é maximizar o uso de fontes renováveis, minimizar o uso de combustíveis fósseis e a quantidade de energia comprada da rede de distribuição, amortecer flutuações de energia e atender a demanda. No caso de micro-redes interligadas é desejada uma estratégia de controle que permita a interação entre micro-redes para compartilhar fontes de energia e reduzir o fluxo de energia com a rede de distribuição. Assim, para uma única micro-rede o controle centralizado parece uma boa opção, enquanto para micro-redes interligadas, quando o intercâmbio de informação é limitado, o controle distribuído aparece como uma solução interessante. Nesta tese é considerado o problema de controle de micro-redes em diferentes cenários, dentre eles uma microrrede de laboratório com armazenador de hidrogênio, o estudo de microrredes interligadas e uma planta de geração da indústria da cana de açúcar. O objetivo principal é propor soluções baseadas em controle preditivo para atender os requisitos de operação do sistema.

Abstract of the thesis presented to the Federal University of Santa Catarina as a partial fulfillment of the requirements for the degree of Doctor in Automation and Systems Engineering.

PREDICTIVE CONTROL FOR ENERGY MANAGEMENT OF RENEWABLE ENERGY BASED MICROGRIDS

Paulo Renato da Costa Mendes

Agosto/2016

The objective of this thesis is to address the energy management of power generation and energy storage systems. These systems are nowadays a reality in countries where a diversification of energy sources and a higher penetration of renewable sources is desired. In particular, Brazil has a diversified energy matrix based on water resources, biomass (ethanol), natural gas and oil. But the expectation for the near future is an increase in the use of renewable sources, mainly solar and wind. Thus, this work attacks a current and important economic problem for the country. A large scale energy network can be subdivided into subsystems called Microgrids, that can be seen as set of dispatchable and/or non-dispatchable generators that uses fossil and/or renewable energy, storage units and consumers. A microgrid can operate in island mode, grid-connected mode and interconnected with other microgrids as the so called networked microgrids. It is known that an ideal operation of each unit does not guarantee the perfect operation of the overall microgrid, which leads to an unacceptable behavior. Thus it becomes necessary coordination between all microgrid elements. The same philosophy should be applied in the networked microgrids problem. From modeling point of view, the top level energy management system models have hybrid characteristics due to the need to introduce binary variables, for example, to model storage dynamics or different prices for economic operations like sell/purchase of energy. Thus, a natural approach to control these systems is the use of predictive control, which is already widely used in the process

industry and can deal with hybrid optimization problems. In a microgrid operating in grid connected mode the control challenges are to maximize the use of renewable sources, minimize the use of fossil sources an the amount of energy bought from distribution network operator (DNO), mitigate energy fluctuating and meet the demand. In an interconnected case a control strategy that allows the interaction between microgrids to share energy sources and reduce the energy flow with DNO is desired. Thus for a single microgrid the centralized control seems to be a good option and for networked microgrids, when information sharing is limited, the distributed control appears as an interesting solution. In this thesis the problem of control of microgrids in different scenarios is considered, among them a laboratory microgrid with hydrogen storage, the study of four interconnected microgrids and a sugar cane industry power plant. The main objective is to propose solutions based on model predictive control to attend the system operation requirements.

Contents

Nomenclature

Acronyms

BS	Binary Search
BSDC	Binary Search with Distributed Coordination
CSMU	Charging Station Management Unit
CMIQP	Centralized MIQP
DMPC	Distributed Model Predictive Control
DNO	Distribution Network Operator
EMS	Energy Management System
MHL	Metal Hydrid Level
MISO	Multiple inputs and single input
MIMO	Multiple inputs and multiple outputs
MIQP	Mixed Integer Quadratic Programming
MLD	Mixed Logical Dynamic
MPC	Model Predictive Control
OLE	Object Linking and Embedding
OPC	OLE for Process Control
PLC	Programmable Logic Controller
QP	Quadratic Programming
SISO	Single input and single output
SIMO	Single input and multiple outputs
SOC	State of charge
SQP	Sequential Quadratic Programming
TIO-MPC	Time Instant Optimization - MPC
V2G	Vehicle-to-grid

List of Symbols

Indexes

r	Hub inputs
p	Hub outputs
q	Inputs of the input storage units
m	Inputs of the output storage units
s	Storage interface
L	Converters
E	Storage units
rad	Radiation
g	Gas
e	Electricity
h	Heat
E	Model storage flow
L	Model input flow
$+$	Storage charging
$-$	Storage discharging
c	Continuous variable
l	Discrete variable
$H2$	Hydrogen
DNO	Distribution Network Operator
B	Battery
S	Solar
W	Wind
ev	Electric vehicle
ez	Electrolyzer
fc	Fuel cell
$Renewable$	Renewable energy source
$PVCh$	Charging Station photovoltaic energy source
in	Input

out	Output
i, j	Hub index
$\rightarrow, \leftarrow$	Flow direction
dem	Demand
aug	Augmented Lagrangian
fix	Fixed values for binary variables
b	binary
TU	Turbine
C	Boiler
CHP	Combined heat and power plant
Ch	Chiller
TC	Heat exchanger
Esc	Escape
Net	Network
Proc	Process
Sale	Sale
V	Steam
M	Middle
L	Low
Variables	
A,B,C,D	State-space system matrices
γ	Steady state conversion efficiency of the converter
n_r	Number of hub inputs
n_p	Number of hub outputs
e	Storage charge/discharge efficiency
u	Model input
x	State vector
y	Model output
δ	Binary variable
z	Continuous auxiliary variable
Λ	Storage coupling matrix
Γ	Converter coupling matrix
ϵ	Electric vehicle binary variable
P	Power
w	Interconnecting variables
Π	Interconnecting matrix
λ	Lagrange multipliers
J	Objective function
C	Objective function cost
CI	Controller instance

SCI	Set of controller instances
BCI	Best cost instance
Q	Weighting matrix
f	Weighting vector
e	Error
γ_c, γ_b	DMPC weights
N	Horizon
MG	Microgrid
SP	Set-point
$Wind$	Wind speed
$Irrad_{in}$	Solar irradiation
Bag	Bagasse
Str	Straw
Bg	Biogas
α	blending factors

List of Figures

List of Tables

Chapter 1

Introduction

Efficient energy generation and consumption is a key factor to achieve ambitious goals for sustainable development and activities related to air pollution and climate change. Efficient and safe power distribution along with minimized and balanced electricity power consumption is nowadays an important part of the economic activity of most countries. One of the largest issues is that generation power systems have to supply energy at greatly varying demands. Abrupt changes in the large-scale energy demand status can cause severe problems to production facilities, and since these changes cannot be accurately predicted they may lead to outages.

Energy generation fundamentals of today are about to undergo a profound change: affordable fossil fuel reserves are being reduced every year while, at the same time, energy demand increases in every country [63]. Moreover, the aim to reduce greenhouse gas emissions is moving its attention to more environmentally-friendly and sustainable energy sources [104]. With an increased utilization of small distributed energy resources for generation of electricity and heat [11], renewable energy generation will constitute an important part of the overall energy scenario in the coming years.

Notably, in the instance of this work, the Brazilian energy scenario will be taken into account. Brazil has an immensely diversified energy matrix. This can be seen in Brazilian energy reports of 2015 [26] (related to the energy generation of 2014, seen in table 1.1): hydraulic energy sums up to $11,5\%$ of total energy generation, almost 16% of the generated energy came from sugar cane (ethanol and electric energy from biomass) and other bio-energy sources contributed with up

to $12, 2\%$ of total generation. The rest of Brazilian energy generation corresponds to: natural gas, summing up $13, 5\%$, petroleum and derived sources, related with $39, 4\%$, nuclear sources, corresponding to $1, 3\%$ and coal, corresponding to 6% of the totality. In respect to the Brazilian electric matrix (seen in table 1.2), 74.6% of the total electric energy was generated by renewable energy sources.

The investment in solar energy has vastly risen in recent years and Brazil has good climatological conditions in several regions to explore this kind of energy source, showing competitive costs [108]. Solar and wind energies can be considered potential energy sources to enlarge the renewable energy share in the Brazilian electric energy matrix for the next years. According to [24] the share of wind energy in the total electric energy produced in 2024 will increase to 11.6% ($24GW$) while solar energy will contribute with 3.3% ($7GW$). Beyond that, the prospect to next years is that renewable energy sources will increase their contribution in 84% to the electric energy matrix.

Table 1.1: Brazilian Internal Energy Offer

Energy Source	Structure (%)
Non-renewable	60.6
Petroleum and derivatives	39.4
Natural Gas	13.5
Mineral Coal and derivatives	5.7
Uranium ($U3O8$) and derivatives	1.3
Other non-renewable	0.6
Renewable	39.4
Hydraulics and Electricity	11.5
Firewood and Charcoal	8.1
Sugar Cane derivatives	15.7
Other Renewable	4.1
Total	100

The sugar cane and ethanol power plants are particularly significant to this study [53], as the sugar cane process has a great amount of residue that can be treated as biomass. To allow technological improvements [35] and to increase ethanol production, per ton of processed sugar cane, the amount of sugar cane fiber made available in the plant has to be as great as possible. A plausible solution to resolve this matter is to harvest the crops of cane without pre-burning the crop area, and, by this, recover a significant portion of straw available in the canebrakes

Table 1.2: Brazilian Internal Electrical Energy Offer

Energy Source	Structure (%)
Hydraulic	59.8
Sugar Cane derivatives	5.2
Wind	2
Solar	0.003
Other renewable	2.2
Petroleum and derivatives	5.1
Natural Gas	13.0
Mineral Coal and derivatives	2.9
Nuclear	2.5
Other non-renewable	1.9
Imported	5.4
Total	100

[22]. The straw is composed of unseasoned leafs, dry leafs and by the sugar cane pointer, and can be used, for example, to boost up heating boilers. This biomass is not yet exploited in its plenitude, although this situation will be reversed in the near future, knowing that Brazilian environmental legislation [73] predicts gradual prohibition of pre-burning canebrakes. Apart from the straw, the bagasse is also an important [2] and useful residue of the sugar cane processing. The bagasse is the final residue of the compression process to retrieve the sugar cane juice and is commonly used in sugar cane energy plants. From the ethanol production process, it is, in the instance of this work, worth mentioning the vinasse. The vinasse [96] represents the residue made available after the distillation of fermented sugar cane broth (*garapa*). For every liter of ethanol produced, 12 liters of vinasse appear as left-overs. Typically, the vinasse is used as a fertilizer for newer crops, which is actually linked to environmental damaging issues, as contamination of soil and underground water. Even if not often, the vinasse can be used as a renewable power source. This is grounded in the technology of anaerobic digestion of the vinasse, that ends up transformed in biogas. This biogas can be used in thermodynamical applications: generation of heat and power. In sum, there are three very important renewable sources of energy in the sugar-ethanol plants: the bagasse, the straw and the vinasse.

One of the main problems associated with these kind of systems is the reliability and quality of the power supply. As a matter of fact,

since the renewable source is intermittent, unpredictable fluctuations may appear in power output [3]. Also, electrical generation from renewable sources is not subjected to demand, which creates imbalance in the system. One way to overcome this problem is to include intermediate storage, such as batteries, water pumping, super-capacitors, compressed air, fly wheels, superconducting magnetic energy storage unit, etc. [33]. This buffering capability can help to avoid the consideration of renewable as an undispatchable source, due to its inherent unpredictability and variability.

The use of storage systems enables the opportunity to decide the microgrid optimal operating point both in the islanded and connected to the grid modes, being possible to manage the appropriate time to exchange energy with the external network. There are several energy storage technologies and the possibility of hybridization among them has aroused great interest [38], [54]. Specifically, the combination of hydrogen storage together with electric batteries and supercapacitors seems to be a suitable solution for renewable generation [62]. The use of hydrogen for storing electrical energy from renewable sources is based on the possibility of producing hydrogen by electrolysis, store it and subsequently use it again to generate electricity through fuel cells.

A structural solution that has been studied in recent years is the splitting of the electrical network into smaller self-generation units based on renewable energy where the use of energy storage compensates the fluctuations in renewable generation and the randomness of consumer behavior. Thus, the concept of microgrid, introduced by [68], becomes a powerful tool to improve the electrical system quality and reliability. A microgrid is defined as a hybrid system which includes several sources and storage devices to fulfill the local loads [41]. According to [86] a microgrid can be seen as a set of loads, generators and storage units whose management can be done independently or connected to the external network in a coordinated way to contribute to the whole system stability.

On the other hand, V2G systems (Vehicle-to-grid) consist of the use of electric car batteries, during periods when they are not used, as energy storage units for an electrical network. Taking into account the current size of the fleet and the expectation of a gradual increase in the number of electric vehicles, it is expected that the energy storage capacity that can be provided in a near future will be sufficient to balance the supply and demand on an electricity grid or microgrid, and hence, improve the performance and stability of the network. According to recent publications of the Brazilian Science, Technology and Innova-

tion Ministry ([23], [25]), the use of electric vehicles connected to the smart grid is a trend for the future and the development of algorithms for managing the use of vehicle batteries is a strategic research area.

It is estimated that a electric vehicle is in motion only 4% of time, so the rest of the time it could be available as an electrical energy storage unit [47]. Furthermore, in normal use, the car batteries are recharged overnight (which is the period of low electricity demand) and are parked in the workplace during periods of high electrical demand, so this power could be used to meet the peak demand. This storage capacity is especially useful with renewable energy sources, as the fluctuating nature makes it harder to adjust production and demand.

In addition, the V2G systems enable to set new business models in which new actors appear, such as Load Managers that would be responsible for recharging infrastructure, providing service to vehicles, buying or selling electrical energy and building relationships with the network managers. In the last years control algorithms for charging electric vehicles in intelligent networks appeared in the literature. In [28] and [97] the problem is solved by real-time optimization algorithms, whereas in [52] an MPC-based algorithm is presented. Also solutions based on hierarchical distributed algorithms have been presented ([5]; [36]; [43]).

Regarding modeling aspects, most part of the algorithms proposed in literature use very simplified models of power systems, vehicle motion and load characteristics. In particular, the modeling framework called Energy hubs ([49], [31]) allows the integration of different forms of production and storage of a microgrid, V2G system [44] and the interconnection of different microgrids or a microgrid connected to an electric network.

With an increasing demand on improving productivity and efficiency, the operation requirements of energy systems are getting tighter. This leads to the necessity of investing on automatic operation and control of the plants aimed to achieve an enhanced efficiency of the whole plant. It is known that an optimal operation of each subsystem composing the energy plant does not ensure the optimal operation of the whole system possibly leading to an even not admissible behavior. This makes necessary the coordination between the elements of the whole plant. This is typically carried out by a supervised automatic system which relies on an upper level in the control hierarchy of the plant. Thus, targets of each subsystem are provided by the upper level such that the quality of the service is ensured and, if possible, operation is done close to the optimal operating point. From the efficiency

point of view, the best control technique should take into account simultaneously the efficient operation of each subsystem while quality requirements are fulfilled.

The development of new results for modeling, identification and control of hybrid energy systems including renewable energy would imply a significant improvement in the operation, efficiency and safety of this class of relevant systems. Due to the incomplete nature of the results on this topic, new methodologies and strategies are of potential great relevance in this emerging field.

Model Predictive Control (MPC) is the most natural approach to the optimal control of processes subject to constraints [17]. This explains why MPC is the advanced control strategy that has the greatest acceptation in process industry. However, there are still many open issues related to MPC techniques to be applied to energy systems, such as cooperation, robustness, real-time optimization, that must be deeply explored.

In general, microgrid management is carried out by heuristic algorithms [55], although there are applications that use MPC strategies, such as those presented in [38] and [112]. Optimal control of distributed energy resources using model predictive control with battery storage system is developed in [82]. In the case of hybrid storage systems, MPC appears to be a good solution as shown in [30], [115] and [54].

Several works ([59]; [126];[51]) use the hysteresis band (HB) method for energy management of microgrids with hybrid storage. Regarding the performance advantages of MPC over optimized hysteresis band, there are several papers comparing these approaches and others ([113]; [14]; [46]). The main difference between MPC and HB is that MPC guarantees optimality while HB does not. MPC solves an optimization problem each sampling time to determine minimal running cost while meeting the demand and considering technical and physical limits. A dramatic reduction in operation cost can be observed when comparing both techniques [115].

Recent works have brought to light MPC-based control structures used to master microgrids with renewable sources. Reference [114] shows a hydrogen-based domestic microgrid being controlled by an MPC-based structure; [45] and [93] also refer to optimal generation for renewable microgrids, considering hydrogen storage systems. [42] considers plug-in hybrid electric vehicles based on multi-carrier systems and [75] proposes a MPC to energy management of a microgrid connected to an electric vehicle charging station. In terms of renewable source applications, [44] is specific about wind balancing capabilities

using heuristics and MPC, whereas [76] focuses on a renewable micro-grid in an isolated load area. Generic MPC-based structures are seen in [4] and [92]. Economic optimization is exposed in [15] and [91]. Cogeneration is discussed in [106] and [101].

Recent studies have shown that connecting multiple microgrids can further improve the system operation and reliability ([85], [37], [121]). Those benefits are assigned to some properties of networked microgrids, such as coordinated energy management and interactive support and exchange. According to [122], self-healing capability intro-duced by interconnecting microgrids, is an important feature in smart grids, especially when a fault occurs in a part of the system.

The study of interconnected microgrids is a growing research field. A centralized control model for optimal management and operation of a smart network of microgrids was presented in [88]. [83] and [77] addressed the optimal power dispatch problem considering uncertain-ties in load and probabilistic modeling of generated power by renewable small-scale energy resources. A review on distributed control techniques for all hierarchy levels and a discussion of future research trends in this area was presented in [125]. A game theoretic coalition formulation strategy was proposed in [123] to allow the microgrids autonomously cooperate and self-organize into coalitions. In [121] a bi-level stochas-tic solution for the coordinated operation of multiple microgrids and a distribution system is presented. A self-healing operation mode based on average consensus algorithm for optimal operation of autonomous networked microgrids was developed in [122]. In [105] a distributed energy management system for the optimal operation of alternating current (AC) microgrids was designed with consideration of the under-lying power distribution network and the associated constraints.

Due to the complexity of large-scale networks, the distribution of the control effort between local control agents can be a very convenient choice. In many cases, parts of the network belong to different organi-zations, which makes centralized control impossible to be implemented [31]. In interconnected microgrids scenario the coordination among all microgrids and between the microgrids and Distribution Network Operator (DNO) brings new challenges for the overall system energy management. In this scenario a distributed control structure becomes a good option for sharing information about energy exchange to de-cide the optimal operating point for the whole system. In the last years many distributed control techniques were proposed in literature ([71],[72],[1],[18]).

The control of hybrid energy systems including renewable and

non-renewable generation is an important problem to be studied in the following years to allow the optimal operation of these new generation units. The integration of V2G systems can be a key factor in network stability guarantee against load fluctuations. In this context this thesis aims to contribute with this research area through the study and development of control algorithms applied to renewable energy microgrids.

1.1 Objectives and Organization of the Thesis

This thesis has a general objective to develop MPC algorithms to the economic management of hybrid energy systems based on renewable energy sources. The specific objectives are:

1. Model hybrid energy systems integrating renewable energy sources (wind and solar), hybrid storage units (batteries, hydrogen and biomass) and electric vehicles (V2G).

2. Develop load controllers strategies and manage the electric vehicles batteries usage as energy storage connected to microgrid in the context of V2G systems.

3. Apply the control algorithms to an experimental microgrid located at the *Departamento de Ingeniería de Sistemas y Automática* (DISA) of the *Universidad de Sevilla* (US) in Seville, Spain.

4. Develop an Hybrid MPC and Distributed MPC strategies for the optimal economic management of single grid-connected microgrids and networked microgrids respectively.

5. Apply these techniques in a Brazilian case study of hybrid power plants in sugar cane distilleries.

This thesis is organized as follows. In Chapter 2 the energy hub modeling framework is described. Chapter 3 presents a review of MPC, Hybrid MPC and Distributed MPC Strategies. Chapter 4 proposes an Hybrid Distributed MPC algorithm. Chapter 5 focuses on the application of modeling and control methodologies described in previews chapters to the problem of single grid-connected microgrid and networked microgrids. Finally, chapter 6 presents the case of hybrid power plants in sugar cane distilleries and the use of the discussed techniques to optimize their operation. The thesis ends with some conclusions presented in chapter 7.

Chapter 2

Energy Hubs Modeling Framework

This chapter presents a literature review of the energy hub modeling methodology, introduced in [48]. An energy hub can be used to model the interface between energy producers, consumer and the transmission line. From the standpoint of the system, an energy hub can be identified as a unit that provides the following features:

1. input and output power;

2. energy conversion;

3. energy storage.

The hub serves as interface between the energy sources, producers and consumers or between the different energy sources. In practice a microgrid can be modeled as a hub and a power system can be divided in many microgrids interconnected by transmission lines, where each network node corresponds to one hub. The system model is designed in two parts: power flow within and between hubs. The model is based on some assumptions and simplifications:

- it is considered that the network is in steady state. Such a state is achieved after the end of all transitory dynamics and all variables oscillate uniformly or remain essentially constant;

- the interconnection between hubs is carried out through inputs and outputs interconnection;

- losses only occur in converter and storage unit elements;

- within a hub, it is assumed that the flow is unidirectional from the inputs to the outputs of the converters, except when considering the storage elements, where the bidirectional flow (charge/discharge) is allowed.

2.1 Modeling Framework

Hereafter the modeling of converters and storage elements will be presented. For a description of input and output variables a standard based on the generic variable:

$$g_{sub}^{sup}(k) \qquad\qquad (2.1)$$

was used, where g can be represented by y for outputs and u for inputs. When sub-index sub refers to input variables the letter r will be used; for hub outputs, the letter p; to the inputs of the inputs storage units, the letter q; for inputs of the output storage units, the letter m; and for storage interface the letter s. The super-index sup is the element type that the variable belongs, being L for converters and E to storage units.

2.1.1 Converters

Input-output conversion can be described considering the converter as a black box. Converter combinations can lead to different hub input-output settings according the following four cases below:

- single input and single output (SISO);

- single input and multiple outputs (SIMO);

- multiple inputs and single input (MISO);

- multiple inputs and multiple outputs (MIMO).

A single converter can be seen as presented in figure 2.1. This element converts, in every time instant k, a generic r input flow $u_r^L(k)$ of a generic hub into a generic p output flow $y_p(k)$, where superscript L is associated to converter input flows. The input-output conversion is

defined through coupling factors $\gamma^L_{p,r}$, which correspond to steady state conversion efficiency of the converter between the input and output flows:
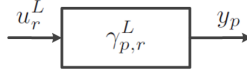
Figure 2.1: SISO converter

$$y_p(k) \quad = \quad \gamma^L_{p,r} u^L_r(k) \tag{2.2}$$

with $u^L_r(k) > 0$, which implies unidirectional flow from the input to the output of a converter. From a physical point of view, coupling factors have the meaning listed in table 2.1, considering lossy, lossless and gainy conversions. When considering applications where flow conservation laws have to be fulfilled (such as energy-related systems), coupling factors are limited in the sense that the output of a converter element must be less than or equal to the input:

$$y_p(k) \quad \leq \quad u^L_r(k) \Rightarrow 0 \leq \gamma^L_{p,r} \leq 1 \tag{2.3}$$

Table 2.1: Coupling factors meaning

Type of converter	Coupling factor
Lossy conversion	$0 \leq \gamma^L_{p,r} \leq 1$
Lossless conversion	$\gamma^L_{p,r} = 1$
Gainy conversion	$\gamma^L_{p,r} \geq 1$

Considering the converter model described above, a generic hub is composed of a converter cluster, shown in figure 2.2, linking all flow inputs $\mathbf{u}^L(k) = \{u^L_1(k), \ldots, u^L_{n_r}(k)\}$ with all flow outputs $\mathbf{y}(k) = \{y_1(k), \ldots, y_{n_p}(k)\}$, where n_r and n_p are the total number of hub inputs and outputs respectively. A set of converters is expressed by the converter coupling matrix Γ^L, which describes the flows from the input to the output and is composed by the converter coupling factors $\gamma^L_{p,r}$.
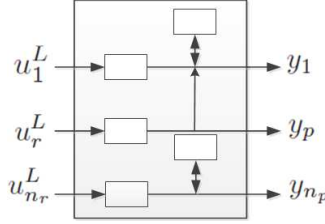
Figure 2.2: Hub with multiple converters

$$
\underbrace{\begin{bmatrix} y_1(k) \\ \vdots \\ y_{n_p}(k) \end{bmatrix}}_{\mathbf{y}(k)} = \underbrace{\begin{bmatrix} \gamma^L_{1,1} & \cdots & \gamma^L_{1,n_r} \\ \vdots & \ddots & \vdots \\ \gamma^L_{n_p,1} & \cdots & \gamma^L_{n_p,n_r} \end{bmatrix}}_{\Gamma^L} \underbrace{\begin{bmatrix} u^L_1(k) \\ \vdots \\ u^L_{n_r}(k) \end{bmatrix}}_{\mathbf{u}^L(k)} \tag{2.4}
$$

As the coupling factors are assumed constant, equations (2.2) and (2.4) result in linear relations.

Application example

In this example, the concepts presented above are applied to model the energy hub shown in figure 2.3, composed of a photovoltaic panels, a CHP (combined heat and power plant) and a battery bank. First input $u^L_1(k)$ is referred to solar radiation, while second input $u^L_2(k)$ is referred to natural gas. First and second outputs $y_1(k)$, $y_2(k)$ are referred to electricity and heat demand respectively. Hub inputâoutput description is obtained utilizing the converter coupling matrix Γ^L in equation (2.5).

$$
\begin{bmatrix} y_1(k) \\ y_2(k) \end{bmatrix} = \begin{bmatrix} \gamma^L_{1,1} & \gamma^L_{1,2} \\ 0 & \gamma^L_{2,2} \end{bmatrix} \begin{bmatrix} u^L_1(k) \\ u^L_2(k) \end{bmatrix} \tag{2.5}
$$

In the example application described herein, coupling factors have the physical meaning of energy conversion efficiencies η. Specifically, the photovoltaic panels are characterized by its radiationâ electric conversion efficiency $\eta^S_{rad,e}$. Analogously, the CHP is characterized by its gasâelectric conversion efficiency $\eta^{CHP}_{g,e}$ and its gas-heat conversion efficiency $\eta^{CHP}_{g,h}$. This way the converter coupling matrix has the following form:
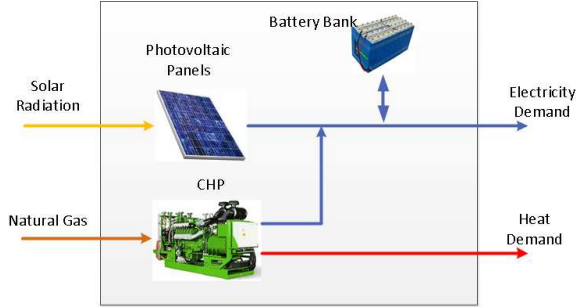
Figure 2.3: Energy Hub that contains a photovoltaic panels, a CHP and a battery bank

$$\Gamma = \left[\begin{array}{cc} \eta_{rad,e}^{S} & \eta_{g,e}^{CHP} \\ 0 & \eta_{g,h}^{CHP} \end{array} \right] \tag{2.6}$$

2.1.2   Storage Units

The modeling of a generic storage considers that the device is composed of an interface and an internal storage, as shown in figure 2.4. The interface can be seen as a flow converter, which modulates a generic storage interface input flow $u_s^E(k)$ into another generic storage interface output flow $\breve{u}_s^E(k)$. The converted energy is then stored in an ideal internal stage. Mathematically, the storage interface is modeled analogously to a converter device, where the steady-state input-output flow values are described by the relation:
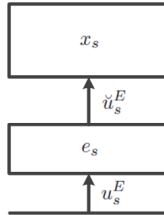
Figure 2.4: Hub storage

$$\breve{u}_s^E(k) = e_s(k)u_s^E(k) \tag{2.7}$$

where $e_s(k)$ represents the efficiency of the charge/discharge interface s of the Hub, which describes how much of the flow exchanged with the system affects the storage. This factor depends on the direction of the exchanged flow, if the storage is being charged or discharged:

$$e_s(k) = \begin{cases} e_s^+ & \text{if} \quad u_s^E(k) \geq 0 \quad (charging) \\ e_s^- & \text{else} \qquad\qquad (discharging) \end{cases} \quad (2.8)$$

where e_s^+ and e_s^- are respectively the charging and discharging efficiencies.

From a discrete-time point of view, internal storage state x_s at sampling time $k+1$ depends on the state at previous sample k and on the total exchanged flow $\breve{u}_s^E(k)$ during the period ΔT ranging from k to $k+1$, assuming $\breve{u}_s^E(k)$ to remain constant during ΔT:

$$x_s(k+1) = x_s(k) + \breve{u}_s^E(k)\Delta T \quad (2.9)$$

Thus, vector $\mathbf{x}_s(k+1)$ containing all the storage states $x_s(k+1); s = 1, \ldots, n_s$ depends on the state vector at previous time step $\mathbf{x}_s(k)$, on matrix $\Lambda^E(k)$ containing all the interface efficiencies $e_s(k); s = 1, \ldots, n_s$ and on vector $\mathbf{u}_s^E(k)$ containing all the interface flow inputs $u_s^E(k); s = 1, \ldots, n_s$, where n_s is the total number of storage elements:

$$\underbrace{\begin{bmatrix} x_1(k+1) \\ \vdots \\ x_{n_s}(k+1) \end{bmatrix}}_{\mathbf{x}_s(k+1)} = \underbrace{\begin{bmatrix} x_1(k) \\ \vdots \\ x_{n_s}(k) \end{bmatrix}}_{\mathbf{x}_s(k)} + \underbrace{\begin{bmatrix} e_1(k) & & \\ & \ddots & \\ & & e_{n_s}(k) \end{bmatrix}}_{\Lambda^E(k)} \underbrace{\begin{bmatrix} u_1^E(k) \\ \vdots \\ u_{n_s}^E(k) \end{bmatrix}}_{\mathbf{u}_s^E(k)}$$

$$(2.10)$$

where

$$\Lambda^E(k) = \left\{ \Lambda^{E+}, \Lambda^{E-} \right\} = \begin{bmatrix} \{e_1^+, e_1^-\} & & \\ & \ddots & \\ & & \{e_{n_s}^+, e_{n_s}^-\} \end{bmatrix} \quad (2.11)$$

where each element of $\Lambda^E(k)$ is a signal function of $u_s^E(k)$, so, if $u_s^E(k)$ is positive this means that the storage is charging and $e_s(k) = e_s^+$, otherwise $u_s^E(k) \leq 0$ and the storage is discharging and $e_s(k) = e_s^-$.

Multiple Storage

As storage elements may be connected to both hub inputs and outputs, as shown in figure 2.5, a mathematical transformation of the corresponding storage flows has to be performed in order to obtain an input-output description independently of where the storage device is physically connected.
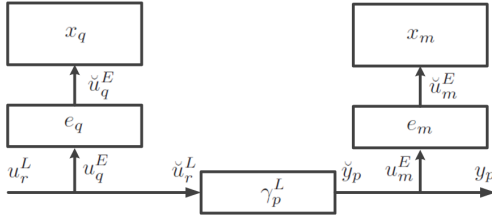
Figure 2.5: Hub with multiple storage units

As shown in figure 2.5, the flow $\breve{u}_r^L(k)$ entering the converter is equal to the hub input flow $u_r^L(k)$ minus the input side storage flow $u_q^E(k)$:

$$\breve{u}_r^L(k) = u_r^L(k) - u_q^E(k). \tag{2.12}$$

The converter output can be described as:

$$\breve{y}_p(k) = y_p(k) + u_m^E(k) \tag{2.13}$$

where $\breve{y}_p(k)$ is the converter output flow, $y_p(k)$ is the hub output flow and $u_m^E(k)$ is the output storage flow. Using equation (2.2) in this case gives:

$$\breve{y}_p(k) = \gamma_p^L \breve{u}_r^L(k). \tag{2.14}$$

Substituting equations (2.12) and (2.13) into (2.14), both converter sides storage flows can be explicitly included in the following input-output description:

$$y_p(k) = \gamma_{p,r}^L \left(u_r^L(k) - u_q^E(k) \right) - u_m^E(k) = \gamma_{p,r}^L u_r^L(k) + \gamma_{p,r}^E u_r^E(k), \tag{2.15}$$

where $\gamma_{p,r}^E$ are the coupling factors related to storage variables $u_r^E(k)$. Vector $\mathbf{y}(k)$ contains all hub outputs $y_p(k) \in \{y_1(k), \ldots, y_{n_p}(k)\}$ and can be extended in order to include storage elements through the storage coupling matrix Γ^E. Such a matrix describes how changes of the storage flows affect the converter output flows, resulting in 2.16.

$$
\underbrace{\begin{bmatrix} y_1(k) \\ \vdots \\ y_{n_p}(k) \end{bmatrix}}_{\mathbf{y}(k)} = \underbrace{\begin{bmatrix} \gamma_{1,1}^L & \cdots & \gamma_{1,n_r}^L \\ \vdots & \ddots & \vdots \\ \gamma_{n_p,1}^L & \cdots & \gamma_{n_p,n_r}^L \end{bmatrix}}_{\Gamma^L} \underbrace{\begin{bmatrix} u_1^L(k) \\ \vdots \\ u_{n_r}^L(k) \end{bmatrix}}_{\mathbf{u}^L(k)} \qquad (2.16)
$$

$$
+ \underbrace{\begin{bmatrix} \gamma_{1,1}^E & \cdots & \gamma_{1,n_s}^E \\ \vdots & \ddots & \vdots \\ \gamma_{n_p,1}^E & \cdots & \gamma_{n_p,n_s}^E \end{bmatrix}}_{\Gamma^E} \underbrace{\begin{bmatrix} u_1^E(k) \\ \vdots \\ u_{n_s}^E(k) \end{bmatrix}}_{\mathbf{u}^E(k)}
$$

Application example

Consider the hub shown in figure 2.3, which is composed of two converters and one storage device: photovoltaic panels, CHP and battery bank. The state $x1(k)$ is related to the battery bank state of charge while the input u_1^E is related to the charging/discharging interface. As described herein, state variables can be modeled as:

$$
x_1(k+1) = x_1(k) + e_1(k)u_1^E(k) \qquad (2.17)
$$

where

$$
e_1(k) = \begin{cases} e_1^+ & \text{if} \quad u_1^E(k) \geq 0 \quad (charging) \\ e_1^- & \text{else} \quad (discharging) \end{cases} \qquad (2.18)
$$

with e_1^+ being the charge efficiency and e_1^- the discharge efficiency. Including the storage input into the equation (2.5), results in:

$$
\begin{bmatrix} y_1(k) \\ y_2(k) \end{bmatrix} = \begin{bmatrix} \gamma_{1,1}^L & \gamma_{1,2}^L \\ 0 & \gamma_{2,2}^L \end{bmatrix} \begin{bmatrix} u_1^L(k) \\ u_2^L(k) \end{bmatrix} + \begin{bmatrix} -1 \\ 0 \end{bmatrix} u_1^E(k) \qquad (2.19)
$$

when the battery bank is charging ($u_1^E \geq 0$) the direction of energy

flow is from the converters to the storage, otherwise ($u_1^E < 0$) and the storage is providing energy to the first output.

2.1.3   State-space Representation

Summarizing equations (2.11) and (2.16) yields to a complete state-state representation of a generic hub:

$$
\begin{aligned}
x(k+1) &= x(k) + \Lambda^E(k)u^E(k) \\
y(k) &= \Gamma^L u^L(k) + \Gamma^E u^E(k),
\end{aligned}
\tag{2.20}
$$

which can be condensed by defining the complete converter interface efficiency matrix $\Lambda_i(k)$, the complete coupling matrix Γ_i and the complete hub input vector $\mathbf{u}_i(k)$ as follows:

$$
\begin{aligned}
\Lambda(k) &= \left[\ 0 \mid \Lambda^E(k)\ \right] \\
\Gamma &= \left[\ \Gamma^L \mid \Gamma^E\ \right] \\
\mathbf{u}(k) &= \left[\ u^L(k)^T \mid u^E(k)^T\ \right]^T,
\end{aligned}
\tag{2.21}
$$

which results in the following representation:

$$
\begin{aligned}
x(k+1) &= x(k) + \Lambda(k)u(k) \\
y(k) &= \Gamma u(k).
\end{aligned}
\tag{2.22}
$$

Using this formulation, a generic network hub can be described by the set of matrices $H = \{\Lambda(k), \Gamma\}$.

2.2   Mixed Logical Dynamical Systems (MLD)

This section is a literature review about Mixed Logical Dynamic systems based in [7]. According to [29], the state-space representation of equation (2.22) is not linear as it includes bilinear terms related to equation (2.7) and (2.8). In order to avoid these terms, the state space representation can be transformed into a Mixed Logical Dynamic system (MLD) [7], where logic, dynamics and constraints are integrated according to:

$$x(k+1) \quad = Ax(k) + B_1u(k) + B_2\delta(k) + B_3z(k) \quad (2.23)$$
$$y(k) \quad = Cx(k) + D_1u(k) + D_2\delta(k) + D_3z(k) \quad (2.24)$$
$$E_2\delta(k) + E_3z(k) \qquad \leq E_1u(k) + E_4x(k) + E_5 \qquad (2.25)$$

where $x(k) = \begin{bmatrix} x_c(k) & x_l(k) \end{bmatrix}^{\mathrm{T}}$ is the state vector with $x_c(k) \in \Re^{n_c}$ and $x_l \in \{0,1\}^{n_l}$, $y(k) = \begin{bmatrix} y_c(k) & y_l(k) \end{bmatrix}^{\mathrm{T}}$ is the output vector with $y_c(k) \in \Re^{p_c}$ and $y_l(k) \in \{0,1\}^{p_l}$, $u(k) = \begin{bmatrix} u_c(k) & u_l(k) \end{bmatrix}^{\mathrm{T}}$ is the input vector with $u_c(k) \in \Re^{m_c}$ and $u_l(k) \in \{0,1\}^{m_l}$, $z(k) \in \Re^{r_c}$ are the continuous auxiliary variables, $\delta(k) \in \{0,1\}^{r_l}$ are the binary auxiliary variables, A, B_1, B_2, B_3, C, D_1, D_2, D_3, E_1, E_2, E_3 and E_4 are constant real matrices, E_5 is a real vector, $n_c > 0$ and $p_c, m_c, r_c, n_l, p_l, m_l, r_l > 0$. The auxiliary variables are new variables introduced in the model to transform the original model into a MLD model.

MDL systems are able of modeling a broad class of systems, as the energy hubs described previously. In order to transform the nonlinear model (2.22) into an MDL description, some basics on propositional calculus and linear integer programming [7] should be firstly revised. To that end, consider the statement $X \triangleq [f(x) \leq 0]$, where $f : R^n \to R$ is linear, assume that $x \in X$, where X is a given bounded set, and define:

$$M \triangleq \underbrace{\max f(x)}_{x \in X} \qquad (2.26)$$

$$m \triangleq \underbrace{\min f(x)}_{x \in X} \qquad (2.27)$$

It is easy to verify that

$$[f(x) \leq 0] \wedge [\delta = 1] \quad \text{is true iff} \quad f(x) - \delta \leq -1 + m(1-\delta) \quad (2.28)$$
$$[f(x) \leq 0] \vee [\delta = 1] \quad \text{is true iff} \quad f(x) \leq M\delta$$
$$\sim [f(x) \leq 0] \quad \text{is true iff} \quad f(x) \geq \epsilon$$

where ϵ is a small tolerance beyond which the constraint is regarded as violated and standard Boolean algebra is utilized, which enables

statements X such as "$x > 0$" to be combined in compound statements by means of connectives: "$\wedge$" (and), "$\vee$" (or), "$\sim$" (not), "$\rightarrow$" (implies), "$\leftrightarrow$" (if and only if). By property

$$X_1 \rightarrow X_2 \quad \text{is the same as} \quad \sim X_1 \vee X_2 \tag{2.29}$$

and (2.28), it also follows

$$[f(x) \leq 0] \rightarrow [\delta = 1] \quad \text{is true iff} \quad f(x) \geq \epsilon + (m - \epsilon)\delta \tag{2.30}$$

$$[f(x) \leq 0] \leftrightarrow [\delta = 1] \quad \text{is true iff} \quad \begin{cases} f(x) \leq M(1 - \delta) \\ f(x) \geq \epsilon + (m - \epsilon)\delta \end{cases} \tag{2.31}$$

Following the reasoning, it is possible to transform products of logical variables, and of continuous and logical variables, in terms of linear inequalities, which can be done by the introduction of some auxiliary variables. Specifically, the generic product term $\delta_1 \delta_2$ can be replaced by an auxiliary logical variable $\delta_3 \triangleq \delta_1 \delta_2$. Then, $[\delta_3 = 1] \leftrightarrow [\delta_1 = 1] \wedge [\delta_2 = 1]$, and therefore

$$\delta_3 = \delta_1 \delta_2 \quad \text{is equivalent to} \quad \begin{cases} -\delta_1 + \delta_3 \leq 0 \\ -\delta_2 + \delta_3 \leq 0 \\ \delta_1 + \delta_2 - \delta_3 \leq 1 \end{cases} \tag{2.32}$$

Also, the term $\delta f(x)$, where $f : \Re^n \rightarrow \Re$, can be replaced by an auxiliary real variable $y \triangleq \delta f(x)$, which satisfies $[\delta = 0] \rightarrow [y = 0]$, $[\delta = 1] \rightarrow [y = f(x)]$. Thus, $y = \delta f(x)$ is equivalent to

$$y \leq M\delta \tag{2.33}$$

$$y \geq m\delta \tag{2.34}$$

$$y \leq f(x) - m(1 - \delta) \tag{2.35}$$

$$y \geq f(x) - M(1 - \delta) \tag{2.36}$$

where M and m are defined as in (2.26) and (2.27).

2.2.1   MLD Procedure applied to Storage Modeling

According to [29], in order to convert the bilinear equation (2.7) in the MLD form and taking into account the concepts of propositional calculus and integer linear programming, the following steps are performed:

1. Condition $u_s^E(k) \geq 0$ is associated with the binary variable $\delta_s(k)$ so that

$$[\delta_s(k) = 1] \leftrightarrow [u_s^E(k) \geq 0] \tag{2.37}$$

   Using transformations (2.30) and (2.31), equation (2.37) is represented by inequalities

$$-m_s \delta_s(k) \leq u_s^E(k) - m_s$$
$$-(M_s + \epsilon)\delta_s(k) \leq -u_s^E(k) - \epsilon$$

   where ϵ is a positive scalar and

$$m_s \triangleq \underbrace{\min}_{k \in \Re, s \in N_s} u_s^E(k)$$
$$M_s \triangleq \underbrace{\max}_{k \in \Re, s \in N_s} u_s^E(k)$$

   and N_s is the storage units set.

2. A new variable is defined $z_s(k) = u_s^E(k)\delta_s(k)$ which can be represented as

$$\begin{aligned}
z_s(k) &\leq M_s \delta_s(k) \\
z_s(k) &\geq m_s \delta_s(k) \\
z_s(k) &\leq u_s^E(k) - m_s(1 - \delta_s(k)) \\
z_s(k) &\geq u_s^E(k) - M_s(1 - \delta_s(k))
\end{aligned}$$

3. The system evolution, (2.20), can be described by the following linear relationships:

$$x_s(k+1) = x_s(k) + e_s^- u_s^E(k) + \left(e_s^+ - e_s^-\right) z_s(k)$$

It should be noted that when $u_s^E(k) > 0$ so $\delta_s(k) = 1$ and consequently $z_s(k) = u_s^E$ and equation results in $x_s(k+1) = x_s(k) + e_s^+ u_s^E(k)$. When $u_s^E(k) < 0$ so $\delta_s(k) = 0$ and $z_s(k) = 0$ and model results in $x_s(k+1) = x_s(k) + e_s^- u_s^E(k)$ satisfying the imposed modeling conditions, but with a linear model.

Vector $\mathbf{x}(k+1)$ containing all the storage states, which was previously described by the nonlinear equation (2.10), can also be described by the following linear relationships:

$$
\underbrace{\begin{bmatrix} x_1(k+1) \\ \vdots \\ x_{n_s}(k+1) \end{bmatrix}}_{\mathbf{x}(k+1)} = \underbrace{\begin{bmatrix} x_1(k) \\ \vdots \\ x_{n_s}(k) \end{bmatrix}}_{\mathbf{x}(k)} + \underbrace{\begin{bmatrix} e_1^- & & \\ & \ddots & \\ & & e_{n_s}^- \end{bmatrix}}_{\Lambda^{E-}} \underbrace{\begin{bmatrix} u_1^E(k) \\ \vdots \\ u_{n_s}^E(k) \end{bmatrix}}_{\mathbf{u}^E(k)} \tag{2.38}
$$

$$
+ \underbrace{\begin{bmatrix} e_1^+ - e_1^- & & \\ & \ddots & \\ & & e_{n_s}^+ - e_{n_s}^- \end{bmatrix}}_{\Lambda^{E+} - \Lambda^{E-}} \underbrace{\begin{bmatrix} z_1(k) \\ \vdots \\ z_{n_s}(k) \end{bmatrix}}_{\mathbf{z}(k)}
$$

$$
\underbrace{\begin{bmatrix} -M \\ m \\ -m \\ M \\ -m \\ -(M + \epsilon(\cdot)) \end{bmatrix}}_{E_\delta} \underbrace{\begin{bmatrix} \delta_1(k) \\ \vdots \\ \delta_{n_s}(k) \end{bmatrix}}_{\delta} + \underbrace{\begin{bmatrix} \mathbf{1}(\cdot) \\ -\mathbf{1}(\cdot) \\ \mathbf{1}(\cdot) \\ -\mathbf{1}(\cdot) \\ \mathbf{0}(\cdot) \\ \mathbf{0}(\cdot) \end{bmatrix}}_{E_z} \underbrace{\begin{bmatrix} z_1(k) \\ \vdots \\ z_{n_s}(k) \end{bmatrix}}_{z(k)}
$$

$$
\leq \underbrace{\begin{bmatrix} \mathbf{0}(\cdot) \\ \mathbf{0}(\cdot) \\ \mathbf{1}(\cdot) \\ -\mathbf{1}(\cdot) \\ \mathbf{1}(\cdot) \\ -\mathbf{1}(\cdot) \end{bmatrix}}_{E_u^E} \underbrace{\begin{bmatrix} u_1^E(k) \\ \vdots \\ u_{n_s}^E(k) \end{bmatrix}}_{u^E(k)} + \underbrace{\begin{bmatrix} \mathbf{0}(\cdot)_f \\ \mathbf{0}(\cdot)_f \\ -m_f \\ M_f \\ -m_f \\ -\epsilon(\cdot)_f \end{bmatrix}}_{E_0}
$$

where,

$$M = \begin{bmatrix} M_1 & & \\ & \ddots & \\ & & M_{n_s} \end{bmatrix}, M_f = \begin{bmatrix} M_1 \\ \cdots \\ M_{n_s} \end{bmatrix},$$

$$m = \begin{bmatrix} m_1 & & \\ & \ddots & \\ & & m_{n_s} \end{bmatrix}, m_f = \begin{bmatrix} m_1 \\ \cdots \\ m_{n_s} \end{bmatrix},$$

$$\mathbf{a}(\cdot) = \begin{bmatrix} a & & \\ & \ddots & \\ & & a \end{bmatrix}, \mathbf{a}(\cdot)_f = \begin{bmatrix} a \\ \cdots \\ a \end{bmatrix}$$

where $\mathbf{a}(\cdot)$ is a matrix with dimension $n_s \times n_s$ and $\mathbf{a}(\cdot)_f$ is a column vector with n_s rows.

Introducing equation (2.16) related to coupling factors and using the condensed formulation (2.21), a generic hub can be expressed by the following MDL form, which is analogous to the nonlinear state-space representation in equation (2.22).

$$\mathbf{x}(k+1) = A\mathbf{x}(k) + \Lambda^{E-}\mathbf{u}^E(k) + \left(\Lambda^{E+} - \Lambda^{E-}\right)\mathbf{z}(k) \qquad (2.39)$$

$$\mathbf{y}(k) = \Gamma^L\mathbf{u}^L(k) + \Gamma^E\mathbf{u}^E(k) \qquad (2.40)$$

$$E_\delta\delta + E_z\mathbf{z}(k) \leq E_u^E\mathbf{u}^E(k) + E_0 \qquad (2.41)$$

2.3   Interconnected Energy Hubs

Consider a generic network composed of a set $\mathcal{N} = 1, \ldots, n_N$ of interconnected hubs, where n_N is the total number of hubs composing the network. The dynamics of sub-network $i \in \mathcal{N}$ can be defined by the following nonlinear time-invariant discrete-time state-space model:

$$x_i(k+1) = x_i(k) + \Lambda_i(k)u_i(k) \qquad (2.42)$$

$$y_i(k) = \Gamma_i u_i(k) + \Pi_{in,i\leftarrow j}w_{in,i\leftarrow j}(k), \qquad (2.43)$$

where $w_{in,i\leftarrow j}(k) \in R^{n_v}$ is the interconnecting inputs vector and $\Pi_{in,i\leftarrow j} \in R^{n_p \times n_v}$ is the input interconnecting matrix, n_p and n_v are the total number of hub outputs and interconnecting constraints, respectively.

The "$\leftarrow$" indicates the power flow direction between the hub j and the hub i. As discussed previously such a nonlinear state-space model can be expressed in the following MDL form:

$$x_i(k+1) = x_i(k) + \Lambda_i^{E-} u_i^E(k) + \left(\Lambda_i^{E+} - \Lambda_i^{E-}\right) z_i(k) \qquad (2.44)$$

$$y_i(k) = \Gamma_i^L u_i^L(k) + \Gamma_i^E u_i^E(k) + \Pi_{in,i\leftarrow j} w_{in,i\leftarrow j}(k) \qquad (2.45)$$

$$E_{i,\delta}\delta_i + E_{i,z} z_i(k) \leq E_{i,u}^E u_i^E(k) + E_{i,0}. \qquad (2.46)$$

Considering the interconnections among hubs, generic interconnecting variables between hub i and its neighbor j can be defined as seen in figure 5.19, where $w_{in,i\leftarrow j}(k)$ and $w_{out,i\rightarrow j}(k)$ are, respectively, generic interconnecting input and output vectors of hub i related to its neighboring hub j, with:
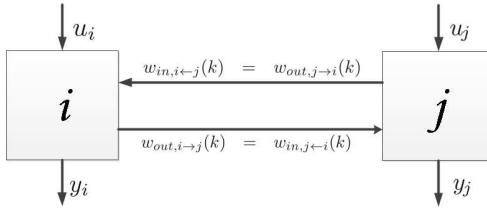
Figure 2.6: Interconnection variables between hub i and j

$$w_{out,i\rightarrow j}(k) = \Pi_{out,i\rightarrow j} y_i(k) \qquad (2.47)$$

where $\Pi_{out,i\rightarrow j}$ is the output interconnecting matrix referred to the coupling of hub i with respect to its neighbor j. The "$\rightarrow$" indicates the power flow direction between the hub i and the hub j. Also, $w_{in,i\leftarrow j}(k)$ and $w_{out,i\rightarrow j}(k)$ are defined as vectors containing, respectively, all interconnecting inputs and outputs of hub i with respect to its neighboring hub set $\mathcal{N}_i = 1, \ldots, n_{N_i}$. Also, interconnecting constraints have to be introduced, as the interconnecting inputs of hub i with respect to hub j must be equal to the interconnecting outputs of hub j with respect to hub i, which results in the following equalities:

$$w_{in,i\leftarrow j}(k) = w_{out,j\rightarrow i}(k) \qquad (2.48)$$

$$w_{out,i\rightarrow j}(k) = w_{in,j\leftarrow i}(k) \qquad (2.49)$$

Taking into account the interconnections among hubs described above, a generic hub i, part of network N, can then be described by the set of matrices $H_i = \Lambda_i, \Gamma_i, \Pi_{in,i\leftarrow j}, \Pi_{out,i\rightarrow j}$.

2.4   Final Remarks

In this chapter a literature review about energy hubs modeling theory and its representation by MLD equations was presented, which is a important tool to model microgrids. In the chapter 3 a review on model predictive control applied to hybrid systems will be presented where the models developed here will be considered.

Chapter 3

Model Predictive
Control (MPC)

This chapter presents some concepts of model predictive control (MPC). First the state space MPC algorithm is revisited and some basic characteristics are broached. Then the idea of distributed MPC is discussed and the Lagrange based DMPC algorithm is presented. Finally a framework to Hybrid distributed MPC is proposed and a convergence analysis is performed.

3.1 State Space MPC

MPC has emerged in the last two decades as a powerful practical control technique. It is one of the few advanced control techniques that have achieved significant impact on industrial process control. The main reason for this success is, perhaps, the ability of MPC to deal with the following situations: the possibility to be applied in SISO (single input single output) and MIMO (multiple inputs multiple outputs) systems, feedback and feedforward actions can be included directly in the MPC formulation, soft and hard constraints can be included in the formulation of the control law through online optimization and the intrinsic compensation of process dead times [84].

MPC is not a specific control strategy, but is the name given to a very large set of control methods that have been developed considering some common ideas and based on the concept of prediction. Figure 3.1 shows the MPC general structure. From the past values of process in-

put and output, future predictions can be calculated using a prediction model. The prediction model is the most important controller element, once it must be able to represent the process dynamics. In the linear case, the process output prediction can be separated into two parts: the free response that corresponds to the output prediction when only past values of the input are considered and the future control is constant and, the forced response that is obtained assuming null values for the past inputs and variations in the future control action. With the values of future predictions, future reference, process constraints and objective function, an optimization module computes the control signal to be applied to the process in the next step. Generally the purpose of the objective function is to minimize the error between the output prediction and the desired reference penalizing control effort [17]. The receding horizon strategy is other important property of the MPC, as only the first element of the obtained control vector is applied to the plant and the procedure is repeated on the next sample.
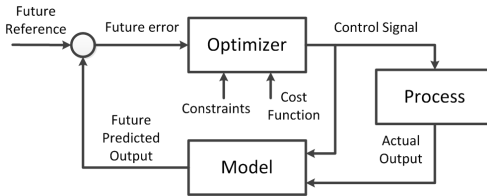
Figure 3.1: MPC block diagram.

All MPC algorithms have some elements in common, being: the prediction model, the objective function and a method for obtaining the control law. Different controllers in the literature differ in the way in which these elements are found [17]. Hereafter some of these concepts are presented.

3.1.1   Prediction Model

The prediction model is composed of the process and disturbance dynamics and is the most important element in predictive control algorithms. As MPC bases its control law computation in the prediction model, all the advantages of predictive control may be lost if the model is not faithful to the process dynamics. Linear models are more common in practice and can be input-output (impulse response, step response and transfer function) or based on state space variables, as the one used in this thesis.

The main theoretical results of MPC related to stability come from a state-space formulation, which can be used for both monovariable and multivariable processes and can easily be extended to nonlinear processes [17]. Consider a process with n_x states, n_u inputs and n_y outputs is described by the following state space equations:

$$x(k+1) = Ax(k) + B\Delta u(k)$$
$$y(k) = Cx(k) + D\Delta u(k) \tag{3.1}$$

where A, B, C, D are matrices with order $n_x \times n_x$, $n_x \times n_u$, $n_y \times n_x$, $n_y \times n_u$; x is the state vector, u the input vector and y the output vector. In this model k represents the discrete time (the sampling time is not written explicitly for simplicity).

The future predicted values of process state and output can be calculated recursively until $k + j$ according to:

$$\hat{x}(k+j|k) = A^j x(k) + \sum_{i=0}^{j-1} A^{j-i-1} B\Delta u(k+i) \tag{3.2}$$

$$\hat{y}(k+j|k) = CA^j x(k) + \sum_{i=0}^{j-1} CA^{j-i-1} B\Delta u(k+i) + D\Delta u(k+j) \tag{3.3}$$

Considering a prediction horizon of N_p and a control horizon of $N_c \leq N_p$, the future state and output predictions are given by:

$$
\underbrace{\begin{bmatrix} \hat{x}(k+1|k) \\ \hat{x}(k+2|k) \\ \vdots \\ \hat{x}(k+N_p|k) \end{bmatrix}}_{\hat{\mathbf{x}}} = \underbrace{\begin{bmatrix} A \\ A^2 \\ \vdots \\ A^{N_p} \end{bmatrix}}_{\mathbf{A}} x(k) +
$$
$$
\underbrace{\begin{bmatrix} B & 0 & \cdots & 0 \\ AB & B & \cdots & 0 \\ \vdots & \vdots & \ddots & \vdots \\ A^{N_p-1}B & A^{N_p-2}B & \cdots & \sum_{i=0}^{N_p-N_c} A^i B \end{bmatrix}}_{\mathbf{B}} \underbrace{\begin{bmatrix} \Delta u(k) \\ \Delta u(k+1) \\ \vdots \\ \Delta u(k+N_p-1) \end{bmatrix}}_{\mathbf{u}} \tag{3.4}
$$

$$\underbrace{\begin{bmatrix} \hat{y}(k+1|k) \\ \hat{y}(k+2|k) \\ \vdots \\ \hat{y}(k+N_p|k) \end{bmatrix}}_{\hat{\mathbf{y}}} = \underbrace{\begin{bmatrix} CA \\ CA^2 \\ \vdots \\ CA^{N_p} \end{bmatrix}}_{\mathbf{C}} x(k) +$$

$$\underbrace{\begin{bmatrix} CB & D & \cdots & 0 \\ CAB & CB & \cdots & D \\ \vdots & \vdots & \ddots & \vdots \\ CA^{N_p-1}B & CA^{N_p-2}B & \cdots & \sum_{i=0}^{N_p-N_c} CA^i B \end{bmatrix}}_{\mathbf{D}} \underbrace{\begin{bmatrix} \Delta u(k) \\ \Delta u(k+1) \\ \vdots \\ \Delta u(k+N_p-1) \end{bmatrix}}_{\mathbf{u}}$$

$$(3.5)$$

or in a condensed form:

$$\hat{\mathbf{x}} = \mathbf{A}x(k) + \mathbf{B}\mathbf{u} \tag{3.6}$$

$$\hat{\mathbf{y}} = \mathbf{C}x(k) + \mathbf{D}\mathbf{u} \tag{3.7}$$

It should be emphasized that the prediction computation depends on the state vector measurement. As in many cases is not possible to obtain these variables directly, a state observer based on Kalman Filter can be used [17].

3.1.2   Objective Function

The various MPC algorithms use different cost functions for computing the control law. The most common objective is to minimize the error between the future output y and desired reference w penalizing the control increment Δu. The standard expression for this objective function is:

$$J = \sum_{l=N_1}^{N_p} \|\hat{y}(k+l|k) - \omega(k+l)\|_Q^2 + \sum_{l=1}^{N_c} \|\Delta \hat{u}(k+l-1)\|_R^2 \tag{3.8}$$

where N_1 e N_p are the minimum and maximum prediction horizons while N_c is the control horizon. In this work the same horizons for

all inputs and outputs was used. These indexes define the limits in which it is desirable for the output to follow the reference and when it is important to limit the control action. These horizons may be used to compensate transmission delays and non-minimum phase. Changing N_c is possible to adjust the time instants where control action is penalized. Q and R are real matrices used to weight error and control effort.

In some systems it is possible to know future values of the reference. For these systems MPC may use this data to compute the control law and allow the system to achieve quickly the new desired value. The reference vector $\omega(k + l)$ used in the objective function does not necessarily coincide with the current reference system. Typically, in practical applications, strategies are used to soften the reference changes, similar to the filters used in classical two-degree-of-freedom control structures.

In practice all processes are subject to constraints. The actuators have a limited field of action and a determined slew rate. Constructive reasons, safety or environmental ones can cause limits in the process variables as states and outputs. The operational conditions are normally defined by the intersection of certain constraints, so that the control system will operate close to the boundaries. The controller must anticipate and correct these violations so they do not happen, preventing the system being unstable. In this context MPC controllers are effective, since they have the ability to predict possible violations over the prediction horizon including constraints on the optimization problem [17].

Generally, bounds in the amplitude and in the slew rate of the control signal and limits in states and outputs are considered [120]. The solution of the constrained MPC is carried out by minimizing the cost function through quadratic programming (QP) algorithms. These algorithms solve problems like:

$$\min_{u} J = \sum_{l=N_1}^{N_p} \|\hat{y}(t+l|t) - \omega(t+l)\|_Q^2 + \sum_{l=1}^{N_c} \|\Delta\hat{u}(t+l-1)\|_R^2$$

(3.9)

Subject to :

$$x(k+1) = Ax(k) + B\hat{u}(k)$$
$$\hat{y}(k) = Cx(k) + D\hat{u}(k)$$
$$\underline{u} \leq \hat{u}(k+l-1) \leq \overline{u}$$
$$\underline{\Delta u} \leq \hat{u}(k+l) - \hat{u}(k+l-1) \leq \overline{\Delta u}$$
$$\underline{x} \leq \hat{x}(k+l) \leq \overline{x}$$
$$\underline{y} \leq \hat{y}(k+l) \leq \overline{y}$$
$$x(k) = \breve{x}(k)$$

where, hat ($\hat{a}$) over variables is used to denote variables over the prediction horizon, $\underline{a}$ and $\bar{a}$ denote minimum and maximum allowed values respectively, and $\breve{a}$ refers to variables whose values are supposed to be known, for example, initial conditions.

3.1.3   Obtaining the Control Law

To compute the control action the following steps are executed:

1. update the initial conditions $\breve{x}(k)$;

2. compute $\hat{y}(k+l)$ as a function of future control actions;

3. substitute $\hat{y}$ and w in the objective function J;

4. minimize J considering the system dynamics and constraints.

The result is a sequence of control actions that should be applied to the system. It is important to emphasize the concept of receding horizon control, i.e., despite the solution of objective function results in an array of control actions through the horizon, only the first control action will be applied and all control actions will be recalculated in the next step according to new information from the real system.

3.2 Distributed MPC

Large scale networks, like power distribution networks, traffic and transportation systems, water distribution networks, logistic operations networks etc., are the pillars of our modern society. Networks of this type are typically spread in a large geographical area, present a modular structure consisting of many subsystems, have many actuators and sensors and in some cases the dynamics evolves over different time scales [78].

In complex or geographically-spread systems, such as large-scale networks, the distribution of the control effort among local control agents can be a very convenient choice. Also, for most networks, the main obstacle to the centralized control is not only technical, but commercial and/or organizational. Typically, technical issues arise from communication delays and too high computational requirements. Commercial issues include unavailability of information from one network operator to another, restricted control access, and costs of sensors. In many cases, parts of the network belong to different organizations, which makes centralized control impossible to implement. Also, robustness and reliability of the network cannot be guaranteed when a single centralized control agent breaks down [29].

In order to distribute the control effort, the network may suitably be divided into exactly defined subsystems, in order to reduce the dynamic coupling. Once partitioned, the overall control objective can be distributed between local control agents, depending on the control structure and the selected communication protocol. This distributed approach results in multi-agent control structures.

The modular nature simplifies the system maintenance, allows expansions of the control system and provides robustness in comparison with a centralized controller [71]. On the other hand, distributed controllers present lower performance in comparison with a centralized controller, that depends on the degree of interaction between the local subsystems and the coordination mechanisms between the agents [71].

In the last years many distributed control techniques were proposed in literature ([71], [72], [79], [1], [18], [100], [20]). In [29] many distributed network control structures described in literature ([118], [100], [67], [82]) were compared. From this assessment, the MPC control structure based on Lagrange multipliers (Lag-MPC), presented in ([78],[32]), appears as a suitable solution for the network control problem providing stability and optimality guaranties and good convergence rate. Hereafter the Lag-MPC structure, that will be applied in chapter

5 to the problem of networked microgrids, is presented in detail.

3.2.1 Control Problem

According [78], in a distributed control structure, the control effort is shared by several agents and each agent solves the control problem of its respective sub-network. Considering a generic network composed of a set $\mathcal{N} = 1, \ldots, n_N$ of interconnected sub-networks, and assuming one control agent for each sub-network i, the general network control problem can be seen as a union of local control problems:

$$
\begin{array}{c}
min \\
\hat{\mathbf{x}}_1(k+1) \ldots \hat{\mathbf{x}}_{n_N}(k+1) \\
\hat{\mathbf{u}}_1(k) \ldots \hat{\mathbf{u}}_{n_N}(k) \\
\hat{\mathbf{y}}_1(k) \ldots \hat{\mathbf{y}}_{n_N}(k)
\end{array}
\qquad \sum_{i=1}^{n_N} J_{local,i}\left(\hat{\mathbf{x}}_i(k+1), \hat{\mathbf{u}}_i(k), \hat{\mathbf{y}}_i(k)\right)
\qquad (3.10)
$$

subject to local dynamics:

$$
\begin{aligned}
x_i(k+1) &= A_i x_i(k) + B_i u_i(k) + B_{qi} q_i(k) + \Pi_{in1,i\leftarrow j} w_{in,i\leftarrow j}(k) & (3.11) \\
y_i(k) &= C_i x_i(k) + D_i u_i(k) + D_{qi} q_i(k) + \Pi_{in2,i\leftarrow j} w_{in,i\leftarrow j}(k) & (3.12) \\
w_{out,i\rightarrow j}(k) &= \Pi_{out,i\rightarrow j} y_i(k) & (3.13)
\end{aligned}
$$

the process constraints:

$$
\begin{aligned}
\underline{x}_i &\leq \hat{x}_i(k+l+1) \leq \overline{x}_i & (3.14) \\
\underline{u}_i &\leq \hat{u}_i(k+l) \leq \overline{u}_i & (3.15) \\
\underline{y}_i &\leq \hat{y}_i(k+l) \leq \overline{y}_i & (3.16) \\
x_i(k) &= \breve{x}_i(k) & (3.17)
\end{aligned}
$$

and the interconnecting constraints

$$
\begin{aligned}
w_{in,i\leftarrow j}(k) &= w_{out,j\rightarrow i}(k) & (3.18) \\
w_{out,i\rightarrow j}(k) &= w_{in,j\leftarrow i}(k) & (3.19)
\end{aligned}
$$

where the sub-index j denotes the neighbor networks.

A typical choice for the local objective function is [78]:

$$
J_{local,i}\left(\hat{\mathbf{x}}_i(k+1), \hat{\mathbf{u}}_i(k), \hat{\mathbf{y}}_i(k)\right) = \qquad (3.20)
$$

$$
\sum_{l=0}^{N_p-1} \begin{bmatrix} \hat{x}_i(k+l+1) \\ \hat{u}_i(k+l) \\ \hat{y}_i(k+l) \end{bmatrix}^T Q_i \begin{bmatrix} \hat{x}_i(k+l+1) \\ \hat{u}_i(k+l) \\ \hat{y}_i(k+l) \end{bmatrix} + f_i^T \begin{bmatrix} \hat{x}_i(k+l+1) \\ \hat{u}_i(k+l) \\ \hat{y}_i(k+l) \end{bmatrix}
$$

where Q_i is a positive definite weighting matrices and f_i is a weighting

vector.

3.2.2 Information Exchange

As the use of a multi-agent control structure implies the information exchange between agents, it is important to analyse and choose the best way of how these agents communicate. According to [80],[81] an agent can use different schemes for communication and decision making:

- synchronous/asynchronous;

- iterative/non-iterative;

- serial/parallel.

In a synchronous communication scheme each agent has to wait for the rest until all of them have finished the current stage calculations. On the other hand, in asynchronous communication each agent runs at its own speed, sending and receiving information and determining what actions should be performed at any time. This mode is potentially faster than synchronous one but the price to pay is the uncertainty of the information updated from neighbouring agents.

Non-iterative communication protocols need smaller amount of information exchange and are potentially faster than iterative schemes, since the time required to take a decision is smaller and only one iteration is performed. However, iterative communication schemes can potentially achieve solutions closer to the ideal. As the information exchange is carried out during the solution of local control problems, it is possible to satisfy the interconnection constraints.

In parallel communication schemes all agents perform the calculating step at the same time, unlike the serial schemes in which there is only one agent, per time step, solving its local control problem. Parallel schemes are potentially faster than serial schemes, but the serial schemes ensure that agents receive the most updated information from its neighbours.

Synchronous communication have been widely studied in literature, such as synchronous non-iterative parallel schemes ([34], [60], [65]) and both serial and parallel synchronous iterative schemes ([18], [50], [61], [78]). The multi-agent control structure discussed in this thesis uses synchronous iterative parallel communication, which is the most developed and utilized communication scheme in literature to solve large-scale networked control problems.

3.2.3   Lagrange MPC

The Augmented Lagrange MPC used in this thesis was developed in [78]. In MPC control structure based on Lagrange multipliers, the general control problem presented in (3.10) and (3.20) is divided into sub-problems and assigned to local control agents [78]. These agents use an augmented Lagrangian formulation to solve the general control problem. This methodology was first presented in [57] and [94] and later new analytical convergence tests were provided in [8]. In a control scheme based on augmented Lagrange formulation each control agent includes terms related to the interconnection constraints in its objective function. As described in [78] and [80], the set of local solutions obtained through an iterative process at each sampling period k is equivalent to the optimal solution calculated in a centralized way. Following is presented the Augmented Lagrange MPC formulation proposed by [78] to be implemented with a parallel communication protocol.

In order to divide the general network problem into local sub-problems, the interconnecting constraints in (3.18), for all control agents $i = 1, \ldots, n_N$, are removed from the set of constraints and added to the objective function in such a way that the following augmented Lagrange function is obtained:

$$
\begin{aligned}
&J_{aug}\left(\hat{\mathbf{x}}(k+1), \hat{\mathbf{u}}(k), \hat{\mathbf{y}}(k), \hat{\mathbf{w}}_{in}(k), \hat{\mathbf{w}}_{out}(k), \hat{\boldsymbol{\lambda}}_{in}(k)\right) \\
&= \sum_{i=1}^{n_N} \Big[J_{local,i}\left(\hat{\mathbf{x}}_i(k+1), \hat{\mathbf{u}}_i(k), \hat{\mathbf{y}}_i(k)\right) \\
&\quad + \sum_{j \in \mathcal{N}_i} \left(\hat{\boldsymbol{\lambda}}_{in,i,j}(k)^T \left(\hat{\mathbf{w}}_{in,i \leftarrow j}(k) - \hat{\mathbf{w}}_{out,j \rightarrow i}(k)\right)\right. \\
&\quad + \frac{\gamma_c}{2} \left\| \hat{\mathbf{w}}_{in,i \leftarrow j}(k) - \hat{\mathbf{w}}_{out,j \rightarrow i}(k) \right\|_2^2 \Big]
\end{aligned} \tag{3.21}
$$

with

$$
\begin{aligned}
\hat{\mathbf{w}}_{in}(k) &= \left[\hat{w}_{in,1}(k)^T, \ldots, \hat{w}_{in,n_N}(k)^T \right]^T \\
\hat{\mathbf{w}}_{out}(k) &= \left[\hat{w}_{out,1}(k)^T, \ldots, \hat{w}_{out,n_N}(k)^T \right]^T \\
\hat{\boldsymbol{\lambda}}_{in}(k) &= \left[\hat{\lambda}_{in,1}(k)^T, \ldots, \hat{\lambda}_{in,n_N}(k)^T \right]^T,
\end{aligned}
$$

where γ_c is a positive constant and $\hat{\lambda}_{in,i}(k)$ are the Lagrange multipliers associated with the interconnections of sub-network $i \in \mathcal{N}$ with its

neighboring sub-networks $j \in \mathcal{N}_i$. Specifically, $\hat{\lambda}_{in,i,j}(k)$ are the Lagrange multipliers related to the constraints $\hat{w}_{in,i\leftarrow j}(k) = \hat{w}_{out,j\rightarrow i}(k)$. Using J_{aug} and by duality theory, the overall control problem can be expressed as:

$$
\max_{\hat{\boldsymbol{\lambda}}_{in}(k)} \left\{ \min_{\substack{\hat{\mathbf{x}}(k+1),\hat{\mathbf{u}}(k),\hat{\mathbf{y}}(k), \\ \hat{\mathbf{w}}_{in}(k),\hat{\mathbf{w}}_{out}(k)}} J_{aug} \left(\begin{array}{c} \hat{\mathbf{x}}(k+1), \hat{\mathbf{u}}(k), \\ \hat{\mathbf{y}}(k), \hat{\mathbf{w}}_{in}(k), \\ \hat{\mathbf{w}}_{out}(k), \hat{\boldsymbol{\lambda}}_{in}(k) \end{array} \right) \right\} \quad (3.22)
$$

subject to sub-network dynamics, constraints and initial conditions.

The optimal solution to problem (3.22) for every instant k is found iteratively by minimizing the objective function with fixed Lagrange multipliers and then updating Lagrange multipliers using the values obtained after the minimization procedure [78]. The ideal solution is found when the Lagrange multipliers converge to new values through an iteration procedure.

This solution is equivalent to the optimal solution of the centralized problem, under assumptions of objective functions convexity and sub-network models affinity [81]. Since these assumptions are satisfied by the objective functions $J_{local,i}$ for all $i \in \mathcal{N}$ and by the sub-network model, both solutions to (3.10) and (3.22) coincide.

Finally, the problem (3.22) must be divided into sub-problems in order to assign them to each of the local control agents. Such a division cannot be directly done due to the presence of quadratic terms in the formulation. In order to approximate the aforementioned non-quadratic terms, the auxiliary problem principle ([6], [66], [98]) was utilized, whose implementation requires a parallel iterative process to be done each time step k, where all the agents perform their local optimization problems at the same time and share between them the results of their computations. This way, the local problem can be written as follows:

$$
\min_{\substack{\hat{\mathbf{x}}_i(k+1),\hat{\mathbf{u}}_i(k),\hat{\mathbf{y}}_i(k), \\ \hat{\mathbf{w}}_{in,i}(k),\hat{\mathbf{w}}_{out,i}(k)}} \begin{array}{l} J_{local,i}\left(\hat{\mathbf{x}}_i(k+1), \hat{\mathbf{u}}_i(k), \hat{\mathbf{y}}_i(k)\right) + \\ J_{inter,i}\left(\hat{\mathbf{w}}_{in,i}(k), \hat{\mathbf{w}}_{out,i}(k)\right) \end{array} \quad (3.23)
$$

where $J_{local,i}$ is the local objective function defined in (3.20) and $J_{inter,i}$

is the following interconnection function:

$$
J_{inter,i}\big(\hat{\mathbf{w}}^{p}_{in,i}(k), \hat{\mathbf{w}}^{p}_{out,i}(k)\big) = \begin{bmatrix} \hat{\boldsymbol{\lambda}}^{p}_{in,i\leftarrow j}(k) \\ \hat{\boldsymbol{\lambda}}^{p}_{out,i\rightarrow j}(k) \end{bmatrix}^{T} \begin{bmatrix} \hat{\mathbf{w}}^{p}_{in,i\leftarrow j}(k) \\ \hat{\mathbf{w}}^{p}_{out,i\rightarrow j}(k) \end{bmatrix} \tag{3.24}
$$

$$
+ \frac{\gamma_c}{2} \left\| \begin{bmatrix} \hat{\mathbf{w}}^{p-1}_{in,j\leftarrow i}(k) - \hat{\mathbf{w}}^{p}_{out,i\rightarrow j}(k) \\ \hat{\mathbf{w}}^{p-1}_{out,j\rightarrow i}(k) - \hat{\mathbf{w}}^{p}_{in,i\leftarrow j}(k) \end{bmatrix} \right\|^{2}_{2}
$$

$$
+ \frac{\gamma_b - \gamma_c}{2} \left\| \begin{bmatrix} \hat{\mathbf{w}}^{p}_{in,i\leftarrow j}(k) - \hat{\mathbf{w}}^{p-1}_{in,i\leftarrow j}(k) \\ \hat{\mathbf{w}}^{p}_{out,i\rightarrow j}(k) - \hat{\mathbf{w}}^{p-1}_{out,i\rightarrow j}(k) \end{bmatrix} \right\|^{2}_{2}
$$

where γ_c and γ_b are positive constants, $\hat{\mathbf{w}}^{p-1}_{in,i\leftarrow j}(k)$ and $\hat{\mathbf{w}}^{p-1}_{out,i\rightarrow j}(k)$ are the own information set of the previous iteration, $\hat{\mathbf{w}}^{p-1}_{in,j\leftarrow i}(k)$ and $\hat{\mathbf{w}}^{p-1}_{out,j\rightarrow i}(k)$ are the information set collected from the neighbouring agent $j \in N_i$ at the previous iteration, the superscript p represents the actual iteration at the time instant k and $\hat{\boldsymbol{\lambda}}^{p}_{in,i\leftarrow j}(k)$ and $\hat{\boldsymbol{\lambda}}^{p}_{out,i\rightarrow j}(k)$ are the Lagrange multipliers.

At each time step k, each local agent must perform the iterative algorithm described below with parallel communication. One of the main drawbacks of Lagrangian methods is the slow convergence [71]. The algorithm convergence speed can be improved through the so-called warm start by initializing the interconnecting inputs and the Lagrange multipliers every step to the values obtained from previous decision step rather than initializing these values arbitrarily. The algorithm is implemented according to the following steps:

1. Make a measurement of current state $\hat{x}_i(k)$

2. Compute the optimal control sequence $\tilde{u}_i^*(k)$. To do so, perform the following steps:

    (a) Parameter initialization:

        • for $k = 0$

$$
\begin{aligned}
p &= 1 \\
e_i &\gg 1 \\
\hat{\boldsymbol{\lambda}}^0_{in,i\leftarrow j}(k) &= 0 \\
\hat{\boldsymbol{\lambda}}^0_{out,i\rightarrow j}(k) &= 0 \\
\hat{\mathbf{w}}^0_{in,i\leftarrow j}(k) &= 0 \\
\hat{\mathbf{w}}^0_{out,i\rightarrow j}(k) &= 0 \\
\hat{\mathbf{w}}^0_{in,j\leftarrow i}(k) &= 0 \\
\hat{\mathbf{w}}^0_{out,j\rightarrow i}(k) &= 0
\end{aligned}
$$

- for $k > 0$ use warm start

$$
\begin{aligned}
\hat{\boldsymbol{\lambda}}^0_{in,i\leftarrow j}(k) &= \hat{\boldsymbol{\lambda}}^p_{in,i\leftarrow j}(k-1) \\
\hat{\boldsymbol{\lambda}}^0_{out,i\rightarrow j}(k) &= \hat{\boldsymbol{\lambda}}^p_{out,i\rightarrow j}(k-1) \\
\hat{\mathbf{w}}^0_{in,i\leftarrow j}(k) &= \hat{\mathbf{w}}^p_{in,i\leftarrow j}(k-1) \\
\hat{\mathbf{w}}^0_{out,i\rightarrow j}(k) &= \hat{\mathbf{w}}^p_{out,i\rightarrow j}(k-1) \\
\hat{\mathbf{w}}^0_{in,j\leftarrow i}(k) &= \hat{\mathbf{w}}^p_{in,j\leftarrow i}(k-1) \\
\hat{\mathbf{w}}^0_{out,j\rightarrow i}(k) &= \hat{\mathbf{w}}^p_{out,j\rightarrow i}(k-1) \\
p &= 1 \\
e_i &\gg 1
\end{aligned}
$$

for all $i \in \mathcal{N}$.

(b) Solve the optimization problem in equation (3.23), subject to local dynamics and constraints.

(c) Send $\hat{\mathbf{w}}^p_{in,i\leftarrow j}(k)$ and $\hat{\mathbf{w}}^p_{out,i\rightarrow j}(k)$ to neighbouring agents $j \in N_i$ and collect $\hat{\mathbf{w}}^0_{in,j\leftarrow i}(k)$ and $\hat{\mathbf{w}}^p_{out,j\rightarrow i}(k)$ from them.

(d) Upgrade the multipliers:

$$
\hat{\boldsymbol{\lambda}}^{p+1}_{in,i\leftarrow j}(k) = \hat{\boldsymbol{\lambda}}^p_{in,i\leftarrow j}(k) + \gamma_c\left(\hat{\mathbf{w}}^p_{in,i\leftarrow j}(k) - \hat{\mathbf{w}}^p_{out,j\rightarrow i}(k)\right) \tag{3.25}
$$

$$
\hat{\boldsymbol{\lambda}}^{p+1}_{out,i\rightarrow j}(k) = \hat{\boldsymbol{\lambda}}^p_{out,i\rightarrow j}(k) + \gamma_c\left(\hat{\mathbf{w}}^p_{out,i\rightarrow j}(k) - \hat{\mathbf{w}}^p_{in,j\leftarrow i}(k)\right) \tag{3.26}
$$

(e) Evaluate the stopping conditions:

$$p > \bar{p} \tag{3.27}$$

$$e_i = \left\| \hat{\boldsymbol{\lambda}}_{in,i\leftarrow j}^{p+1}(k) - \hat{\boldsymbol{\lambda}}_{in,i\leftarrow j}^{p}(k) \right\| \leq \bar{e} \tag{3.28}$$

where $\bar{p}$ is the maximum number of iterations allowed and $\bar{e}$ is the maximum error allowed. If both conditions are false, move on to next iteration $p \to p+1$ and go to step 2b. If (3.27) is true, go to step 3. If (3.28) is true, set agent i termination flag $flag_i(k) = 1$. If all neighboring agents $j \in N_i$ termination flags are equal to 1, go to step 3. If not, move on to next iteration and go to step 2b [78].

3. Implement the optimal control action $\hat{u}_i^*(k)$.

4. Start a new control cycle $k \leftarrow k+1$ and go to step 1.

Selecting $\gamma_b \geq 2\gamma_c$ and ϵ sufficiently small, and due to the fact that the overall control problem is a convex space, the iterative algorithm described above converges to the minimum of the overall network problem.

The positive scalar γ_c penalizes the deviation from the interconnecting variable iterates that were computed during the last iteration. As additional parameter this scheme uses a positive scalar γ_b. If $\gamma_b \geq \gamma_c$, then the term penalizes the deviation between the interconnecting variables of the current iteration and the interconnecting variables of the last iteration of agent i; it thus gives the agent less incentive to change its interconnecting variables from one iteration to the next. When $\gamma_b \geq 2\gamma_c$ and ϵ, and moreover the overall combined problem is convex, it can be proved that the iterations converge toward the overall minimum for sufficiently small $\bar{e}$ ([9], [66]).

3.3   Final Remarks

In this chapter a literature review about centralized and distributed MPC was presented. In the chapter 4 will be presented a DMPC algorithm for hybrid systems.

Chapter 4

Hybrid Distributed MPC

This chapter presents one of the contributions of this thesis. Hybrid systems are a class of dynamical systems whose evolution depends on a coupling between continuous and binary variables. This kind of systems has many applications, for example, in energy management ([31], [82], [12], [75]), in hydrogen production ([103]), in supermarket applications ([99], [107]), in electric vehicles charging ([52]), in process control ([27], [95], [21]) and in traffic light control ([102]).

In [7] a proposal was carried out to generalize MPC to hybrid systems based on Mixed Logical Dynamical (MLD) modeling framework. The solution of the hybrid MPC can be rewritten as a sequence of optimization problems defined as Mixed Integer Quadratic Programming (MIQP), which is computationally complex. The most common methods to solve MIQP problems are cutting-plane methods, decomposition methods, logic-based methods, and branch and bound methods. Several authors report that branch and bound is the most successful method for mixed integer programs [7]. A commonly used commercial software is the solver CPLEX [58].

There are in literature other algorithms to deal with the presence of binary variables. In [102] and [116], the authors use a technique called TIO-MPC (Time Instant Optimization - MPC), where time instants are introduced as control inputs in place of binary variables. The time instants when the changes of the structure state should occur are optimized for a selected number of changes, resulting in a real-valued programming problem. In [99] and [27], a technique is presented that

defines two new continuous manipulated variables for each binary manipulated variable, which corresponds to the duration of the activation/deactivation of the binary variables on the prediction horizon. In this way the original problem is turned into a non-linear optimization with continuous variables that can be solved using Sequential Quadratic Programming (SQP). There are some works in literature focused on distributed MPC to hybrid systems ([56],[13],[40]).

In networked hybrid systems, each subsystem has a certain number of binary variables that describe its discrete state. Let us assume that controller i has nb_i binary variables, which means that the controller can be configured in 2^{nb_i} different ways. Considering that the system is composed by n_N subsystems, from a global point of view, this implies that there are $\prod_{i=1}^{n_N} 2^{nb_i}$ configurations for the binary variables in the system. There are two combinatorial explosions here. One is due to the local binary variables. Another is due to the joint action of the local controllers. All together may make the computation intractable even for systems with a low number of controllers.

In this section an approach is proposed to deal with both combinatorial explosions. First an algorithm is presented to deal with the binary variables of the local controllers. The basic idea is to provide an easy way to solve this kind of problem without a MIQP solver. The proposed technique first decides about the values of the binary variables for each local controller and transforms the optimization problem into a set of quadratic programs (QP). A finite set of instances of each controller is created with the possible solutions.

To overcome the limitations imposed by the second combinatorial explosion, the one derived from the joint action of the controllers, it is assumed that a set of feasible combinations of binary decision variables exists. From a distributed optimization perspective, we have a problem where a set of agents must agree on the value of a set of continuous interconnection variables and the binary variables are computed by each local agent. In this work, we propose to improve the efficiency of this approach by iterating and checking which are the instances with the lowest performance. These instances are penalized at the next iteration step so that their impact in the cost function is reduced. Likewise, the instances with the best cost are rewarded with a higher weight in the overall optimization. Eventually, some of the instances are dismissed, e.g., when their weight is below a certain threshold or simply 0. This procedure is repeated until there is only one instance left in each instance set or after a certain number of iterations has been achieved. In this last case the instance with the optimal cost is chosen and its

value is assigned to the binary variables of the subsystem. In this way a solution for the hybrid DMPC problem can be attained.

4.1 Problem setting

Consider a generic network composed of a set $\mathcal{N} = 1, 2, \ldots, n_N$ of n_N interconnected sub-networks. The dynamics of each sub-network can be described by the following MLD equations:

$$x(k+1) = Ax(k) + B_1 u(k) + B_2 \delta(k) + B_3 z(k) + D_{q1} q(k) + \Pi_{in1} w_{in, i \leftarrow j}(k) \tag{4.1}$$

$$y(k) = Cx(k) + D_1 u(k) + D_2 \delta(k) + D_3 z(k) + D_{q2} q(k) + \Pi_{in2} w_{in, i \leftarrow j}(k) \tag{4.2}$$

$$w_{out, i \rightarrow j}(k) = \Pi_{out} y(k) \tag{4.3}$$

$$E_2 \delta(k) + E_3 z(k) \leq E_1 u(k) + E_4 x(k) + E_5 \tag{4.4}$$

where $x(k) = \begin{bmatrix} x_c(k) & x_l(k) \end{bmatrix}^{\mathrm{T}}$ is the state vector with $x_c(k) \in \Re^{n_c}$ and $x_l \in \{0, 1\}^{n_l}$, $y(k) = \begin{bmatrix} y_c(k) & y_l(k) \end{bmatrix}^{\mathrm{T}}$ is the output vector with $y_c(k) \in \Re^{p_c}$ and $y_l(k) \in \{0, 1\}^{p_l}$, $u(k) = \begin{bmatrix} u_c(k) & u_l(k) \end{bmatrix}^{\mathrm{T}}$ is the input vector with $u_c(k) \in \Re^{m_c}$ and $u_l(k) \in \{0, 1\}^{m_l}$, $q(k)$ is a disturbance vector, $w_{in, i \leftarrow j}(k)$ is a vector of input interconnected variables, $w_{out, i \rightarrow j}(k)$ is a vector of output interconnected variables, $z(k) \in \Re^{r_c}$ are the continuous auxiliary variables, $\delta(k) \in \{0, 1\}^{r_l}$ are the binary auxiliary variables, A, B_1, B_2, B_3, C, D_1, D_2, D_3, D_{q1}, D_{q2}, Π_{in1}, Π_{in1}, Π_{out}, E_1, E_2, E_3 and E_4 are constant real matrices, E_5 is a real vector, $n_c > 0$ and $p_c, m_c, r_c, n_l, p_l, m_l, r_l > 0$.

In this case, it is assumed that $z(k)$ is defined as a product between $\delta(k)$ and $u(k)$. This product is expressed by the mixed-integer linear inequalities in (4.4), by using propositional logic, as explained in chapter 2. The local objective function and constraints are the same as the ones defined in (3.20) and (3.14).

4.2 Hybrid DMPC Framework

The optimization problem formulated previously includes binary and continuous manipulated variables that characterize a mixed integer optimization. In this section a framework to deal with this kind of problems in a distributed fashion will be presented. The proposed algorithm is one of the contributions of this thesis. The main idea is to determine a set of possible solutions for the binary variables and create controller instances related to these solutions. These instances

are tested by a competitive rule in an iterative procedure until the best
solution is found.

4.2.1   Binary Search Algorithm

For each physical binary condition in a subsystem there are N_p
variables related to the prediction horizon. Taking into account that in
a subsystem i there exist nb_i physical binary conditions, the total num-
ber of binary variables in the optimization problem is $nb_i \times N_p$, which
results in $2^{nb_i \times N_p}$ possible instances of the local controller. In practice,
this number can be reduced using some heuristics. For example it could
be assumed that the configuration should not change drastically from
one time instant to another, or that there are no changes in the value
of the binary variables after a few steps in the horizon. Another way
to deal with binary variables is performing a binary search over the
prediction horizon. The controller instances are defined considering all
possible combinations of the binary variables of the first two elements of
the horizon and assuming the remaining control actions to be constant
and equal to the second instant.

Thus,

$$\delta = \delta_{fix} \tag{4.5}$$
$$z = \delta_{fix} \times u \tag{4.6}$$

where δ_{fix} is a matrix with fixed values for all binary variables. This
procedure transforms the original optimization problem into a QP as
the binary variables are known.

After solving the QP problems for the controller instances, a per-
formance index, for example the objective function cost, is analyzed.
The instance that provides the best performance index is fixed for the
first horizon instant and the next two time instants are tested. This
procedure is repeated until the end of the prediction horizon or can be
truncated in a certain instant called binary decision horizon N_b, which
should be lower or equal than the prediction horizon.

A previous simulation study to investigate the algorithm behavior
for different values of N_b is recommended. According to the parsimony
principle the best choice is one that provides a good compromise be-
tween the number of iterations, the calculation time, the number of
changes through the prediction horizon for binary variables, and the
performance. Depending on the nature of the application, this algo-
rithm can be applied to all binary variables together or independently,

and leads a set of $4 \times N_b$ or $4 \times N_i \times N_b$ controller instances respectively. Algorithm 1 shows, the implementation used to solve the optimization problem with all binary variables together.

Algorithm 1 Binary Search Algorithm

Input: Nb
Output: CI,FCI,FIX

    Initialization :
    $FIX = []$;
    LOOP Process

2: **for** $i = 1$ to N_b **do**

    if $i = 1$ {First instant} **then**

4:       Define $\delta_{fix} = \begin{bmatrix} 0 & \mathbf{0}_{\{1 \times N_p - 1\}} \\ 0 & \mathbf{1}_{\{1 \times N_p - 1\}} \\ 1 & \mathbf{0}_{\{1 \times N_p - 1\}} \\ 1 & \mathbf{1}_{\{1 \times N_p - 1\}} \end{bmatrix}$

    else

6:       Define $\delta_{fix} = \begin{bmatrix} FIX & 0 & \mathbf{0}_{\{1 \times N_p - i\}} \\ FIX & 0 & \mathbf{1}_{\{1 \times N_p - i\}} \\ FIX & 1 & \mathbf{0}_{\{1 \times N_p - i\}} \\ FIX & 1 & \mathbf{1}_{\{1 \times N_p - i\}} \end{bmatrix}$

    end if

8:     **for** $j = 1$ to 4 **do**

      Solve the optimization problem for $\delta_{fix\{j,1...Np\}}$

10:       Compute the objective function cost C_j

      Compute the controller instance $CI_{i,j}$.

12:     **end for**

    Analyze C_j and choose the minimum cost $C_{min} = \min C_j$

14:     Update FIX with the value of δ_{fix} that corresponds to C_{min}

    end for

16: With all values of δ_{fix} defined, compute the Final Controller Instance (FCI).

4.2.2   Distributed Coordination

    In this sub-section an algorithm for the coordination of a set of local controllers with continuous and binary decision variables is presented. In particular, the binary decision variables at each local controller are relaxed from the original MIQP problem by considering an instance of the controller for each feasible combination of them. The

number of initial controller instances can be reduced by using the algorithm presented in subsection 4.2.1. Then, a standard distributed control problem in which a set of agents must agree on the value of continuous decision variables is used iteratively.

At each iteration, the instances with lowest expected performance are penalized and those with the best expected performance are rewarded by modifying their corresponding weights in the overall optimization problem. Eventually, instances leading to the worst performance are dropped at each local controller. A way to determine which instances will be dropped is to compute a cutoff index that consists in the middle point between the minimum and the maximum costs obtained by all active instances in current iteration. The process continues until there is only one instance at each local controller. The value of the binary variables of the corresponding instance is then implemented in the system. This procedure is applied at each sampling period. One important characteristic of the proposed methodology is that during the iterations the computational effort decreases proportionally to the decreasing of possible instances, on the other hand, this algorithm does not guarantee the solution optimality. These steps are formalized in Algorithm 2.

Algorithm 2 Distributed Coordination Algorithm

Input: *iteration*
Output: BCI
    if *iteration* $= 1$ {First iteration} **then**
2:    Solve the optimization problem using the binary search algorithm
      Save the initial set of controller instances SCI
4: **else**
      Compute the cost vector C with all active controller instances in SCI
6:    Determine the minimum C_{min} and maximum C_{max} costs of C
      Compute cutoff index $I = 0.5C_{min} + 0.5C_{max}$
8:    Deactivate the instances in SCI with higher costs than the cutoff index
      Apply the instance with best cost BCI
10:   Repeat this procedure until the convergence of the distributed algorithm
    end if

4.2.3   Algorithm Convergence

In order to investigate the convergence and optimality properties of the proposed algorithm, a simulation analysis was performed. The system under study is a generic network composed by two identical sub-networks containing one binary variable. The sub-networks are interconnected through two interconnection variables, and represented by equations (4.1 - 4.4) with the following matrices:

$$u = \begin{bmatrix} u_1 & u_2 & w_{out,i \to j} & w_{in,i \leftarrow j} & \delta & z \end{bmatrix}^T$$

$$A = 1 \quad D_{q1} = D_{q2} = C = 0 \quad \Pi_{out} = \begin{bmatrix} 0 \\ 1 \end{bmatrix}$$

$$B = \begin{bmatrix} B_1 \\ \Pi_{in1} \\ B_2 \\ B_3 \end{bmatrix}^T = \begin{bmatrix} 0 & 23.75 & 0 & 0 & 0 & -0.75 \end{bmatrix}$$

$$D = \begin{bmatrix} D_1 \\ \Pi_{in2} \\ D_2 \\ D_3 \end{bmatrix}^T = \begin{bmatrix} 1 & -1 & -1 & 1 & 0 & 0 \\ 0 & 0 & 1 & 0 & 0 & 0 \end{bmatrix}$$

Each local controller uses the following objective function:

$$
\begin{aligned}
J_{local} =\ & \sum_{l=0}^{N_p-1} \hat{u}(k+l)^T Q \hat{u}(k+l) \\
& + \sum_{l=0}^{N_p-1} \left(\hat{x}(k+l) - \hat{x}_{ref}(k+l) \right)^T Q_x \left(\hat{x}(k+l) - \hat{x}_{ref}(k+l) \right) \\
& + \sum_{l=0}^{N_p-1} \left(\hat{u}(k+l) - \overline{u} \right)^T Q_e \left(\hat{u}(k+l) - \overline{u} \right)
\end{aligned}
\tag{4.7}
$$

subject to local dynamics (4.1) and (4.4) and following constraints:

$$\underline{x} \leq \hat{x}(k+l+1) \leq \overline{x} \tag{4.8}$$

$$\underline{u} \leq \hat{u}(k+l) \leq \overline{u} \tag{4.9}$$

$$\hat{y}(k+l) = y_{dem}(k) \tag{4.10}$$

$$x(k) = \breve{x}(k) \tag{4.11}$$

for $l = 0, \ldots, N_p - 1$, where Q, Q_x, Q_e are positive definite weighting matrices, and N_p is the prediction horizon. With respect to the notation, hat ($\hat{a}$) over variables is used to denote variables over the prediction horizon, $\underline{a}$ and $\bar{a}$ denote minimum and maximum allowed

values respectively, and $\breve{a}$ refers to variables whose values are supposed to be known, for example, the initial conditions.

A simulation with 24 steps was performed using the software Matlab [74] with Yalmip toolbox [69] and the solver CPLEX [58]. A prediction horizon of $N = 6$ was used totalizing 6 binary variables per sub-network, i.e., 2^6 possible instances to the local controller, which results in $\prod_{i=1}^{2} 2^6$ configurations for the binary variables in the global optimization problem.

First, the differences between the use of binary search algorithm (BS) and binary search with distributed coordination (BSDC) are investigated. A simulation analysis to determine the influence of N_b, testing $N_b = 1$ until $N_b = 6$ was performed. Figure 4.1 shows the number of iterations for each time instant and the calculation time for each N_b. The number of iterations varies between 206 and 207 for BS and 213 and 217 for BSDC, and the calculation time increases with N_b. The BSDC provides the solution with less time than BS for all values of N_b, which may be explained by the exclusion of instances that do not have good performance during the iteration procedure. This way the number of optimization problems tested at each iteration is reduced. Both algorithms presented similar dynamical behavior for all values of N_b, as can be seen in Figure 4.2. In this case, $N_b = 1$ was chosen because it provided the best compromise between the number of iterations and the calculation time.

Table 4.1 presents a comparison between the BS, the BSDC (both using $N_b = 1$), the centralized MIQP (CMIQP) solved by the CPLEX branch and bound solver and the all instances possible combinations (COMB). As expected, the computation time expended by BSDC was smaller than BS and COMB, and closer to CMIPQ. Assuming that the CMIPQ is the best solution that can be computed, the total and the average costs can be used to compare the algorithms with respect to the distance from the optimum. All algorithms presented similar costs, but BS obtained the closest solution while BSDC obtained the farthest. It is possible that, for one specific time instant, the exclusion of the worst performance instances performed by BSDC can miss untimely an instance that can probably be the best at the end of iteration procedure when compared to BS. In despite of the proposed Hybrid DMPC being a suboptimal algorithm, the reduction in calculation time provided by BSDC can be useful in applications with a great number of binary variables.
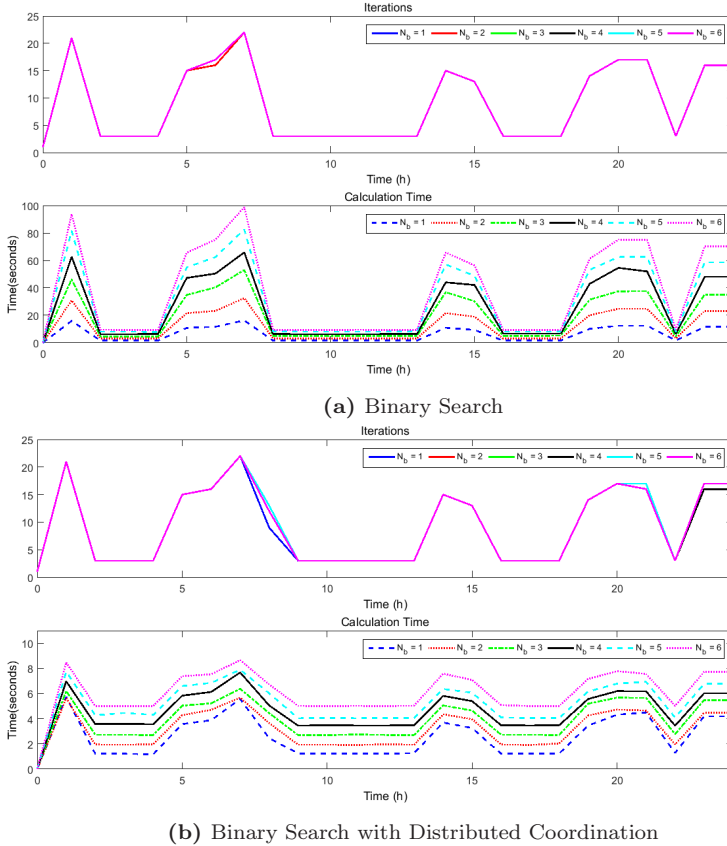
(a) Binary Search

(b) Binary Search with Distributed Coordination

Figure 4.1: Number of iterations and calculation time varying N_b.

4.3 Final Remarks

In this chapter an hybrid DMPC framework was presented as a contribution of this thesis and a discussion about convergence and optimality was performed. In the chapter 5 these algorithms will be applied to a microgrid energy management.
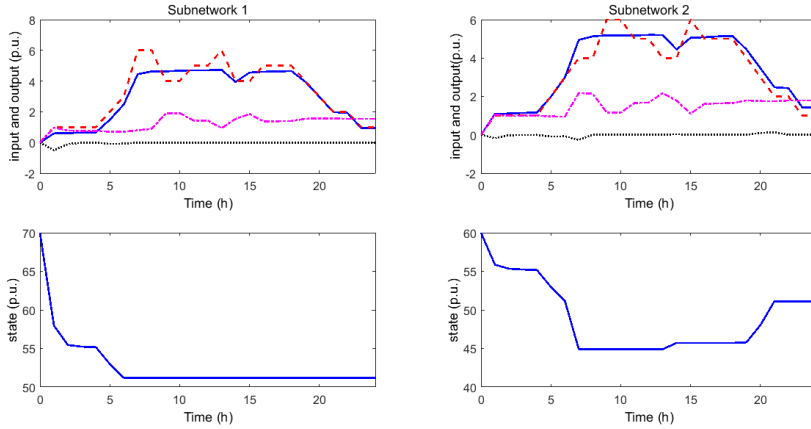
Figure 4.2: Input, output and state variables. (blue - u_1, red - y, black - u_2, magenta - w_{out})

Table 4.1: Performance Indexes

	BS	$BSDC$	$CMIQP$	$COMB$
Total Iterations	206	213	—	207
Total time (s)	35.44	14.85	3.23	2266.9
Average time (s)	1.48	0.62	0.14	94.45
Total cost	402.99	405.25	402.82	403.22
Average cost	16.79	16.88	16.78	16.80

Chapter 5

Microgrid Control

This chapter presents some concepts of microgrid control. First the different control levels are discussed. Then a two level MPC algorithm is applied to a laboratory microgrid, and different weather conditions are tested. Finally the problem of optimization of networked microgrids is discussed and a Hybrid distributed MPC is applied.

5.1 Energy Management in Microgrids

A microgrid is a concept which refers to a small-scale power system with a cluster of loads and distributed generators operating together with energy management, control and protection devices and associated software [111]. A microgrid can be a DC [124], AC or even a high frequency AC grid [19] and hybrid AC/DC [110].

Microgrids are planned to operate in grid-connected and/or islanded mode. For each operating mode operational requirements are different and distinct control schemes are required [111]. In grid-connected scenario, the microgrid sells/purchases energy with the Distribution Network Operator (DNO), which usually produces energy from fossil energy sources. Minimize the amount of energy purchased from DNO is an important goal to reduce greenhouse gas emissions and promote sustainable consumption practices. An interesting alternative is to connect neighboring microgrids in a network so to cooperate each other [87].

A crucial issue in microgrid operation is the use of energy storage, that allows to compensate imbalances between consumption and generation and ensure the energy quality. According to ([38]) and ([54]) the possibility of hybridization among several energy storage technologies is

of great interest. In this chapter, the combination of hydrogen storage together with electric batteries is used to reduce the energy fluctuation and store energy in an experimental microgrid.

From the control point of view, many authors ([16], [70], [117], [10], [86], [90], [89], [110]) agree on the existence of three control levels. The primary level operates on a fast time scale and maintains the voltage and frequency stability during changes on the generation or load or after switching to the island mode. This control is implemented locally. The secondary level is responsible for ensuring that the voltage and frequency deviations are adjusted to zero after a load or generation change is produced within the microgrid. It is responsible to eliminate any steady-state error introduced by the primary control and is also used for synchronization with the DNO during the transition from island mode to grid connection.

The third level is related to energy management system (EMS) and is the main topic of this thesis. This tertiary control is used to control the power flow between the microgrid and the DNO and for the optimal operation on large time scales. This level may include many optimization strategies, according to the time scales, and it includes planning and economic dispatch. For a single microgrid the energy management is usually done by a microgrid central controller (MGCC). In case of networked microgrids a good solution is to use an agent-based distributed EMS.

5.2 Laboratory Microgrid Control

This section presents an economic optimization of a laboratory microgrid located at the University of Seville (US), Spain. The system modeling was carried out using the Energy Hubs methodology.

A hierarchical control structure is proposed based on Model Predictive Control and acting in different time scales, where the first level is responsible for maintaining the microgrid stability and the second level has the task of performing the management of electricity purchase and sale to the power grid, maximize the use of renewable energy sources, manage the use of energy storage units and perform the charge of the parked vehicles. Practical experiments were performed with different weather conditions of solar irradiation and wind.

5.2.1 V2G Experimental Microgrid

In this work the experiments were carried out at HyLab microgrid connected to an electric vehicle charging system. This microgrid was designed to study control strategies applied to energy management of a network based on renewable energy sources and hydrogen storage ([112], [113], [114]). The facility has special features that allow the implementation and study of different operating modes and control strategies. Figure 5.1 shows the outline of the studied system.
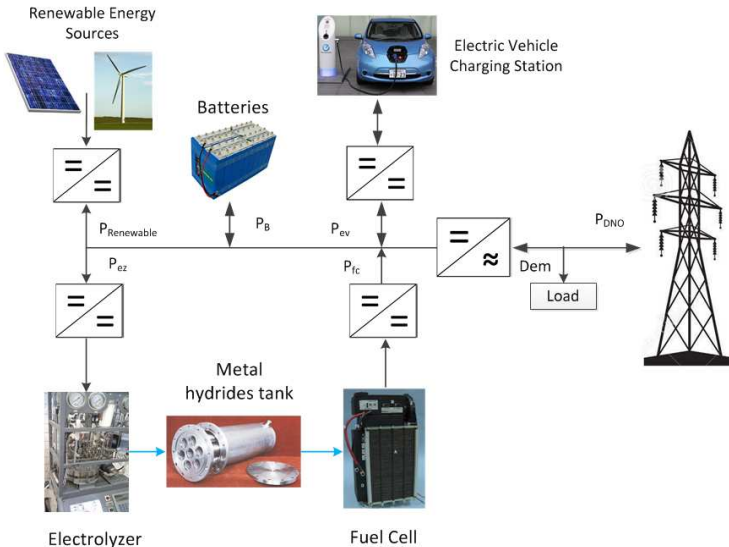
Figure 5.1: Hylab microgrid

To replicate renewable energy systems, the microgrid has a programmable power supply that can emulate the dynamic behavior of a wind turbine and/or a photovoltaic field. It also includes a battery bank, an electronic load to emulate different consumption systems and, finally, includes a hydrogen storage system comprising a PEM (Proton Exchange Membrane) electrolyzer to produce hydrogen, a metal hydride tank to store hydrogen and PEM fuel cell to produce energy. The electric car charging station has the capacity to charge four cars simultaneously. The charging station was emulated by a hardware-in-the-loop methodology. The dynamics of the electric vehicle batteries were simulated by a Simulink model and interfaced with the microgrid through the programmable power supply and the electronic load. The

technical characteristics of the equipments are summarized in table 5.1.

Table 5.1: Microgrid Units

Equipment	Nominal Value
Programmable Power Supply	6kW
Electronic Load	2.5kW
Electrolyzer	$0.23\text{Nm}^3/\text{h}$ at 1kW
Metal Hydride Tank	7Nm^3 at 5bar
Fuel Cell	1.5kW at 20Nl
Battery Bank	$C120 = 367\text{Ah}$

From the microgrid operation point of view, usually the energy produced does not match the demand. Then, the excess of energy from renewable sources can be stored in batteries or used to produce hydrogen through electrolysis. The hydrogen produced is stored in the metal hydride tank. Finally, when power from renewable sources is not available, the fuel cell uses hydrogen to supplement the lack of demand. Additionally, the microgrid has a connection to the DNO allowing the energy purchase and sale. The hybrid storage allows operation strategies on two time scales: the battery can absorb/provide small amounts of energy on fast transients while hydrogen storage supplements bigger oscillations. In this sense, when the cars are parked, their batteries can be used by the microgrid to expand the buffer capacity during fast transients. The idea of the control system is then to compute the different powers $P_{Renewable}$ (the generated renewable energy power), P_{DNO} (the power exchanged with the DNO), P_B (the power of the battery bank), P_{H2} (the power of the hydrogen storage) and P_{Bev1}, P_{Bev2}, P_{Bev3}, P_{Bev4} (the powers of vehicle batteries) in such a way that the performance of the overall system is optimized.

5.2.2 System Modeling

In this section, the methodology presented in chapter 2 is applied to the microgrid and electric vehicles charging station modeling. As the battery bank is considered to have the same charging/discharging efficiency it is not necessary to define binary variables for it. The batteries of electric vehicles are modeled in the same way as the microgrid battery bank, however a binary variable ϵ is added, which is directly related to the physical connection between the vehicle and the charging station. This variable provides a change in the prediction model

without using an hybrid modeling, as the value of ϵ is informed by the vehicle connection and is not a decision variable. If the vehicle is connected $\epsilon = 1$ and a state related to electric vehicle battery SOC is enabled in the prediction model; if it is not $\epsilon = 0$, and the state is disabled. The final state equation of the electric cars batteries is

$$x(k+1) \quad = \quad \epsilon x(k) + \epsilon \Lambda u(k) \tag{5.1}$$

To model the hydrogen storage dynamics it is necessary to define the variable $z_{H2}(k) = P_{H2}(k)\delta_{H2}(k)$ that is related to charging/discharging the hydrogen storage. To manage the purchase and sale of energy to the DNO, different weights for sale and purchase were used. To make this possible a new variable $z_{DNO}(k) = P_{DNO}(k)\delta_{DNO}(k)$ was defined and the corresponding MLD constraints were introduced. Thus, the complete decision vector (manipulated variables) is:

$$u = \begin{bmatrix} u^L \\ u^E \\ \delta \\ z \end{bmatrix} = \begin{bmatrix} P_{Renewable} \\ P_{DNO} \\ \hline P_B \\ P_{H2} \\ P_{Bev1} \\ P_{Bev2} \\ P_{Bev3} \\ P_{Bev4} \\ \hline \delta_{H2} \\ \delta_{DNO} \\ \hline z_{H2} \\ z_{DNO} \end{bmatrix} \tag{5.2}$$

The model in equation (2.39) can be rewritten in a condensed form:

$$x(k+1) = Ax(k) + \Lambda u(k) \tag{5.3}$$
$$y(k) = \Gamma u(k)$$

$$A = \begin{bmatrix} 1 & 0 & 0 & 0 & 0 & 0 \\ 0 & 1 & 0 & 0 & 0 & 0 \\ 0 & 0 & \epsilon_1 & 0 & 0 & 0 \\ 0 & 0 & 0 & \epsilon_2 & 0 & 0 \\ 0 & 0 & 0 & 0 & \epsilon_3 & 0 \\ 0 & 0 & 0 & 0 & 0 & \epsilon_4 \end{bmatrix}$$

$$\Lambda = \left[\begin{array}{cc|cccccc|cc|cc} 0 & 0 & \lambda_1 & 0 & 0 & 0 & 0 & 0 & 0 & 0 & 0 & 0 \\ 0 & 0 & 0 & \lambda_2 & 0 & 0 & 0 & 0 & 0 & 0 & \lambda_3 & 0 \\ 0 & 0 & 0 & 0 & \lambda_4 & 0 & 0 & 0 & 0 & 0 & 0 & 0 \\ 0 & 0 & 0 & 0 & 0 & \lambda_5 & 0 & 0 & 0 & 0 & 0 & 0 \\ 0 & 0 & 0 & 0 & 0 & 0 & \lambda_6 & 0 & 0 & 0 & 0 & 0 \\ 0 & 0 & 0 & 0 & 0 & 0 & 0 & \lambda_7 & 0 & 0 & 0 & 0 \end{array} \right]$$

$$\lambda_1 = \eta_B \qquad \lambda_2 = \eta_{H_2,e}^{FC} \qquad \lambda_3 = \eta_{e,H_2}^{E} - \eta_{H_2,e}^{FC}$$

$$\lambda_4 = \epsilon_1 \eta_{Bev1} \quad \lambda_5 = \epsilon_2 \eta_{Bev2} \qquad \lambda_6 = \epsilon_3 \eta_{Bev3} \qquad \lambda_7 = \epsilon_4 \eta_{Bev4}$$

$$\Gamma = \left[\begin{array}{cc|cccccc|cc|cc} \eta_{rad,e}^{S} & 1 & -1 & -1 & -1 & -1 & -1 & -1 & 0 & 0 & 0 & 0 \end{array} \right]$$

where η is the storage and conversion efficiency, $P_{Renewable}$ is the generated renewable energy power, P_{DNO} is the power exchanged with the DNO, P_B is the power of the battery bank, P_{H2} is the power of the hydrogen storage and P_{Bev1}, P_{Bev2}, P_{Bev3} and P_{Bev4} are the powers of vehicle batteries. The states are the battery bank SOC (state of charge), the MHL (metal hydrid level) of the hydrogen storage and the SOC of each electric vehicle battery.

5.2.3   Control Algorithm

A two-level hierarchical control structure based on MPC, as shown in figure 5.2, is proposed. Both controllers were implemented in the tertiary level and act in different time scales. The MPC1 acts directly on the microgrid and charging station with a sampling period of one second (T_s = 1s), and it is responsible for ensuring the constraints, operation conditions and power flow exchange between the microgrid elements and the charging station, following the upper level targets. The MPC2 is designed to achieve the microgrid economic optimization managing the energy selling and purchasing. This controller uses a sampling period of five minutes (T_s = 5min). The Charging Station Management Unit runs at the second level controller and manages the use of electric vehicles batteries as a storage and guarantees that the charging constraints (charging type and time) are satisfied. Figure 5.3

shows the flowchart containing the steps for implementation the two-level MPC controller.
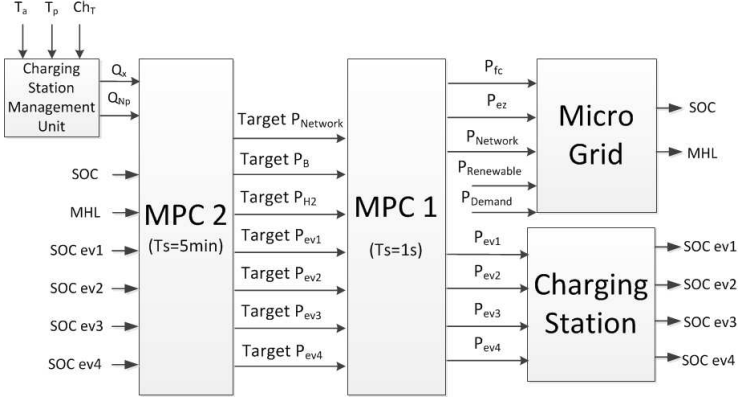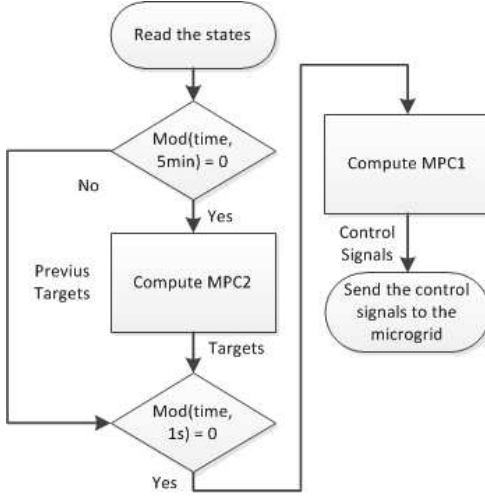

Figure 5.2: Control Structure

First Controller (MPC_1)

The first MPC has the following objective function:

$$J_1 = \sum_{l=0}^{N_c-1} \hat{u}_1(k+l)^T Q_{u1} \hat{u}_1(k+l)+ \tag{5.4}$$

$$\sum_{l=0}^{N_p-1} (\hat{x}_1(k+l) - \hat{x}_{ref}(k+l))^T Q_{x1} (\hat{x}_1(k+l) - \hat{x}_{ref}(k+l)) +$$

$$\sum_{l=0}^{N_c-1} \Delta \hat{u}_1(k+l)^T Q_{\Delta u1} \Delta \hat{u}_1(k+l)+$$

$$\sum_{l=0}^{N_c-1} (\hat{u}_1(k+l) - \hat{u}_{Target}(k+l))^T Q_{Target1} (\hat{u}_1(k+l) - \hat{u}_{Target}(k+l))$$

subject to local dynamics (5.3) and the following constraints:

Figure 5.3: Implementation Flowchart

$$\underline{x}_1 \quad \leq \quad \hat{x}_1(k+l+1) \leq \overline{x}_1 \qquad (5.5)$$

$$\underline{u}_1 \quad \leq \quad \hat{u}_1(k+l) \leq \overline{u}_1 \qquad (5.6)$$

$$\hat{y}_1(k+l) \quad = \quad y_{dem}(k) \qquad (5.7)$$

$$\hat{u}_1(k+l) \quad = \quad P_{Renewable} = P_{Available} \qquad (5.8)$$

$$\hat{u}_{Target}(1, k+l) \quad = \quad \hat{u}_2(k+l) \qquad (5.9)$$

$$x_1(k) \quad = \quad \breve{x}_1(k) \qquad (5.10)$$

for $l = 0, \ldots, N_p - 1$, where Q_{u1}, Q_{x1}, $Q_{\Delta u1}$ e $Q_{Target1}$ are positive definite weighting matrices, N_p and N_c are the prediction and control horizon respectively [1]. With respect to the notation, hat $(\hat{a})$ over variables is used to denote variables over the prediction horizon, $\underline{a}_i$ and $\bar{a}_i$ denote minimum and maximum allowed values respectively, and $\breve{a}_i$ refers to variables whose values are supposed to be known, for example, initial conditions. In this work we have assumed a bidirectional energy flow between the hub and the DNO so that the negative threshold is

---

[1]The weighting matrices were formulated as: $Q_\mu = \begin{bmatrix} q\mu_1 & \cdots & 0 \\ \vdots & \ddots & \vdots \\ 0 & \cdots & q\mu_{n_\mu} \end{bmatrix}$, for

$\mu = \{u1, x1, \Delta u1, Target1\}$ where n_μ is the number of variables μ.

used.

Matrix Q_{u1} is adjusted to minimize the use of the DNO and the storage units. Matrix Q_{x1} is used to maintain the value of SOC and MHL next to 50%. Matrix $Q_{\Delta u1}$ is adjusted to minimize the control increments in the electrolyzer and fuel cell. Weights of matrix $Q_{Target1}$ are set to guarantee that the controller will follow the targets sent by the second MPC.

Second Controller (MPC_2)

The second MPC was implemented with the following objective function:

$$J_2 = \sum_{l=0}^{N_c-1} \hat{u}_2(k+l)^T Q_{u2} \hat{u}_2(k+l) + f_{u2}^T \hat{u}_2(k+l)+ \tag{5.11}$$

$$\sum_{l=0}^{N_c-1} (\hat{u}_2(k+l) - \hat{u}_{ref}(k+l))^T Q_{e2} (\hat{u}(k+l) - \hat{u}_{ref}(k+l))+$$

$$\sum_{l=0}^{N_p-1} (\hat{x}_2(k+l) - \hat{x}_{ref}(k+l))^T Q_{x2} (\hat{x}_2(k+l) - \hat{x}_{ref}(k+l))+$$

$$(\hat{x}_2(k+N_p) - \hat{x}_{ref}(k+N_p))^T Q_{N_p} (\hat{x}_2(k+N_p) - \hat{x}_{ref}(k+N_p))$$

subject to local dynamics (5.3) and the following constraints:

$$\underline{x}_2 \leq \hat{x}_2(k+l+1) \leq \overline{x}_2 \tag{5.12}$$
$$\underline{u}_2 \leq \hat{u}_2(k+l) \leq \overline{u}_2 \tag{5.13}$$
$$\hat{y}_2(k+l) = y_{dem}(k) \tag{5.14}$$
$$x_2(k) = \breve{x}_2(k) \tag{5.15}$$

The first term of the objective function is used for the management of renewable energy sources and purchasing power for the DNO. The weights Q_{u2} and f_{u2} are tuned according to the price of each energy source. The second term is responsible for ensuring the maximum use of renewable energy sources in order to minimize the error between the amount of power available and the amount of energy used. The third term is responsible for maintaining the load level of storage around 50% of the maximum. This way deviations form this value are allowed when there is need to store more energy or use the stored energy. This term is also used to charge the batteries of electric vehicles according

to the charging type, as will be explained below. Finally, the fourth term relative to the final state weights is introduced to ensure that the vehicle batteries will be fully charged at the end of the charging time.

Different weights for sale and purchase were used to manage the purchase and sale of energy to the DNO. The part of the objective function related to the energy exchanged with the DNO is:

$$
\begin{aligned}
J_2 = \sum_{l=0}^{N_p-1} & \hat{P}_{DNO}(k+l)^T Q_{sale} \hat{P}_{DNO}(k+l)+ \qquad\qquad (5.16)\\
& \hat{z}_{DNO}(k+l)^T \left(Q_{purchase} - Q_{sale} \right) \hat{z}_{DNO}(k+l)+ \\
& f_{sale}\hat{P}_{DNO}(k+l) + \left(f_{purchase} - f_{sale} \right) \hat{z}_{DNO}(k+l)
\end{aligned}
$$

Note that when power $\hat{P}_{DNO} > 0$ we have $\delta_{DNO} = 1$ and $\hat{z}_{DNO}(k) = \hat{P}_{DNO}(k)$, which means that energy is purchased from the DNO and therefore the purchase weight is used. Otherwise $\hat{P}_{DNO} < 0$ implies $\delta_{DNO} = 0$ and $\hat{z}_{DNO}(k) = 0$ and the sale weight is used. This makes it possible to use different weights for the same variable. The values of the weights were adjusted according to the price of energy.

Charging Station Management Unit

A Charging Station Management Unit (CSMU) was designed to manage the use of the electric vehicle batteries over the microgrid. The CSMU decides the operation mode of each electric vehicle battery and communicate it to the second level MPC. This supervisor was implemented by the algorithm 3.

At the time of vehicle connection to the charging station, the user must inform the charging type Ch_T(slow or fast), the arrival time T_a and the parking time T_p. If slow charge is chosen the battery charges over the parking time using low-power charge. In the case of fast charge the battery is charged with maximum power, this is done only half an hour before the pre-set parking time, and in the rest of the time the battery is available for use as a storage for microgrid. During the period of slow or fast charge the weights Q_x and Q_{N_p} are tuned to a positive value in order to ensure that the load is charged on time. When the battery is used as storage these weights assume null values.

Algorithm 3 Charging Station Management

Input: T_a, T_p, Ch_T, ϵ, $Time$
Output: Q_x, Q_{N_p}, $\overline{u}$
 1: **for** $i = 1$ to nc **do**
 2:     **if** $\epsilon(i) = 1$ {Test if there is a parked vehicle} **then**
 3:         **if** $Ch_T(i) = 1$ {Fast Charge} **then**
 4:             **if** $Time \geq T_a + T_p - 30$ minutes **then**
 5:                 Set $Q_x(i, i)$ to the fast charge value
 6:                 Set $Q_{N_p}(i, i)$ to the fast charge value
 7:             **else** {Use the battery as a grid storage}
 8:                 Set $Q_x(i, i)$ to zero
 9:                 Set $Q_{N_p}(i, i)$ to zero
10:             **end if**
11:         **else** {Slow Charge}
12:             Set $Q_x(i, i)$ to the slow charge value
13:             Set $Q_{N_p}(i, i)$ to the slow charge value
14:             Set $\overline{u}(i)$ to the slow charge value
15:         **end if**
16:     **end if**
17: **end for**

Switching between electrolyzer and the fuel cell

In relation to the operation of the fuel cell and electrolyzer, it must be taken into account that both equipments have a minimum time to reach the steady state. Another important point is that abrupt switching between them should be avoided to maximize the useful life. Thus an algorithm was developed to attempt the following objectives:

1. Minimal time between switch on and switch off ($T_{on(ez,fc)} - T_{off(ez,fc)} \geq T_{min(ez,fc)}$);

2. Maintain the equipment on (or off) during the longest time interval;

3. Number of switching in the horizon less than a maximum (MS).

To attempt the first objective the constraint (5.17) is added to the optimization problem while $T_{on(ez,fc)} - T_{off(ez,fc)} \leq T_{min(ez,fc)}$. This way no switching throughout the prediction horizon is guaranteed.

$$\hat{\delta}_{H_2}(k + l) = \hat{\delta}_{H_2}(k + l - 1) \tag{5.17}$$

To satisfy the second objective, an additional variable $\hat{\Delta}_{\delta_{H2}}(k + l) = abs(\hat{\delta}_{H2}(k + l) - \hat{\delta}_{H2}(k + l - 1))$ is included, that is the absolute value of the binary variable increment and the following term is added to the objective function to minimize the number of switches:

$$J = \sum_{l=0}^{N_p-1} \hat{\Delta}_{\delta_{H2}}(k + l)^T Q_{\Delta\delta} \sum_{l=0}^{N_p-1} \hat{\Delta}_{\delta_{H2}}(k + l) \qquad (5.18)$$

Finally, the following constraint that imposes a maximum number of switches (MS) in the prediction horizon is introduced:

$$\sum_{l=0}^{N_p-1} \hat{\Delta}_{\delta_{H2}}(k + l) \quad \leq \quad MS \qquad (5.19)$$

In the proposed method, practical requirements, as the minimal operational time and reduced number of switching, are introduced explicitly in the optimization problem. As the MPC methodology consists of solving an optimization problem for every instant of prediction horizon, the switching constraints are taken into account by the MPC over the prediction horizon, influencing future decisions of energy management. This way the algorithm provides an optimized solution to the hydrogen storage management problem.

5.2.4   Experimental Results

In this section, the experimental results of the proposed control strategy applied to the physical microgrid are presented. The control strategy was implemented using the software Matlab [74] with Yalmip toolbox[69] and solver CPLEX [58] connected to a Programmable Logic Controller (PLC) through OPC. The microgrid is equipped with a high number of sensors and actuators directly controlled by a PLC (Schneider M340). A hierarchical architecture is adopted for reliable microgrid operation. A lower control level is managed by the PLC which monitors critical variables. If any of the critical variables (bus voltage, pressure, current, SOC etc.) is out of safety bounds, the PLC stops the operation carrying out an emergency stop. Above this control layer, the Matlab interface allows to implement advanced controllers. This interface includes the estimation of the states, such as battery state of charge (SOC) and Metal Hydride Level (MHL). All experiments were conducted during a period of 24 hours. Electric vehicles 1 and 3 receive

fast charge while 2 and 4 receive slow charge. The microgrid control objectives are to maximize the use of renewable energy sources, make the purchase and sale management of electricity to the DNO, coordinate the use of the battery bank and the hydrogen storage to minimize the oscillations between the production and demand, perform the charging of electric vehicles and ensure the load demand at all periods of time. All parameter values are presented in appendix A.

Three different experiments were carried out for the controller validation. Three representative weather patterns were selected. In particular, for the first experiment the electronic power supply was used to emulate a solar photovoltaic generator in a sunny day as shown in figures 5.4 and 5.5.

During the period from 0h to 8h and from 19h to 24h, the battery and the fuel cell worked uninterruptedly to provide most part of energy required to meet the demand and reduce the amount of energy imported from the external grid. When there is high irradiation (8h to 18h), part of energy excess is sold to the DNO and other part is used to charge the battery and the hydrogen storage through the electrolyzer operation. This way the proposed control strategy provides an optimal power distribution between the batteries, the electrolyzer and exported to the grid, which is a fundamental difference of this controller compared to traditional heuristic controllers. At the end of the day (18h to 19h), when there is less irradiation, happened a switching between the fuel cell and the electrolyzer, respecting the minimum operation time of each equipment.

As can be seen in figure 5.5, when EV1 was parked at 7h, its battery is used to avoid fluctuations, and after 8h EV1 was charged. There exist some oscillations in the power of EV1 and EV3 during the charge procedure that probably were caused by an aggressive tune of the controller parameters. EV2 and EV4 were charged in a slow charge mode.

The second experiment was performed in a cloudy day scenario, as can be seen in figures 5.6 and 5.7. A cloudy day represents a great challenge for renewable microgrids, since the control has to cope with high power fluctuations. In this sense the storage system should have the ability to absorb such fluctuations. As the microgrid is composed by a hybrid storage system, it is expected that the battery bank absorbs high frequency oscillations while the hydrogen storage provides energy for a long time when the irradiation is not sufficient to meet the demand. Another challenge is to minimize the switching in the hydrogen storage which may be caused by oscillatory conditions.
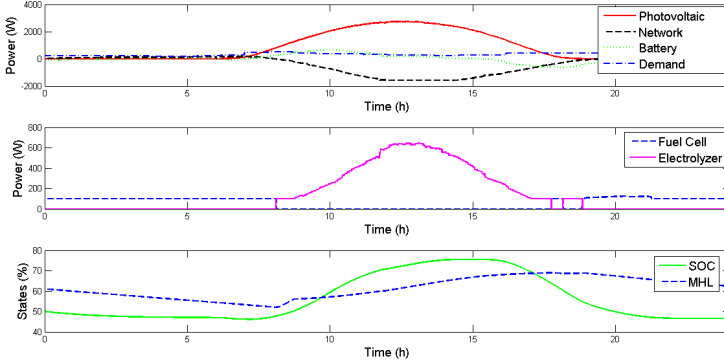
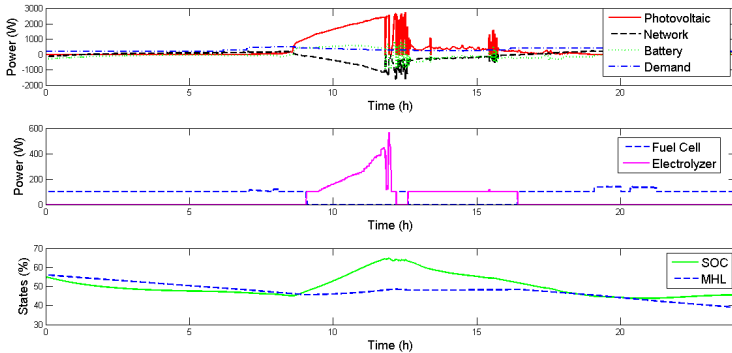**Figure 5.4:** Energy sources and storage units - Sunny day
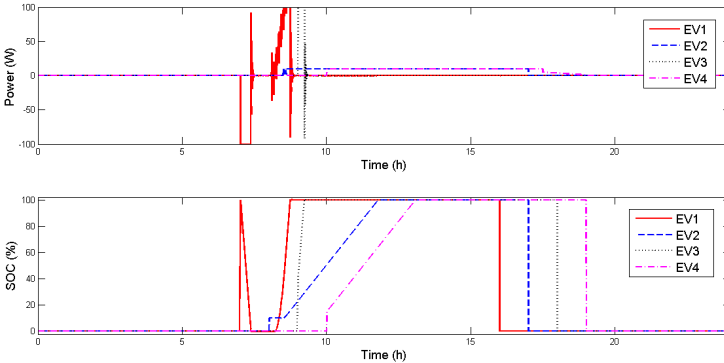
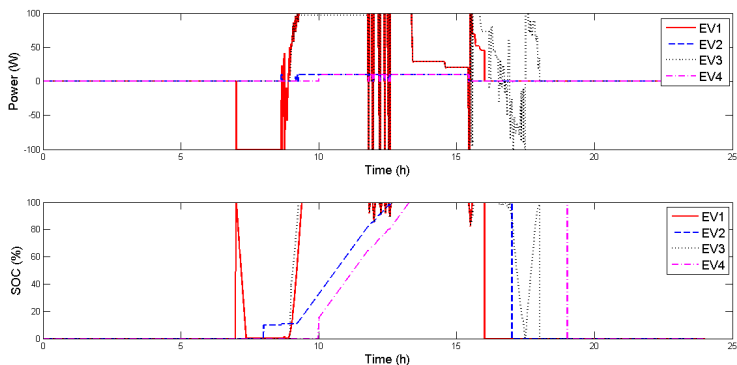**Figure 5.5:** Electric vehicles charge management - Sunny day

When the weather is cloudy, between 12h and 17 : 30h, the battery bank and the batteries of electric vehicles absorbed most of the power fluctuation. It was observed a short switching between the electrolyzer and the fuel cell, from 12h to 13h, that is caused by the radiance oscillation. In the rest of the experiment the hydrogen storage provided energy to the system at night and stored energy during the day. The difference between the initial and the final MHL is greater than compared to the sunny day experiment, that is expected once the radiance during the day is not sufficient to replace the energy expended at night. The radiance oscillation, caused by the clouds, affects directly the profile of energy sold to the DNO and the battery life as the number of charge/discharge cycles increase with fluctuation condition. Otherwise

fuel cell and electrolyzer operation is less affected thanks to the algorithm presented in section 5.2.3 that limits the switching between both equipment.

When EV1 was parked at 7h, its battery is used to provide energy to the load, and after 9h EV1 was charged as can be seen in figure 5.7. The batteries of EV1 and EV3 were used to mitigate the power fluctuation during the cloudy period that caused energy oscillation, from 12h and 16h to EV1 and from 12h and 17 : 30h to EV3. A slow charge was applied in EV2 and EV4.

Figure 5.6: Energy sources and storage units - Cloudy day

Figure 5.7: Electric vehicles charge management - Cloudy day

The third experiment was conducted using a wind turbine as renewable energy source and the results are shown in figures 5.8 and 5.9. In this experiment, the fluctuations are not so abrupt like in the cloudy

day. However, it still presents a high stochastic behavior in the wind turbine production. There are some switching in the hydrogen storage, at 10h when a wind fluctuation happens and after 20h when it is necessary provide energy to the load. In this case the final value of MHL at the end of the day is greater than at the beginning, as a consequence of the electrolyzer operation in most part of the day. The batteries of electric vehicles are scarcely used by the microgrid as can be seen in figure 5.9.

In all experiments there are four switches between the fuel cell and the electrolyzer. This occurs because of the effect of the proposed constraints and the penalty function to maximize the operating time of each equipment (once it has been switched on).
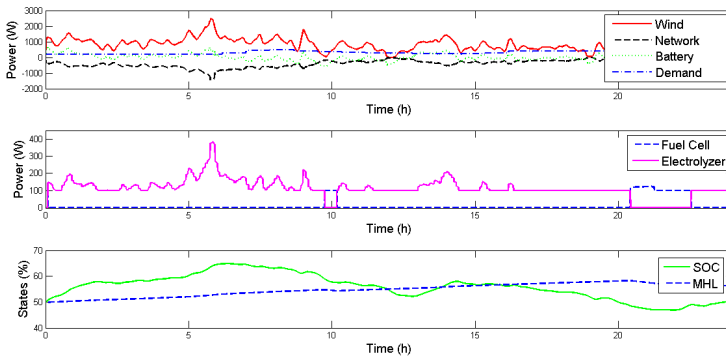
Figure 5.8: Energy sources and storage units - Windy day
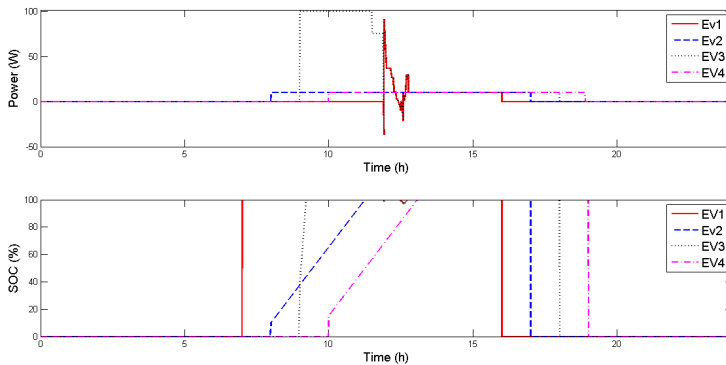
Figure 5.9: Electric vehicles charge management - Windy day

5.3 Networked Microgrids

The objective of this section is to present a distributed energy management system for optimizing direct current (DC) networked microgrids where each microgrid is composed by renewable energy sources and a V2G system to charge electric vehicles.

The microgrids are interconnected to each other and with the distribution network operator (DNO) by a physical common bus. Again in this case the system modeling was carried out using the Energy Hubs methodology. In normal operation the proposed energy management system (EMS) is responsible for performing the energy management between microgrids and purchase and sale energy to the DNO, maximizing the use of renewable energy sources, managing the use of energy storage units and performing the charge of the parked vehicles. During a fault the EMS has the task of ensuring that all microgrids will cooperate to mitigate the fault effects. On the other hand the proposed controller performs, for each microgrid, the management of the use of renewable energy sources, energy storage units, vehicles charge and the purchase and sale of electric power to the DNO.

5.3.1 V2G Networked Microgrids

The analyzed network is composed of four microgrids as shown in figure 5.10, although the methodology can be used with a network of any number of microgrids. The microgrids are connected each other through a common physical point and it is assumed that each microgrid can sell/purchase energy to DNO.

The microgrids are composed of a renewable energy source (solar/wind), a energy storage system (bank of batteries), an electric vehicle charging station and a load that represents residential or industrial consumers. Microgrids 1 and 2 are composed of a grid of photovoltaic panels, while, 3 and 4 are powered by wind turbines. The charging station has capacity to charge ten vehicles simultaneously and it is provided with a photovoltaic energy source. For the battery bank and the electric vehicle batteries different charge/discharge efficiencies were considered as pointed in [45] and [42]. The technical characteristics of all equipments are summarized in table 5.2.

5.3.2 System Modeling

All the modeling aspects of the microgrids are equal to the ones presented in section 4.3. Hereafter the modeling aspects related to
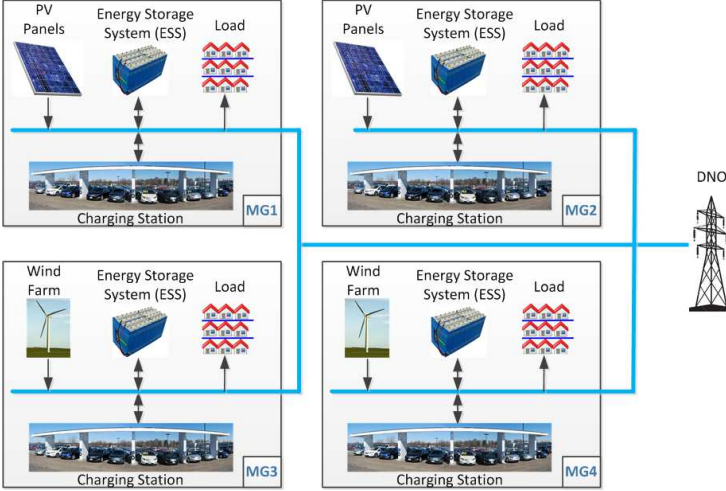
Figure 5.10: Network of Microgrids

the connection between the microgrids are presented. The complete decision vector (manipulated variables) is $u = \begin{bmatrix} u^L & u^E & \delta & z \end{bmatrix}^T$; with $u^L = P_{DNO}$ where P_{DNO} is the power exchanged with DNO; $u^E = \begin{bmatrix} P_B & P_{Bev1} & \dots & P_{Bev10} \end{bmatrix}^T$ where P_B and $P_{Bev1to10}$ are respectively the power of battery bank and electric vehicles batteries; $\delta = \begin{bmatrix} \delta_{DNO} & \delta_B & \delta_{Bev1} & \dots & \delta_{Bev10} \end{bmatrix}^T$ where δ_{DNO}, δ_B and $\delta_{Bev1to10}$ are binary variables; $z = \begin{bmatrix} z_{DNO} & z_B & z_{Bev1} & \dots & z_{Bev10} \end{bmatrix}^T$ where z_{DNO}, z_B and $z_{Bev1to10}$ are continuous auxiliary variables.

As all power generated by the renewable energy sources (photovoltaic and wind) has to be used by the system, they were modeled as disturbances according to vector

$$r = \begin{bmatrix} P_{Renewable} \\ P_{PVCh} \end{bmatrix} \tag{5.20}$$

where $P_{Renewable}$ can be photovoltaic or wind energy source depending on the microgrid and P_{PVCh} is the charging station photovoltaic energy source. Interconnection variables that represent the power exchanged among the microgrids were inserted in the model through the following in/out interconnection vectors:

Table 5.2: Microgrids Components

Photovoltaic panels	Wind Turbines
Micro Grid 1: $P_S = 1.5$MWp	Micro Grid 3: $P_W = 2$MWp
Micro Grid 2: $P_S = 2$MWp	Micro Grid 4: $P_W = 3$MWp
Li-Ion Battery bank	
Power: $P_B = 1$MW	Charge efficiency: $\eta_{Ch} = 0.92$
Capacity: $C_B = 0.5$MWh	Discharge efficiency: $\eta_D = 0.95$
Charging Station	
PV panels: $P_S = 0.03$MWp	
Li-Ion Ev Battery	
Power: $P_B = 0.06$MW	Charge efficiency: $\eta_{Ch} = 0.92$
Capacity: $C_B = 0.023$MWh	Discharge efficiency: $\eta_D = 0.95$

$$w_{in,i \leftarrow j} = \begin{bmatrix} w_{in,i \leftarrow j1} \\ w_{in,i \leftarrow j2} \\ w_{in,i \leftarrow j3} \end{bmatrix}, w_{out,i \rightarrow j} = \begin{bmatrix} w_{out,i \rightarrow j1} \\ w_{out,i \rightarrow j2} \\ w_{out,i \rightarrow j3} \end{bmatrix} \tag{5.21}$$

where $w_{in,i \leftarrow j}$ is the power received by the microgrid i from the microgrid j and $w_{out,i \rightarrow j}$ is the power sent from the microgrid i to the microgrid j. The model can be written in a condensed form:

$$x(k+1) = Ax(k) + \Lambda u(k) \tag{5.22}$$

$$y(k) = \Gamma u(k) + Dr(k) + \Pi_{in} w_{in,i \leftarrow j}(k) \tag{5.23}$$

$$w_{out,i \rightarrow j}(k) = \Pi_{out,i \rightarrow j} y(k) \tag{5.24}$$

$$E_\delta \delta + E_z z(k) \leq E_u^E u^E(k) + E_0, \tag{5.25}$$

where the states are the battery bank SOC (state of charge) and the SOC of each electric vehicle battery.

5.3.3 Control Algorithm

This section gives details of the proposed distributed predictive control structure focusing on optimizing the operation. In this control structure, the global optimization problem is distributed between agents in the form of local optimization goals. Figure 5.11 shows the control structure of each microgrid. The MPC is designed to achieve the

microgrid economic optimization managing the storage state of charge and the energy selling and purchasing to DNO. The CSMU, described in previous section, manages the use of electric vehicles batteries as storage and guarantees that the charging constraints (charging type and time) are satisfied. The microgrid interconnection selector is responsible for analyzing if the microgrid has excess or deficiency of energy and classifies the microgrids as an energy provider or receptor. In this way the interconnections are selected to manage the energy flow from providers to receptors.
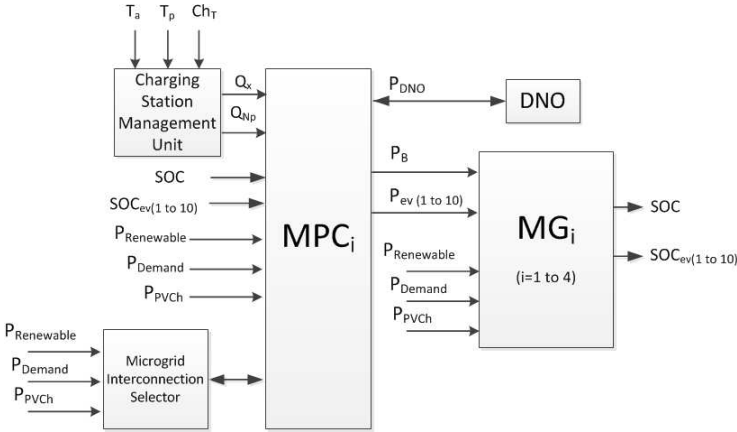
Figure 5.11: Control Structure

Objective Function

The optimization problem for each microgrid uses the following local objective function:

$$
J_{local} = \sum_{l=0}^{N_p-1} \hat{u}(k+l)^T Q \hat{u}(k+l) + f^T \hat{u}(k+l) +
$$

$$
\sum_{l=0}^{N_p-1} (\hat{x}(k+l) - \hat{x}_{ref}(k+l))^T Q_x (\hat{x}(k+l) - \hat{x}_{ref}(k+l)) +
$$

$$
(\hat{x}(k+N_p) - \hat{x}_{ref}(k+N_p))^T Q_{N_p} (\hat{x}(k+N_p) - \hat{x}_{ref}(k+N_p))
$$

$$(5.26)$$

subject to local dynamics (5.22) and (5.25) and the following constraints:

$$\underline{x}_i \quad \leq \quad \hat{x}_i(k+l+1) \leq \overline{x}_i \qquad (5.27)$$
$$\underline{u}_i \quad \leq \quad \hat{u}_i(k+l) \leq \overline{u}_i \qquad (5.28)$$
$$\hat{y}_i(k+l) \quad = \quad y_{dem}(k) \qquad (5.29)$$
$$x_i(k) \quad = \quad \breve{x}_i(k) \qquad (5.30)$$

for $l = 0, \ldots, N_p - 1$, where Q, Q_x are positive definite weighting matrices, f is a vector and N_p is the prediction horizon. It was assumed a bidirectional energy flow between the microgrid and the DNO so that the negative threshold is used.

The first term of the objective function is used for the management of the renewable energy sources and for purchasing power from the DNO. The weights Q and f are tuned according to the price of each energy source. The second term minimizes the error between the state and the state reference and is responsible for maintaining the storage level around 50% of the total load, and allows deviations from this value when there is need to store more energy or use the stored energy. The third term which weights the error between the final state and desired value is introduced to ensure that the vehicle batteries will be fully charged at the end of the charging time. These last two terms are used to charge the batteries of electric vehicles according to the charging type, as will be explained below. As described in previous section the different prices of energy sold/purchased with DNO are treated in the optimization problem by a MLD transformation in the objective function.

Interconnection Selector

The interaction between microgrids is only psychically possible when there is at least one microgrid with energy excess and another or others with deficiency of energy. To impose this physical restriction an interconnection selector was created, that classifies the microgrids. The algorithm performs the logic test $P_{Renewable} + P_{PVCh} \geq P_{Demand}$; if the test is true the microgrid is classified as a provider ($Q_{provider} = 1$ and $Q_{receptor} = 0$) and in case the test is false the microgrid is a receptor ($Q_{provider} = 0$ and $Q_{receptor} = 1$).

In order to ensure the energy flow direction, from providers to receptors, the following constraints were added to each local optimization

problem:

$$Q_{receptor} \sum_{j=1-3} w_{out,i \to j} = 0 \tag{5.31}$$

$$Q_{provider} \sum_{j=1-3} w_{in,i \leftarrow j} = 0 \tag{5.32}$$

$$Q_{provider} \sum_{j=1-3} w_{out,i \to j} \leq \|P_{Renewable} + P_{PVCh} - P_{Demand}\| \tag{5.33}$$

$$Q_{receptor} \sum_{j=1-3} w_{in,i \leftarrow j} \leq \|P_{Renewable} + P_{PVCh} - P_{Demand}\| \tag{5.34}$$

The first and second constraints were used to force null value to the interconnection variable that will not be used. For example, if the microgrid is a provider just the output interconnection variables will be used and the input variables will be null. The third and fourth constraints were used to limit the energy flow between the microgrids.

In the studied system all microgrids can communicate each other by the interconnection variables and can buy/sell energy to the DNO. Each microgrid optimization problem has to satisfy the interconnections constraints $w_{in,j \leftarrow i} = w_{out,i \to j}$ and $w_{out,j \to i} = w_{in,i \leftarrow j}$. To ensure that these constraints will be satisfied it is necessary to apply a distributed control algorithm based on communication between the agents. This way, the Hybrid Distributed MPC framework presented in chapter 4 was used.

5.4 Results

The proposed Hybrid DMPC strategy was applied to the networked microgrids described in section 5.3.1. A simulation with a period of 24 hours and a sampling time of 10 minutes was performed using the software Matlab [74] with Yalmip toolbox[69] and solver CPLEX [58]. The control objectives of each microgrid are to maximize the use of renewable energy sources, make the purchase and sale management of electricity to the DNO, use the storage to minimize the oscillations between the production and demand, perform the charging of electric vehicles and ensure the load demand at all periods of time. From the interconnected systems point of view it is desired to maximize energy exchange between microgrids in a way to reduce the amount of energy purchased from the DNO. In this simulation scenario renewable sources data extracted from experimental microgrid described in [113] were used. All parameter values are presented in appendix A.

As each microgrid has 12 binary variables related to the physical dynamics (one related to energy sells/purchases to DNO, another related to battery bank and ten related to electric vehicles) and a pre-

diction horizon of $N = 6$ was used, the total number of binary variables is 72. This way each microgrid has 2^{72} possible instances to the local controller which results in $\prod_{i=1}^{4} 2^{72}$ configurations for the binary variables in the global optimization problem.

As explained in chapter 3, the proposed algorithm reduces the set of controller instances to 4 using $N_b = 1$ and 24 for $N_b = 6$. A simulation analysis to determine the influence of N_b, testing $N_b = 1$ until $N_b = 6$ with $N = 6$ and $N_c = 2$ was performed. Figure 5.20 shows the number of iterations for each time instant and the calculation time for each N_b. To facilitate the figure visualization a zoom of the first ten hours is provided. In this case the number of iterations varies between 1839 and 3693, and the calculation time increases with N_b. As shown in Table 5.3, $N_b = 3$ offers the best compromise between the number of iterations and the calculation time, getting 1094 iterations in 13.92 minutes with an average time of 5.80 seconds per iteration. For the other values of N_b, the system presented peaks of maximum iterations between 17h and 20h. Hence, in this context the best choice is $N_b = 3$.
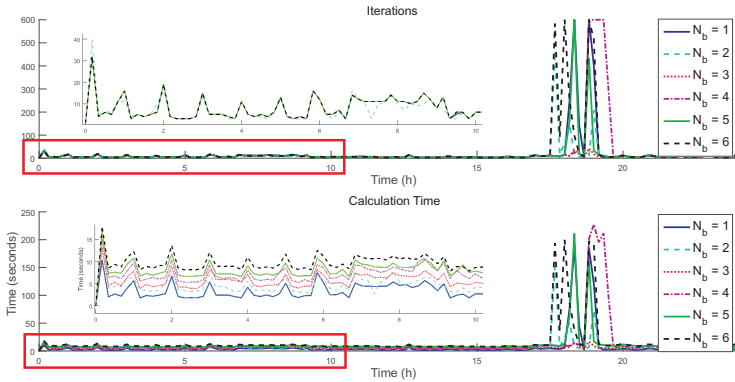
Figure 5.12: Number of iterations and calculation time varying N_b.

Table 5.4 presents a comparison between the proposed hybrid DMPC framework and centralized MIQP (CMIQP) solved by CPLEX branch and bound solver. As expected, the computation time expended by the hybrid DMPC was greater than the centralized solution and this result is explained by the number of optimization problems solved at each iteration. However hybrid DMPC has an average calculation time of 5.8 seconds that is much smaller than the sampling of 10 minutes. Both algorithms presented similar costs, a fact that shows that the proposed DMPC can deal properly with problems composed by a great

Table 5.3: Analysis of N_b

|	Iterations	Total time (min)	Average time (s)
$N_b = 1$	2949	17.3	7.21
$N_b = 2$	1839	15.7	6.56
$N_b = 3$	1094	13.92	5.80
$N_b = 4$	3687	32.13	13.39
$N_b = 5$	2214	27.33	11.39
$N_b = 6$	3693	37.65	15.65

number of binary variables in a distributed fashion and provide a solution close to the optimal obtained by centralized algorithm.

Table 5.4: Performance Indexes

	$HybridDMPC$	$CMIQP$
Iterations	1094	–
Total time (min)	13.92	2.45
Average time (s)	5.8	1.01
Total cost	1.9×10^{15}	1.81×10^{15}
Average cost	1.31×10^{13}	1.25×10^{13}

In order to investigate the interconnection advantages a comparison between the networked microgrids with distributed controller and the isolated microgrids with local centralized controllers was performed. Figures 5.14 and 5.15 show the energy sources graphs for simulation with interconnected and isolated microgrids respectively, while figure 5.16 shows the state of charge of each microgrid in both simulation scenarios. To facilitate the visualization of charging station, photovoltaic source and battery powers were plotted multiplied by a factor of 10. Figure 5.13 shows the sell and purchase prices of energy exchanged with DNO.

In respect to the amount of energy exchanged with the DNO, as shown in table 5.5, in networked arrangement all microgrids sold energy to DNO and only microgrids 1 and 2 purchased 0.067MWh and 0.047MWh respectively. However in isolated scenario microgrids 1 and 2 purchased more energy (3.85MWh and 10.02MWh) and microgrids 3 and 4 sold a great amount of energy to DNO. As the prices of energy exchanged with DNO are variable over the day and the amount of en-
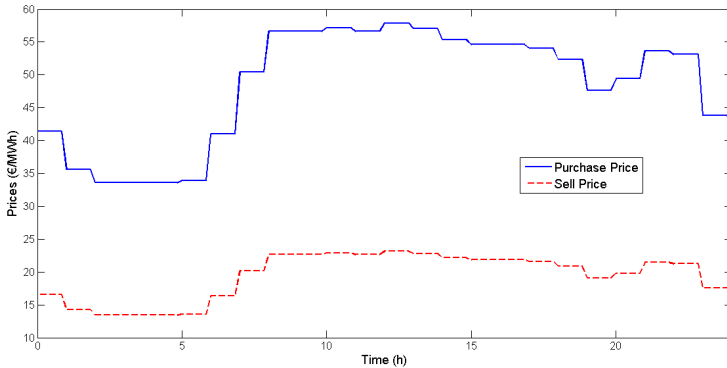
Figure 5.13: Energy prices

ergy exchanged in both scenarios are different, there are distinct energy costs for each microgrid. In isolated case all microgrids sold 980.41€and purchased 618.34€totalizing a profit of 362.07€while in the interconnected case the total profit is 932.19€. These differences between both schemes is because when microgrids are interconnected they exchange energy with each other and consequently minimize the amount of energy purchased from DNO, while in isolated case microgrids just had the DNO to exchange energy. From a sustainable viewpoint the networked case is better because it uses less DNO energy that is usually generated from fossil energy sources.

Analyzing figures 5.16 it is possible to see that in the isolated case microgrids 1 and 2 had more variability of SOC in the battery bank than in the interconnected case. The reason of this fact is that when microgrids are interconnected all systems cooperate to mitigate the power fluctuations while in the isolated case there is only battery bank for this function.

During interconnected simulation microgrids 3 and 4 had excess of energy and were classified as providers while microgrids 1 and 2 as receptors. The energy flow between microgrids is shown in figure 5.19 (a). Microgrids cooperate each other in periods when, for one or more microgrids, demand is greater than power of energy source.

Figure 5.17 displays the vehicles batteries management in isolated case. For all microgrids Vehicles 2, 3, 6 and 10 use slow charge. Other vehicles use fast charge so that part of the time that they are connected to the microgrid they operate as storage elements and only in the last 30 minutes the batteries are actually charged. This functionality was

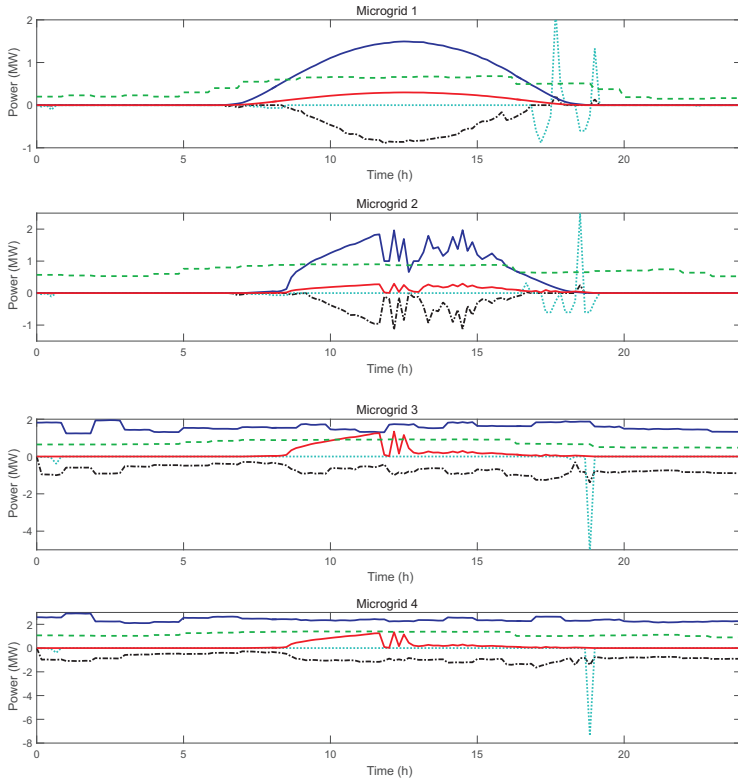**Table 5.5:** Energy exchanged with DNO

	Energy (MWh)		Cost (€)	
	Sold	Purchased	Sold	Purchased
Interconnected Case				
$MG1$	4.57	0.067	103.26	3.47
$MG2$	3.34	0.047	75.33	2.46
$MG3$	17.54	0	345.45	0
$MG4$	20.8	0	414.08	0
Total	46.25	0.0114	938.12	5.93
Isolated Case				
$MG1$	4.60	3.85	103.68	168.45
$MG2$	3.41	10.02	77.26	449.89
$MG3$	21.05	0	408.11	0
$MG4$	30.00	0	391.36	0
Total	59.06	13.87	980.41	618.34

better used in case of isolated microgrids, as highlighted in figure 5.17, because in this situation microgrids have only the storage units to deal with fluctuations. In interconnected arrangement it was not necessary to use the electric vehicles as storage units because this fluctuations are handled through interconnection.

In the second simulation a fault in the energy source of microgrid 3 was applied starting at 10h and extinguishing at 14h. The main purpose of this test is to investigate how distributed controller deal with disturbances and maintain interconnected system stability. As shown in figure 5.18, during the fault the amount of energy sold to DNO is reduced compared with no fault case. Part of this energy is exchanged between microgrids to support microgrid 3 as shown in figure 5.19. During the fault the number of iterations increases compared to the simulation without fault and in few moments reaches the maximum limit of 600 iterations (see figure 5.20).

5.5   Final Remarks

In this chapter the problem of control of microgrids integrating renewable generation, hybrid storage technologies and an interaction with a V2G system was presented. A hierarchical MPC structure was proposed to perform the economic optimization and management of storage systems. Constraints and penalty functions were introduced

Figure 5.14: Interconnected simulation energy sources. (blue - renewable energy sources, red - charging station photovoltaic source, black - power exchanged with DNO, cyan - battery power, green - Demand)

in order to deal with the switching between the fuel cell and the electrolyzer and to maximize the time each equipment is on. The charging station management algorithm performed the use of the electric vehicles batteries as a microgrid storage.

In the second part of this chapter the control of networked microgrids was discussed. The hybrid DMPC developed in chapter 4 was used as energy management system to perform the economic energy management and guarantee the cooperation between microgrids in normal and fault operation. The interconnection selector showed usefulness ensuring the energy flow direction from providers to receptors. As shown in the simulation results, the proposed controller presented satisfactory results for different operating conditions.
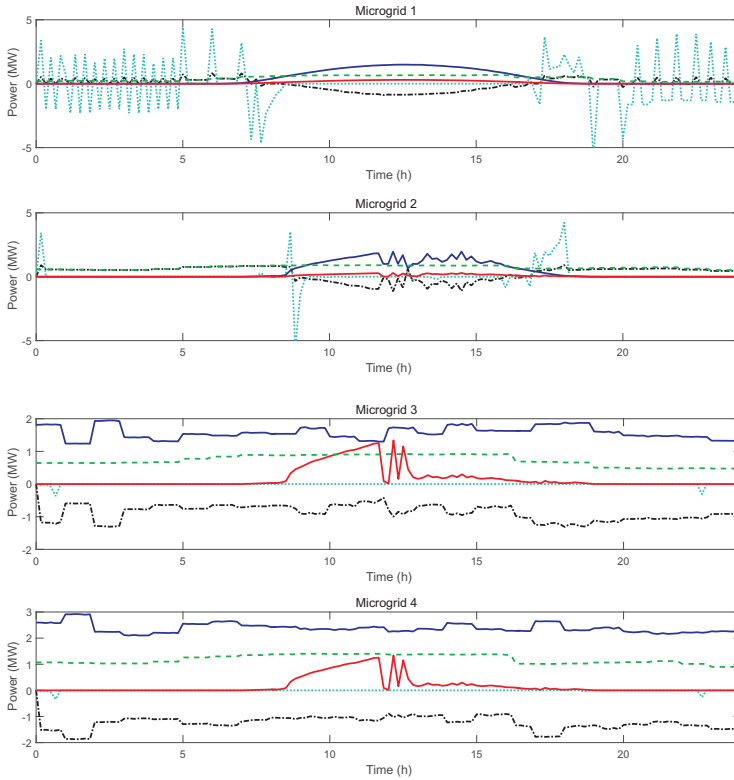
Figure 5.15: Isolated simulation energy sources. (blue - renewable energy sources, red - charging station photovoltaic source, black - power exchanged with DNO, cyan - battery power, green - Demand)

To complete the study of this thesis, in the chapter 6, the Brazilian energy scenario will be taken into account by the modeling and control of a hybrid generation power plant on the sugar cane industry.
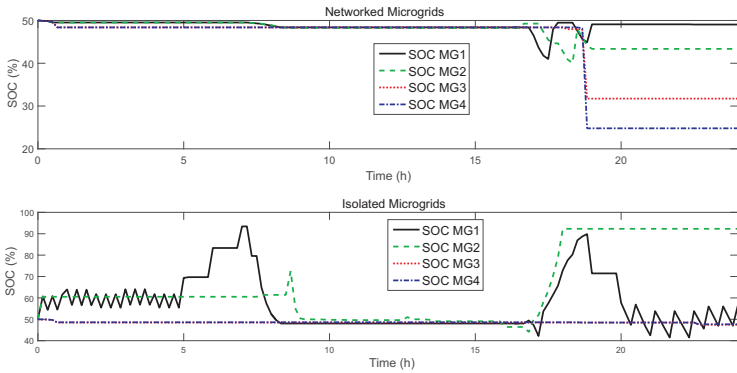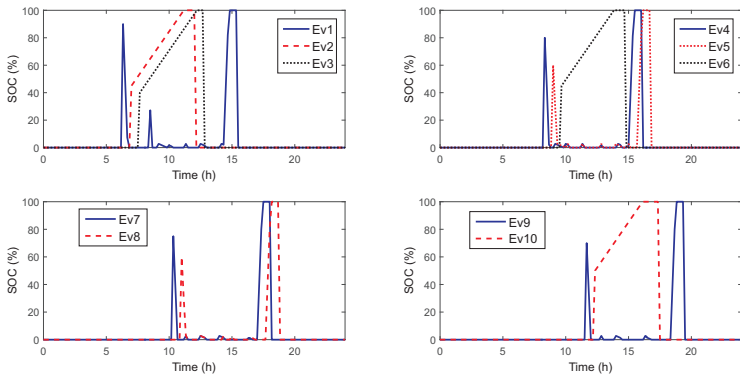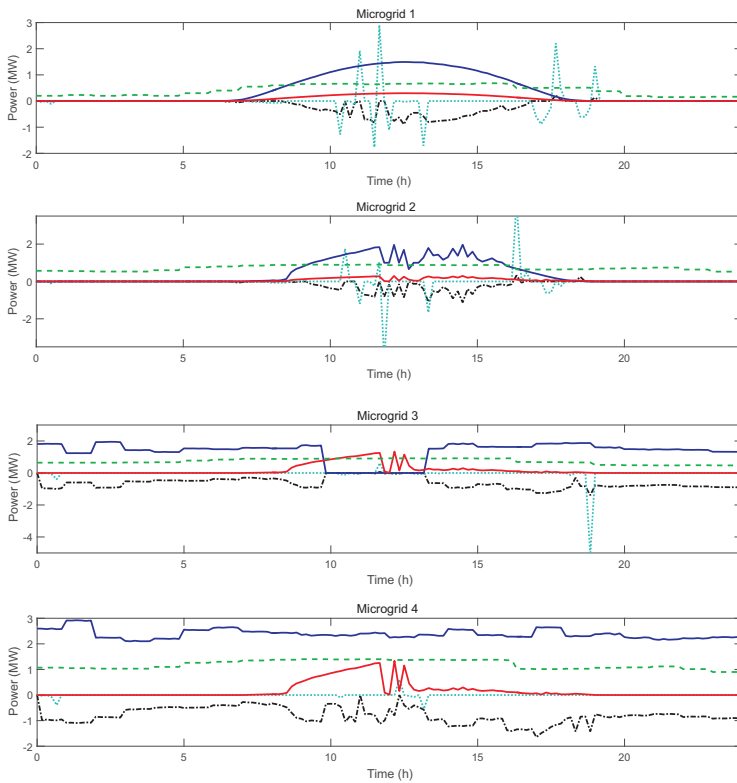
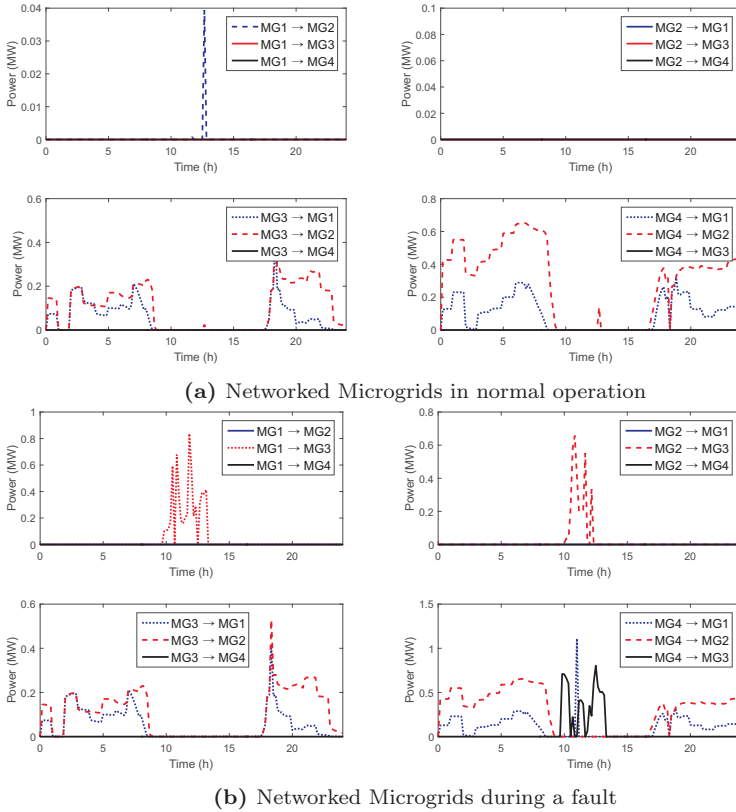**Figure 5.16:** Battery SOC

Figure 5.17: Electric vehicles charge management (Isolated Microgrids)

Figure 5.18: Energy sources during a fault. (blue - renewable energy sources, red - charging station photovoltaic source, black - power exchanged with DNO, cyan - battery power)

(a) Networked Microgrids in normal operation

(b) Networked Microgrids during a fault

Figure 5.19: Interconnection variables in the two analyzed scenarios.
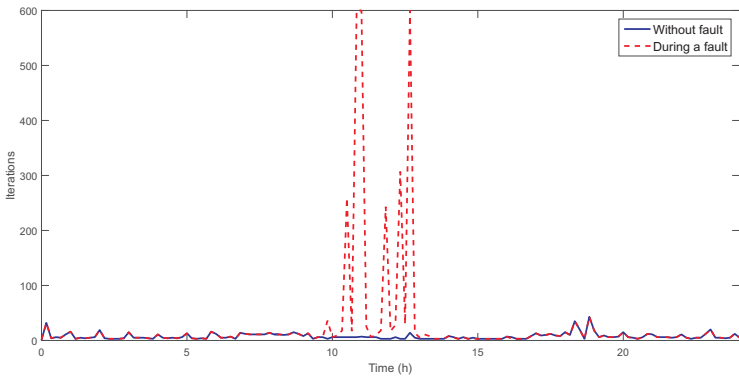
Figure 5.20: Number of iterations (without fault and during a fault)

Chapter 6

Sugar Cane Industry Case

Given the importance of sugar-ethanol power plants in the Brazilian energy setting and knowing that these are mostly established in high insolation sites, they become potential candidates to be managed as distributed power plants of hybrid sources, as seen in [39], considering biomass, biogas, solar and wind power energy and natural gas. Thus, the control of hybrid generation and storage, including renewable and non-renewable sources, is a significant issue to be studied in order to allow the optimal management and operation, carrying out a coordination between legal standards, minimal environmental standards and *state of the art* techniques [54], [38].

Multi-carrier systems represent a crucial need for future research. Traditionally, energy networks have been considered employing only one source of energy (for example, electricity or natural gas). Recent works urge to combine modeling and scrutiny of energy systems including various energy carriers and system intercommunication and the integrated planning of different networks [49].

With greater demands for improvements in production and efficiency, the operational requisites of energy systems are evermore restrict and, for that, the operation and automatic control have to aim optimal efficiency of these energy plants. Knowing that individual optimal conditions of subsystems do not imply the optimal condition of a whole system, a coordination between every subsystem of a whole energy system becomes necessary. This coordination is typically done by an automatic supervisor, in a higher level in the hierarchy of the

control structure of these energy plants, and, by this, the operational set-points of each subsystem are brought so that the operation of the whole energy system is near its optimal operational point.

This chapter presents the proposal of a new hybrid energy generation system, with the reuse of the sugar cane residues coupled with the use of other renewable sources, external to the plant, as photovoltaic panels and wind turbines, that aims to prevent and, when not possible, reduce emissions and the global environmental impact. The proposed microgrid is based on a real sugar cane processing unit, with the addition of subsystems based on renewable generation. First some details about the power plant will be presented and the modeling framework will be detailed. Then an optimization of the hybrid energy system based on MPC is proposed.

6.1   The Hybrid Generation Power System

In this section a generic hybrid energy generation system, based on a sugar cane processing plant, that produces sugar and ethanol is proposed. The energy power plant is based on a real Brazilian industrial plant, whose structure is seen in figure 6.1. The proposed system, shown in figure 6.2, is composed by the following subsystems:

- two boilers, with different efficiencies;

- two steam turbines, with different efficiencies;

- one combined heat and power system (herein denoted as CHP);

- one water chiller;

- one hot water tank;

- photovoltaic panels;

- water heating solar panels;

- one wind turbine;

- two pressure reduction valves;

- one heat exchanger;

- stocks of bagasse, straw and compressed biogas;

- a battery bank.

The tendered system, being a plausible adaptation from a real plant, is interesting in an economic and sustainable point-of-view, as it proposes the use of renewable sources and the recycling of the sugar cane residues. This implies directly on the increase of the total energy generation capacity and, also, on the efficiency and the sustainability of the system - that, herein, does not use any fossil fuel or energy source external to the sugar-ethanol production process. The system aims to use the best possible technology, that conducts a dynamic between legal norms, minimum environmental standards and the state of the art techniques. Figure 6.2 shows the outline of the proposed system. The technical characteristics of these equipments can be seen in table 6.1. Other important data to this study, like average bagasse income from the canebrakes, can be found in table 6.2.
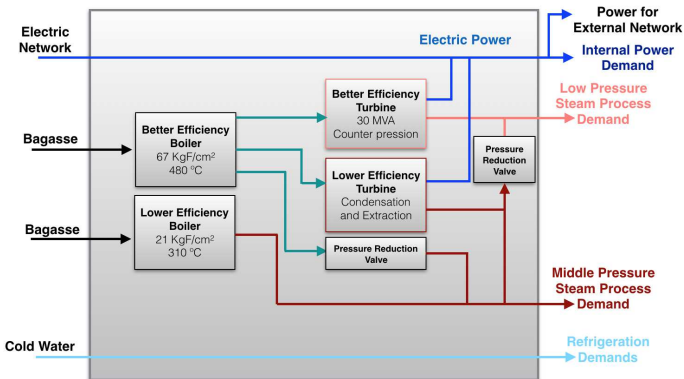
Figure 6.1: Original Power Generation Plant

The two boilers, here nominated better efficiency and lower efficiency, produce, respectively, higher (67kg/) and middle pressure (21kg/) steam. They are both powered by the biomass mixture of straw and bagasse. The lower efficiency boiler produces less amount of steam, which is used in order to comply to the process's (ethanol and sugar) middle pressure steam demands. The other boiler's steam is used to propel the plant turbines. The turbines, likewise the boilers, are here nominated better efficiency and lower efficiency. The better efficiency turbine has a low pressure steam residue (1.5kg/) that is used to meet the process low pressure steam demands, while the lower efficiency turbine steam residue meets the middle pressure steam demands. Both turbines produce electric power that, with the CHP and the renewable energy generation, are related to the electric demands. The CHP is a
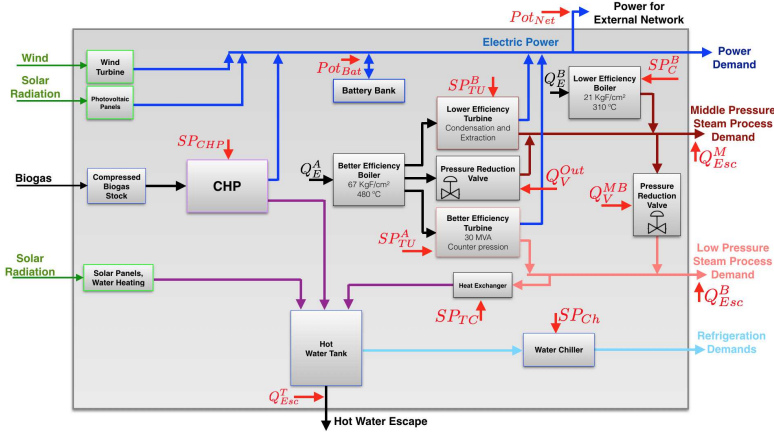
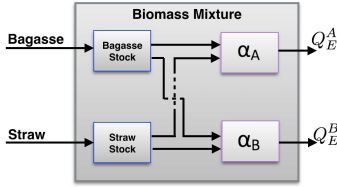**Figure 6.2:** Proposed Power Generation Plant

Figure 6.3: Biomass Mixture

gas engine that uses energy present in the biogas to drive a crankshaft, that, through an alternator, produces electric energy. With the combustion of the gas, heat is released and recovered to warm water, making the CHP a highly efficient system. The CHP, in this scenario, is boosted by the compressed biogas, made from the vinasse. The use of intermediate storage units (battery bank and biomass stocks) allows the system to accumulate energy (or biomass, that can be converted into energy) when the renewable generation is high and use it when there is no renewable production. All these subsystems operating points can be seen in table 6.3. More specific data on the stocks can be found in table 6.4.

The whole problem here studied is subject to several constraints. Firstly, the efficiencies of the boilers fluctuate according to the mixture of biomass that boosts them. The straw is a moist left-over from the sugar cane, so too much straw causes problems with the ignition of

Table 6.1: Microgrid Equipments

Equipment	Efficiency	Used Area	Other
Better Eff. Boiler	87.8 %	-	-
Lower Eff. Boiler	76.5 %	-	-
Better Eff. Turbine	70 %	-	-
Lower Eff. Turbine	65 %	-	-
High-Middle Press. Reducing Valve	25 %	-	-
Middle-Low Press. Reducing Valve	20 %	-	-
CHP	≈ 90 %	-	-
Battery Bank (charge)	95 %	-	-
Battery Bank (discharge)	92 %	-	-
Photovoltaic panels	15.85 %	200m^2	1.8MW$_{peak}$
Solar Water Heater	68.7 %	150m^2	-
Wind Turbine	20 %	-	-
Heat Exchanger	60 %	-	-
Water Chiller	78 %	-	-

Table 6.2: Microgrid Data

Days of Harvest	200 days/year	-
Produced Sugar Cane	1610kt/$_{crop}$	335t/$_h$
Retrieved Bagasse	450.75kt/$_{crop}$	93.90t/$_h$
Retrieved Straw	42.028kt/$_{crop}$	8.756t/$_h$
Amount of Steam used in plant processes	5000t per day	-
Average Middle Pressure Steam Demand	84t/$_h$	21kg/
Average Low Pressure Steam Demand	125t/$_h$	1.5kg/
Average Refrigeration Demands	67t/$_h$	$\approx 1.6 \times 10^6$ L per day
Average Power Process Demands	8MW	192MWh per day

the boilers. It is known that the best possible mixture of bagasse and straw to boost boilers is 50% of each ([119],[109],[64]). The static gains of the boilers vary according to the mixture of biomass used; mixtures with greater amount of straw have bigger calorific power, but are wetter. This is an issue of optimal control, once the amount of bagasse, available in a canebrake, is always bigger than the amount of straw - in the studied plant, there is an average income of 93t/$_h$ of bagasse and 8.7t/$_h$ of straw. For this, this work takes into account biomass blending factors, α_A and α_B, varying from 0.5 to 1, for each boiler, as seen in figure 6.3.

The proposed plant has four demands to satisfy: electric power demand, due to ethanol and sugar production process; middle and low

Table 6.3: Microgrids Subsystems Operating Points

Better Efficiency Turbine	$11 \text{ MW} \leq SP_{TU}^{A} \leq 27 \text{ MW}$
Lower Efficiency Turbine	$3 \text{ MW} \leq SP_{TU}^{B} \leq 20 \text{ MW}$
Better Efficiency Boiler	$105 \text{ t}/_{\text{h}} \leq \frac{SP_{TU}^{A}}{160} + \frac{SP_{TU}^{B}}{85} + Q_{V}^{Out} \leq 190 \text{ t}/_{\text{h}}$
Lower Efficiency Boiler	$18 \text{ t}/_{\text{h}} \leq SP_{C}^{B} \leq 58 \text{ t}/_{\text{h}}$
CHP	$0.8 \text{ MW} \leq Pot_{CHP} \leq 8 \text{ MW}$

Table 6.4: Microgrids Storage Units

	Minimum	Maximum
Bagasse Stock	2000 t	20000 t
Straw Stock	0	2000 t
Compressed Biogas Stock	10 m^3	120 m^3
Hot Water Tank	30 m^3	300 m^3
Battery Bank	−3000 MWh	3000 MWh

pressure steam demands, defined by the process; refrigeration (cold water) demands, also defined by the process. It is important to mention that satisfying each demand alone is not adequate, as they are inextricably linked. As an example: increasing the amount of power supplied by the turbines also increases the amount of steam produced.

The electric power that has to be produced by the microgrid consists of two factors: the internal power demands, to maintain the sugar cane processing - in average 8MW, and the amount of energy that is sold to the Distribution Network Operator (DNO) (this is defined by a fixed contract, 11.52GWh per month). This power generation can be continuous, maintaining an average electric power, or varied, with different values of electric power made available at each hour of the day. This is placed as the main optimization problem of this study, more deeply discussed in further sections.

The steam demands of the system correspond to the sugar and ethanol processing steam demands. These are used to boost water bombs, spray bombs, fans, chippers, shredders and other equipments. The refrigeration demand of the microgrid is used to cool down generators, oil tanks from the distillery process and other systems present on the plant.

6.2 System Modeling

In this section the system modeling methodology is explained.

6.2.1 Manipulated Variables

The system manipulated variables are:

- The lower efficiency boiler set-point, SP_C^B ($^t/_h$);

- The lower efficiency turbine set-point, SP_{TU}^B (kW);

- The better efficiency turbine set-point, SP_{TU}^A (kW);

- The charge/discharge power the battery bank, P_B (kW);

- The CHP set-point, SP_{CHP} (kW);

- The water chiller set-point, SP_{ch} ($^{m^3}/_h$);

- The heat exchangers set-point, SP_{TC} ($^{m^3}/_h$);

- The high-middle pressure reduction valve set-point, (Q_V^{Out} $^t/_h$);

- The middle-low pressure reduction valve set-point, (Q_V^{MB} $^t/_h$);

- The hot water escape flow, (Q_{Esc}^{Tank} $^{m^3}/_h$);

- The middle pressure steam escape flow, (Q_{Esc}^M $^t/_h$);

- The low pressure steam escape flow, ($Q_{Esc}^B$$^t/_h$) and

- The instant electric power that is made available, by the micro-grid, to the DNO (for sale), represented by (P_{Net} (kW));

- The binary variable associated with battery charge/discharge, (δ_B);

- The auxiliary continuous variable associated with battery charge/discharge, (z_B (kW))

These manipulated variables, will be treated as set-points by lower level internal controls. The internal control of each subsystem is not a concern to this work. The complete manipulated variables vector is:

$$u = \begin{bmatrix} SP_{TU}^A & SP_{TU}^B & P_{Net} & SP_C^B & Q_V^{Out} & Q_{Esc}^M & Q_{Esc}^B & SP_{CHP} \end{bmatrix} \quad (6.1)$$

$$\begin{bmatrix} SP_{Ch} & SP_{TC} & P_B & Q_V^{MB} & Q_{Esc}^{Tank} & \delta_B & z_B \end{bmatrix}^T \quad (6.2)$$

6.2.2   Disturbance Vector

The external disturbances to the system are:

$$z = \begin{bmatrix} Wind_{in} & Irrad_{in} & Bag_{in} & Str_{in} & Bg_{in} \end{bmatrix}^{T}, \qquad (6.3)$$

where $Wind_{in}$ is the amount of wind (measured in $km/_{h}$) present in the microgrid area, used by the wind turbines to generate electric power, and $Irrad_{in}$ is the amount of solar irradiation (measured in $W/_{m^2}$) on the microgrid solar panels (photovoltaic and water heating). As the wind and the solar irradiation are considered disturbances, in the rest of this thesis they will be referred as non-dispatchable renewable sources. Bag_{in}, Str_{in} and Bg_{in} are measured in $t/_{h}$ and represent the income of bagasse, straw and compressed biogas to the respective stocks.

6.2.3   System Output

The system output vector is defined as:

$$y = \begin{bmatrix} D_{Proc} & Q_V^M & Q_V^L & Q_{CW} & P_{Sale}, \end{bmatrix}^{T} \qquad (6.4)$$

with D_{Proc} the electric demand referred to the distillery process (kW); Q_V^M the flow of middle pressure steam ($t/_{h}$); Q_V^L the flow of low pressure steam ($t/_{h}$); Q_{CW} the flow of cold water required by the distillery process ($m^3/_{h}$); finally, P_{Sale} represents the electric power made available for the DNO (kW).

6.2.4   Stock Flows

The system state vector is defined as:

$$x = \begin{bmatrix} x_B & x_{Bag} & x_{Str} & x_{Bg} & x_T \end{bmatrix}^{T}, \qquad (6.5)$$

where x_B is the battery SOC; x_{Bag}, x_{Str} and x_{Bg} are the stored amount of bagasse, straw and biogas in their related stocks and x_T is the hot water tank temperature. The stocks state equations were obtained by mass conservation principles as follows.

Battery Bank

The battery bank was modeled by the MLD procedure described

in section 2.2.1. For this purpose it is necessary to define the auxiliary variable $z_{bat} = P_{bat}\delta_{bat}$ that is related to the battery charging/discharging. The state equation for the battery SOC is

$$\frac{dx_B}{dt} = \eta_{bat}^- P_B + \left(\eta_{bat}^- - \eta_{bat}^+\right) z_B \tag{6.6}$$

where, η_{bat}^+ and η_{bat}^- are respectively the charging and discharging efficiencies, δ_{bat} is a binary variable and z_{bat} is a continuous auxiliary variable.

Bagasse Stock

The percentage of bagasse in the stock x_{Bag} is defined as the bagasse income flow Bag_{in} minus the bagasse outcome flow Bag_{out}:

$$\frac{dx_{Bag}}{dt} = Bag_{in} - Bag_{out} = Bag_{in} - \left(\alpha_A Q_E^A + \alpha_B Q_E^B\right) \tag{6.7}$$

Notice that Bag_{out} is a linear combination of Q_E^A and Q_E^B; α_A and α_B are the biomass blending factors, as seen in figure 6.3.

Straw Stock

The amount of straw in the stock x_{Str} is calculated by subtracting the straw output flow Str_{out} from the straw input flow Str_{in}:

$$\frac{dx_{Str}}{dt} = Str_{in} - Str_{out} = Str_{in} - [(1 - \alpha_A)Q_E^A + (1 - \alpha_B)Q_E^B] \tag{6.8}$$

where Bag_{out} is a linear combination of Q_E^A and Q_E^B that represents the biomass mixture that runs into each boiler, in the respective order.

Compressed Biogas Stock

The rate of compressed biogas x_{Bg} can be modeled as the previous states by calculating the balance between the biogas income Bg_{in} and outcome Bg_{out} flow:

$$\frac{dx_{Bg}}{dt} = Bg_{in} - Bg_{out} \qquad (6.9)$$

Notice that Bg_{out} is a consequence of the CHP operating point, here chosen by the manipulated variable SP_{CHP}.

Hot Water Tank

In the same way percentage of hot water x_{Tank} in the tank is calculated by the mass balance between the hot water inflow and outflow:

$$\frac{dx_T}{dt} = T_{in} - T_{out} = (Q_S + Q_{CHP} + Q_{TC}) - (Q_{Esc}^{Tank} + Q_{Ch}) \quad (6.10)$$

where Q_S is the inflow of hot water from the solar panels, Q_{CHP} is the heated water flow from the CHP; Q_{TC} is the heated water flow from the heat exchanger; Q_{Ch} is the hot water outflow to the chiller (consequence of chiller operating point chosen by the manipulated variable SP_{Ch}) and Q_{Esc}^{Tank} is the water tank escape flow.

6.2.5 Final State-Space Representation

The final state-space representation relates the state vector x, seen in equation (6.5), to the decision vector u, seen in equation (6.1), and the disturbance vector z, seen in equation (6.3) using the energy hub methodology, already mentioned. The discrete-time state space equations are represented by the following matrices:

$$
B=
\begin{bmatrix}
0 & 0 & 0 & 0 & 0 & 0 & 0 & 0 & 0 & 0 & \eta_{bat}^- & 0 & 0 & 0 & \eta_{bat}^- & -\eta_{bat}^+ \\
\beta_1 & \beta_3 & 0 & \beta_5 & \beta_7 & 0 & 0 & 0 & 0 & 0 & 0 & 0 & 0 & 0 & 0 \\
\beta_2 & \beta_4 & 0 & \beta_6 & \beta_8 & 0 & 0 & 0 & 0 & 0 & 0 & 0 & 0 & 0 & 0 \\
0 & 0 & 0 & 0 & 0 & 0 & 0 & \beta_9 & 0 & 0 & 0 & 0 & 0 & 0 & 0 \\
0 & 0 & 0 & 0 & 0 & 0 & 0 & \beta_{10} & \beta_{11} & \beta_{12} & 0 & 0 & \beta_{13} & 0 & 0
\end{bmatrix}
$$

$$
C=
\begin{bmatrix}
0 & 0 & 0 & 0 & 0 \\
0 & 0 & \varrho_{2,3} & 0 & 0 \\
0 & 0 & 0 & \varrho_{3,4} & 0 \\
0 & 0 & 0 & 0 & \varrho_{4,5} \\
0 & \varrho_{5,2} & 0 & 0 & 0
\end{bmatrix}
\qquad
F=
\begin{bmatrix}
\psi_{1,1} & \psi_{1,2} & 0 & 0 & 0 \\
0 & 0 & 0 & 0 & 0 \\
0 & 0 & 0 & 0 & 0 \\
0 & 0 & 0 & 0 & 0 \\
0 & 0 & 0 & 0 & 0
\end{bmatrix}
$$

$$
E=
\begin{bmatrix}
\epsilon_1 & \epsilon_3 & \epsilon_5 & 0 & 0 & 0 & 0 & \epsilon_9 & 0 & 0 & \epsilon_{12} & 0 & 0 & 0 & 0 \\
0 & \epsilon_4 & 0 & \epsilon_7 & \epsilon_8 & \epsilon_{15} & 0 & 0 & 0 & 0 & 0 & \epsilon_{13} & 0 & 0 & 0 \\
\epsilon_2 & 0 & 0 & 0 & 0 & 0 & \epsilon_{16} & 0 & 0 & \epsilon_{11} & 0 & \epsilon_{14} & 0 & 0 & 0 \\
0 & 0 & 0 & 0 & 0 & 0 & 0 & 0 & \epsilon_{10} & 0 & 0 & 0 & 0 & 0 & 0 \\
0 & 0 & \epsilon_6 & 0 & 0 & 0 & 0 & 0 & 0 & 0 & 0 & 0 & 0 & 0 & 0
\end{bmatrix}
$$

where A is an identity matrix that relates the next $(k+1)$ system state vector with the previous (k) state vector. Following the Energy Hub methodology, the variation of the stocks (between k and $k+1$) is the inwards (or outwards) flow times the time interval ΔT. D is a null matrix, for the system output vector has no relationship with the system state vector, at any given instant k. B expresses the relationship between the next system state $(x(k+1))$ and the manipulated variables $(u(k))$. C expresses the relationship between the next system state $(x(k+1))$ and the external disturbances $(z(k))$. F shows the relationship between the system outputs (y) and the external disturbances (z). The matrices variables are detailed in table 6.5. K_A and K_B represent, respectively, the static gains of the boilers, that vary according to α_A and α_B.

6.3 Optimization Problems

In this section the control strategy to solve the optimization problems is explained. There are two optimization obstacles to be solved: the biomass mixture optimization and the demand optimization.

Table 6.5: Auxiliary Variables Index

β_1 $-\frac{\alpha A}{32000 \times K_A} \frac{1}{kW}$	β_3 $-\frac{\alpha A}{17000 \times K_A} \frac{1}{kW}$	β_5 $-\frac{\alpha B}{200 \times K_B} \frac{h}{t}$	β_7 $-\frac{\alpha A}{200 \times K_A} \frac{h}{t}$
β_2 $-\frac{(1-\alpha A)}{3200 \times K_A} \frac{1}{kW}$	β_4 $-\frac{(1-\alpha A)}{1700 \times K_A} \frac{1}{kW}$	β_6 $-\frac{(1-\alpha B)}{20 \times K_B} \frac{h}{t}$	β_8 $-\frac{\alpha A}{20 \times K_A} \frac{h}{t}$
β_9 $-0.011 \frac{1}{kW}$	β_{10} $0.15 \times 10^{-2} \frac{1}{kW}$	β_{11} $-0.42 \frac{h}{m^3}$	β_{12} $\frac{1}{3} \frac{h}{m^3}$
β_{13} $-1 \frac{h}{m^3}$	–	–	–
$\varrho_{2,3}$ $\frac{1}{200} \frac{h}{t}$	$\varrho_{3,4}$ $\frac{1}{20} \frac{h}{t}$	$\varrho_{4,5}$ $0.416 \times 10^{-2} \frac{h}{t}$	$\varrho_{5,2}$ $0.466 \times 10^{-2} \frac{m^2}{W}$
ϵ_1 1	ϵ_3 1	ϵ_5 -1	ϵ_9 1
ϵ_{12} -1	ϵ_4 $0.0117 \frac{t}{kWh}$	ϵ_7 1	ϵ_8 1
ϵ_{13} -1	ϵ_2 $0.625 \times 10^{-2} \frac{t}{kWh}$	ϵ_{11} $-0.025 \frac{t}{m^3}$	ϵ_{14} 1
ϵ_{10} 1	ϵ_6 1	ϵ_{15} -1	ϵ_{16} -1
$\psi_{1,1}$ $100 \frac{W.h}{m}$	$\psi_{1,2}$ $0.8 km^2$	–	–

6.3.1   Biomass Mixture Optimization

The mixture optimization consists in maximizing the boiler gains (conversion factor from amount of biomass mixture to amount of produced steam $t/h / t/h$), that fluctuate according to the biomass mixture composition. The more straw there is in the mixture, the greater the gains (up to 50% of straw, due to misture); this is seen in table 6.6. Notice that these blending factors (statistical dummy variables, α_A and α_B) are respectively related to the high efficiency boiler and the lower efficiency boiler. Q_E^A and Q_E^B represent the biomass mixture that runs into each boiler, in the respective order. The amount of bagasse outflow and straw outflow from the stocks (Bag_{out} and Str_{out}) are shown in equations (6.7) and (6.8).

In the mixture optimization the boiler gains (conversion factor from amount of biomass mixture to amount of produced steam) fluctuate according to the biomass mixture composition. The optimization here proposed is solved by the optimizer, Opt_α, that has to maintain the blending factors as close to 0.5 as possible, knowing the future straw income predictions. This is also subject to the following constraints:

1. maintain the straw stock inside the 10 % and 100 % limits, where the minimum of 10 % is a safety margin for one hour operation;

2. try to maintain the straw stock near a reference of 20 %, whenever possible;

3. preserve the blending factors as dummy variables (values from 0 to 1);

4. limit the outflow of straw.

Table 6.6: Biomass mixtures: Boiler gains and calorific power

Mixture	Calorific Power	B. Eff. Boiler Gain	L. Eff. Boiler Gain
$100\%Bagasse$	2042.205 $^{\text{kCal}}/_{\text{kg}}$	2.14 $^{\text{t/h}}/_{\text{t/h}}$	1.284 $^{\text{t/h}}/_{\text{t/h}}$
$90\%Bagasse + 10\%Straw$	2074.367 $^{\text{kCal}}/_{\text{kg}}$	2.1745 $^{\text{t/h}}/_{\text{t/h}}$	1.3041 $^{\text{t/h}}/_{\text{t/h}}$
$80\%Bagasse + 20\%Straw$	2171.022 $^{\text{kCal}}/_{\text{kg}}$	2.275 $^{\text{t/h}}/_{\text{t/h}}$	1.3644 $^{\text{t/h}}/_{\text{t/h}}$
$70\%Bagasse + 30\%Straw$	2253.348 $^{\text{kCal}}/_{\text{kg}}$	2.3607 $^{\text{t/h}}/_{\text{t/h}}$	1.4158 $^{\text{t/h}}/_{\text{t/h}}$
$60\%Bagasse + 40\%Straw$	2338.029 $^{\text{kCal}}/_{\text{kg}}$	2.4487 $^{\text{t/h}}/_{\text{t/h}}$	1.4686 $^{\text{t/h}}/_{\text{t/h}}$
$50\%Bagasse + 50\%Straw$	2408.374 $^{\text{kCal}}/_{\text{kg}}$	2.5219 $^{\text{t/h}}/_{\text{t/h}}$	1.5125 $^{\text{t/h}}/_{\text{t/h}}$
$100\%Straw$	2894.036 $^{\text{kCal}}/_{\text{kg}}$	3.026 $^{\text{t/h}}/_{\text{t/h}}$	1.8156 $^{\text{t/h}}/_{\text{t/h}}$

6.3.2 Demand Optimization

The other optimization problem, solved by the MPC controller, MPC_{main}, is the main purpose of this study: the microgrid has to produce (sell) the contract-defined amount of electric energy, while still meeting all the system demands: internal power demand, steam demands and refrigeration demands.

As explained beforehand, the contract corresponds to the generation of 11.52GWh of electric energy, per month - herein treated as a daily production of 384MWh. The optimization has to define the manipulated vector (6.1) so that the daily production of energy corresponds to the contract and the system state vector (6.5) follows a reference state (for example: all stocks with 50 %). This is subject to the following restrictions:

1. the manipulated variables have to stay within physical limits;

2. the system output vector (6.4) has to contemplate the system demands;

3. the system state vector (6.5) has to stay within bounded limits - every stock has its operational band.

6.3.3 Control Structure

The proposed control structure is comprised of two levels. The first level is associated with optimizing the biomass blending factors. The second (and main) level is associated with complying the process demands and producing the contract-defined amount of electric energy, in the most efficient and sustainable way possible.

Figure 6.4 shows the proposed two-level hierarchical control structure based on *MPC*. Both the optimizer Opt_α and the controller MPC_{main}

are operating together, on the same time scale (sampling time $\Delta T = 1\,h$). The biomass mixture optimizer acts with information of the biomass mixture flows ($Q_E^A(k)$ and $Q_E^B(k)$) and the straw stock percentage ($X_{Str}(k)$) and transmits to the microgrid and the controller the instant values of the blending factors ($\alpha_A(k)$ and $\alpha_B(k)$). The main controller acts with past blending factor values ($\alpha_A(k-1)$ and $\alpha_B(k-1)$), instant disturbance, system state and system output vectors values ($z(k)$, $x(k)$, $y(k)$) and handles the manipulated variables (acting on the microgrid).

Figure 6.4: Proposed Control Structure

Main Controller (MPC_{Main})

The main MPC has the following objective function:

$$J_{Main} = \sum_{i=0}^{N_c-1} \|P_{Net} - (E_{contract} - E_{sum})/\Delta T\|_{Q_P}^2 \qquad (6.11)$$

$$\sum_{i=0}^{N_c-1} q_u \hat{u}(k) + \sum_{l=0}^{N_p-1} \|\hat{x}(k+i) - \hat{x}_{ref}(k+i)\|_{Q_x}^2 + q_\epsilon \epsilon$$

where q_ϵ and q_u are positive defined vectors, Q_P and Q_x are positive definite weighting matrices, E_{sum} represents the electric energy that has already been produced by the microgrid, at given iteration k; $E_{contract}$ represents the daily production of 38MWh; the system state reference is put as $\hat{x}_{ref}$; ϵ represents a slack variable that is to be minimized, used in the constraints, see equation (6.15); N_p represents the prediction horizon, while N_c represents the control horizon. As it can be seen, ($E_{contract} - E_{sum}$) represents how much electric energy the microgrid still has to produce until the end of the day, due to contract requirement. For this, when minimizing $[P_{Net} - \frac{(E_{contract}-E_{sum})}{\Delta T}]$, the

main controller forces the production of energy at iteration k to approach the necessary amount to end the contract requirement, so, by the end of the day, the amount of electric energy supplied to the DNO is the one defined by contract. The objective function (6.11) is subject to the following constraints:

$$
\begin{aligned}
\underline{x} &\leq \hat{x}(k+i+1) \leq \overline{x} && (6.12) \\
\underline{u} &\leq \hat{u}(k+i) \leq \overline{u} && (6.13) \\
\hat{y}(k+i) &= Demands(k) && (6.14) \\
0 &\leq P_{Net}(k) \leq \chi + \epsilon && (6.15)
\end{aligned}
$$

for $i = 0, \ldots, N_p - 1$, where χ represents the contract constant power (16MW, if maintained at every iteration k, the electric contract would certainly be complied). The notation hat over variables ($\hat{a}$) is used to denote variables over the prediction horizon, $\underline{a}$ and $\bar{a}$ denote minimum and maximum allowed values respectively. The matrix Q_P is adjusted so that the electric energy production is prioritized; Q_x is used to maintain the system state vector values near a referenced region of 50 % of all stocks. The vector q_u is used so that the production of energy comes preferably from the most efficient and sustainable energy sources and so that the use of the battery bank is minimized.

Biomass Mixture Optimizer (Opt_α)

The biomass mixture optimizer was implemented with the following objective function:

$$
J_{Opt_\alpha} = \sum_{i=0}^{N_p-1} \|\hat{\alpha}_A(k+i) - 0.5\|^2_{Q_A} + \sum_{i=0}^{N_p-1} \|\hat{\alpha}_B(k+i) - 0.5\|^2_{Q_B} + \qquad (6.16)
$$
$$
\sum_{l=0}^{N_p-1} \left\|\hat{x}_{Str}(k+i+1) - \hat{x}_{Str}^{ref}\right\|^2_{Q_{Str}}
$$

subject to the following constraints:

$$\underline{x}_{Str} \quad \leq \quad \hat{x}_{Str}(k+i+1) \leq \overline{x}_{Str} \qquad (6.17)$$

$$\underline{\alpha} \quad \leq \quad \hat{\alpha}_A(k+i) \leq \overline{\alpha}_A \qquad (6.18)$$

$$\underline{\alpha}_B \quad \leq \quad \hat{\alpha}_B(k+i) \leq \overline{\alpha}_B \qquad (6.19)$$

$$0 \quad \leq \quad [(1-\alpha_A)Q_E^A + (1-\alpha_B)Q_E^B)] \leq \overline{Str}_{out} \qquad (6.20)$$

The first two terms of this objective function (6.16) represent the approach of the blending factors to the optimal factors (0.5 each). The third term of (6.16) is so that the predicted future straw stock follows a reference of 20 %, if possible. The weighting matrices Q_A, Q_B and Q_{Str} are tuned so that the optimizers main goal is to minimize α_A and α_B.

6.3.4   Final Control Algorithm

As seen in figure 6.4, the proposed control structure is composed of Opt_α and MPC_{main}, working together. This is easier to grasp by the understanding of algorithm 4. In this algorithm, it can be seen, after the initialization of variables and the assembling of matrices, how the control structure is iterating hourly to: reassemble matrix B (that changes with α_A and α_B); call the main controller MPC_{main} (based on the previous iteration model: $\alpha_A(k-1)$ and $\alpha_B(k-1)$); compute K_A, K_B, Q_E^A and Q_E^B; call the optimizer Opt_α to divulge the new blending factors (iteration k); reassemble B (for simulation of microgrid) and apply decision vector to the microgrid; receive (measures) output and state vectors.

6.3.5   Simulation Results

The experimental results of the proposed control strategy, applied to a simulated model of the studied microgrid, are presented in this section. The control strategy was implemented using the software *Matlab* [74] with *Yalmip* toolbox[69] and solver *CPLEX* [58]. The experiments described in this section represent the simulation of one day. The microgrid control objectives are to maximize the use of renewable energy sources, ensure the energy production defined by contract and ensure the load demand at all periods of time. Figure 6.5 shows the system disturbances. In this simulation scenario the process data was extracted from a real power plant from state of Paraná [1].All parameter

---

[1]For confidentiality issues the company name is not mentioned.

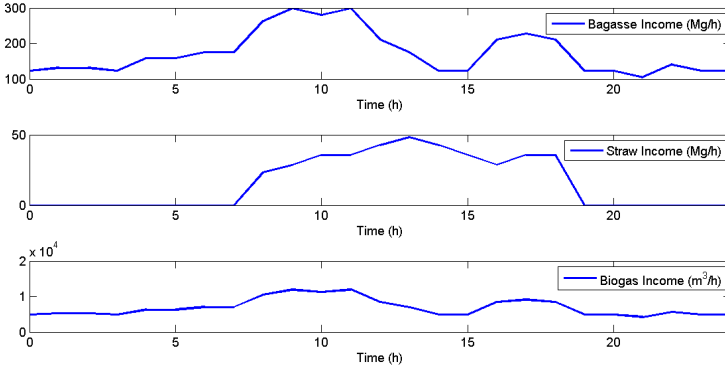**Algorithm 4** Final Microgrid Control Algoritm

---

Input: T_s, z
Output: x, y
    {Inicialize: N_p, N_c, $\alpha_A[0]$, $\alpha_B[0]$, $Pot_{contract}$, X,u}
    {Assemble Matrixes: A, B, C, D, E, F}
    {Assemble Matrixes: q_ϵ,q_u, Q_x, Q_P, Q_A, Q_B, Q_{Str}}
1: **for** $k = 1$ to 24 **do**
2:    Assemble B with $\alpha_A[k-1]$ and $\alpha_A[k-1]$
       $Pot_{sum} = Pot_{sum} + u_3[k-1]$
3:    **Call:** $MPC_{main}[Pot_{sum}; X]$
       {MPC_{main} returns $u[k]$}
       $K_A = \text{lookup}(\alpha_A[k-1])$
       $K_B = \text{lookup}(\alpha_B[k-1])$
4:    Compute: Q_E^A and Q_E^B
5:    **Call:** $Opt_\alpha[Q_E^A; Q_E^B; X_{Str}]$
       {Opt_α returns $\alpha_A[k]$ and $\alpha_B[k]$}
6:    Assemble B with $\alpha_A[k]$ and $\alpha_A[k]$
7:    Apply $u[k]$ to microgrid
8:    Receive $y[k]$,$x[k]$
9: **end for**

---

values are presented in appendix A.

    Figure 6.6 shows a simulation scenario of the proposed microgrid and the use of each subsystem: electric power generated by the *CHP*, by the turbines and by the non-dispatchable renewable sources. The presence of the CHP and the non-dispatchable renewable sources in the proposed system implies reduction on the turbines energy production. As can be seen in figures 6.5 and 6.6 the CHP use depends on the biogas income behavior. The lower efficiency turbine generated around 3MW most part of the day, increasing the production from 18h to 22h when there is an electric demand peak and a reduction in the biogas income. The better efficiency turbine contributed most part of the day with around 15MW with an increasing after 21h when a demand peak and a reduction in the non dispatchable renewable sources occurs. At the end of the day the CHP and the non dispatchable renewable sources contributed with 23.27 % (126.37MW) of the total daily production of 542.97MW (the sum of CHP, both turbines and the non-dispatchaple renewable sources was considered).

    On the other hand, figure 6.7 shows a scenario of the original system. In this scenario only the turbines generated energy to attending
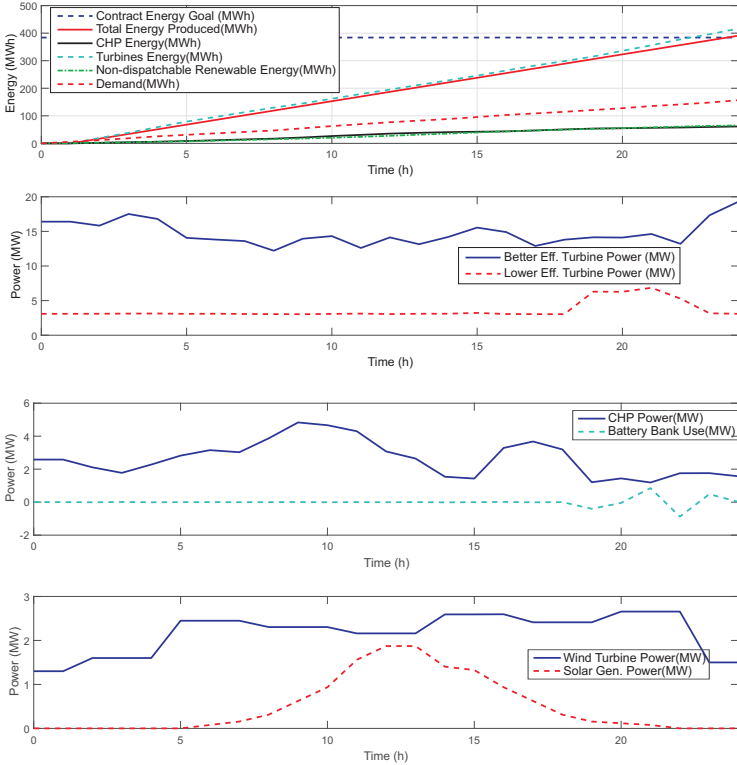
Figure 6.5: System Disturbances

the demand and the energy sale contract. In both scenarios it can be seen that the generation is enough to comply to the energy contract. Figure 6.8 shows that both systems met all system demands.

Figure 6.9 shows the stocks behavior of the proposed system. In this simulation the battery bank acted to mitigate small energy imbalances between the microgrid equipments, staying around 50 %. At the end of the day, from 18h to 22h, when a high energy fluctuation happened as a consequence of the electric demand peak, the battery bank presented a SOC variation of 25 % (between 50 % and 75 %) in order to absorb the energy generated excess. The biogas stock started with 80 % and decreased until around 50 %, that is the state reference, and is directly related with the CHP production. The stock of bagasse is maintained continuously loaded, due to the great amount of income, as seen in figure 6.6. The straw stock, on the other hand, gradually decreases, due to the biomass mixture optimization, and the smaller amount of income.

Figure 6.10 shows the optimizer Opt_α performance when applied to the proposed and system. The optimizer Opt_α is able to maximize the gain of the boilers by reducing α_A and α_B to 0.5, whenever possible. It can be noticed that the optimizer cannot maintain the blending factors at the optimal condition (0.5), because this forces the straw outcome flow to be too voluminous and violate the minimum straw stock constraint, as shown in figure 6.9. So, the blending factors are gradually tending to 1, except the α_B in proposed scenario, that are near 0.5 as the lower efficiency boiler production is very low, due to the low biomass mixture flow Q_E^B.

Figure 6.6: Electric power generation of the proposed system

The behavior of the variables involved in steam production are shown in figure 6.11. As shown in figure 6.8 both steam demands are attended. As the high efficiency boiler presented a high steam production as a consequence of the both turbines energy production, the lower efficiency boiler is not widely used, and production was near the minimum all the time. The middle pressure steam demand is attended by the high-middle pressure reduction valve and the lower efficiency boiler. As this production is greater than the demand, the residual steam is converted to low pressure steam. The low pressure steam demand is attended by the production of the lower efficiency turbine and the converted middle pressure steam. The steam excess is discarded by the middle and low pressure escape valves.

Figure 6.12 shows the variables involved to attend to the refrigeration demands. As can be seen the CHP, the solar water heater and

Figure 6.7: Electric power generation of the original system

Figure 6.8: Fulfillment of the Demands

the heat exchanger are responsible for production. The water chiller is responsible for consuming the hot water and attend the refrigeration demand. The tank escape valve was not used because, as shown in figure 6.9, the hot water tank level does not reach the maximum level.

Table 6.7 evidences the energy gains and approximate economic profit of using the CHP, the photovoltaic panels, and the wind turbine in a daily simulation. It was considered the average biogas production of $3750/_h$, from the anaerobic digestion of the vinasse and the Megawatt average price as R\$386.66. As expected the gain of the non dispatchable sources depends on the weather condition that changes over the year and presents stochastic behaviors as wind gusts and cloudy days. Among the non dispatchable sources the wind turbine contributes with

Figure 6.9: Stocks of the proposed system

Figure 6.10: Blending Factors of the proposed system

more energy and consequently more economic profit.

A series of daily simulation scenarios, considering different prediction errors are detailed in table 6.8. It is important to notice that the total energy generation, in these simulations, has been set within a limited percentage (5 %) to the reference set-point production of 384MWh per day. Analyzing the table data it is possible to see that the prediction error in the renewable energy sources practically did not affected the total energy generation. This occurs because the turbines and the CHP compensated the energy loss.

Figure 6.11: Variables involved in steam production (proposed scenario)

Figure 6.12: Variables involved in hot water production (proposed scenario)

6.4   Final Remarks

In this chapter the study of a hybrid power plant based on a sugar cane industry was discussed. First the original process was described and after a new structure was proposed in order to increase and diversify the use of renewable energy and maximize the reuse of the sugar cane residues. The proposed system became more complex than the original and use the renewable sources and residues to attend a multi carrier demands, being electrical, steam in different pressure levels and cold water for refrigeration. The energy hubs framework was applied to model the system. A two-level hierarchical MPC control structure was proposed to perform the electric energy production optimization, management of storage and subsystems and biomass blending optimization. As showed by the simulation results, the proposed control

Table 6.7: Full-Month Simulation Scenario Details

Subsystem	Power Gains	Economic Gains
CHP	61.39 MWh	R$23,738.00
Photovoltaic Panels		
High Insolation	12.36 MWh	R$4,780.00
Medium Insolation	9.51 MWh	R$3,677.00
Low Insolation	6.34 MWh	R$2,451.00
Wind Turbine		
High Wind Speed	52.62 MWh	R$20,346.00
Medium Wind Speed	29.66 MWh	R$11,470.00
Low Wind Speed	16.61 MWh	R$6,423.00

Table 6.8: Different Daily Simulation Scenarios

Error (%)	Non-dispatchable Renewable Energy	Total Energy Generation
1%	42.573MWh	395.60MWh
2%	42.143MWh	395.50MWh
5%	40.853MWh	395.10MWh
10%	38.703MWh	395.26MWh
15%	36.553MWh	395.33MWh
20%	34.400MWh	394.96MWh
25%	32.252MWh	394.66MWh
35%	30.108MWh	394.86MWh

structure presented satisfactory results. In the chapter 7, conclusions about this thesis and future work are discussed.

Chapter 7

Conclusions and Future Works

This thesis addressed the problem of energy management in microgrids including renewable energy, which is an important research subject and interest of many countries since increasingly seeking of a sustainable world. Different MPC based solutions were presented taking into account the characteristic of the studied systems.

First the integration of a V2G system with an experimental microgrid was discussed. A hierarchical control structure was developed to perform the energy management including the different equipment dynamics and control objectives. The proposed controller got good results under sunny, cloudy and windy weather conditions.

Other theme addressed in this thesis was the problem of controlling networked microgrids. For this issue a hybrid distributed MPC was developed. In the proposed approach the MIQP original local problem was solved by a binary search algorithm that performs a sequence of quadratic programmings and the algorithm distributed nature was considered to coordinate the solution of the binary variables during the iteration procedure. The proposed framework showed a good performance in a simulation scenario with different weather conditions and in presence of faults.

Finally the Brazilian energy production scenario was explored. A sugar cane industry power plant was studied and a new structure was proposed, where non-dispatchable renewable sources and reuse of biomass were included in the plant structure. This power system is composed by different energy carriers which is a challenge to the con-

trol algorithm. The proposed controller had the objective to manage different energy sources, meeting the demands and performing the optimization of bagasse and straw mixture.

7.1   Contributions

The main contributions of this thesis can be highlighted as follows:

- The development of a hybrid distributed MPC framework, where the effect of subsystems interaction in the binary variables decisions is taken into account.

- The study of the integration of a microgrid with electric vehicles charging stations in a V2G philosophy. The proposed charging station management proved very useful to manage the charge of electric vehicles and their batteries usage as a storage to help on the energy fluctuation mitigation.

- A MPC strategy was proposed to deal with the switching between an electrolyzer and a fuel cell in a microgrid taking into account the switching constraints providing an optimized solution to the hydrogen storage management problem.

- The insertion of a MLD formulation on the MPC objective function of the microgrid to manage the energy sell/purchase with the distribution network operator (DNO), which proved to be an interesting solution.

- The use of the hybrid DMPC as energy management system to the problem of networked microgrids based on renewable energy sources appeared as a good solution to perform the economic energy management and guarantee the cooperation between microgrids in different weather and operating conditions.

- The integration of the sugar cane power plant with non-dispatchable renewable sources, the use of biogas (generated from vinasse fermentation) with the CHP to generate energy and heat and the mix between the bagasse and straw to improve the boilers calorific power proved to be a sustainable solution once perform the maximum use of the energy sources to generate electricity, steam and cold water. The use of energy hubs to model the proposed system was very efficient once this methodology allows to integrate different energy carriers in the same model.

- The development of a two-level hierarchical MPC strategy to perform the management of different energy carriers. The proposed controller presented good results ensuring the electric energy production, managing the use of renewable energies and performing the biomass blending optimization.

As a result of the study of energy management of renewable energy based microgrids presented in the thesis the following publications were produced:

- Mendes P. R. C., Normey-Rico J. E., Bordons C.. Economic Energy Management of a Microgrid Including Electric Vehicles. Innovative Smart Grid Technologies Latin America, 2015, Montevideo - Uruguay.

- Mendes P. R. C., Normey-Rico J. E., Valverde L., Bordons C.. Gestión Energética de una Micro Red acoplada a un sistema V2G. XXXVI Jornadas de Automática, 2015, Bilbao - Spain.

- Mendes P. R. C., Maestre J. M., Normey-Rico J. E., Bordons C.. Binary Search Algorithm for Mixed Integer Optimization: Application to energy management in a microgrid. European Control Conference, 2016, Alborg - Denmark.

- Mendes P. R. C., Valverde L., Bordons C., Normey-Rico J. E.. Energy Management of an Experimental Microgrid coupled to a V2G system. Journal of Power Sources.

- Mendes P. R. C., Bordons C., Normey-Rico J. E.. Distributed MPC for Energy Management of V2G Networked Microgrids. IEEE Transactions on Sustainable Energy. (under review)

- Mendes P. R. C., Maestre J. M., Bordons C., Normey-Rico J. E.. Hybrid Distributed MPC. Journal of Process Control. (under review)

- Morato M. M., Mendes P. R. C., Bertol D. W., Cembranel D., Bordons C., Normey-Rico J. E.. Estudo de uma Planta Híbrida de Geração de Energia na Indústria da Cana-de-açúcar. Congresso Brasileiro de Automática, 2016, Vitória - Brazil.

- Morato M. M., Mendes P. R. C., Bertol D. W., Cembranel D., Bordons C., Normey-Rico J. E.. Efficient Hybrid Generation Power Plants in the Sugar Cane Industry. Renewable Energy. (under review)

- Morato M. M., Mendes P. R. C., Normey-Rico J. E. , Bordons C.. Optimal Operation of Hybrid Power Systems Including Renewable Sources in the Sugar Cane Industry. IET Renewable Power Generation.

During the period of Ph.D. studies about subspace predictive control were carried out and the following works were published:

- Mendes P. R. C., Normey-Rico J. E., João V. Jr.. A Bilinear FSP-SPC in a Solar Desalination Plant Collector Field. International Renewable Energy Congress (IREC), 2014, Hammamet - Tunisia;

- Mendes P. R. C., Normey-Rico J. E., João V. Jr., Cruz D. M.. A Filtered Smith predictor based subspace predictive controller. 19*th* World Congress of the International Federation of Automatic Control, Cape Town, South Africa.

7.2   Future Work

The energy management of microgrids is an interesting and open research area involving different fields of knowledge. With respect to the solutions presented in this thesis remarkable future research topics are:

- The investigation of methods to accelerate the convergence of the proposed hybrid DMPC is an important issue thinking in the application in a greater networked microgrids scenario.

- The comparison of the proposed hybrid DMPC with other distributed MPC algorithms.

- The investigation of the effect of weather prediction errors in the Hybrid DMPC and integration with robust and stochastic strategies to deal with this matter.

- The investigation of the energy management of charging stations with renewable energy sources and their impact in the charge electricity price taken into account the Brazilian market.

- The study of integrate many sugar cane power plants of the same company to cooperate each other and attend a multi objective contract. In many cases one company is the owner of many sugar cane processing plants and it is expected that with this integration

it is possible to attend a given contract by the overall company instead of isolated contracts for each power plant. This way the amount of energy sold to DNO as well as the economic gains tend to increase.

Appendix A

Simulation Parameters

A.1 Laboratory Microgrid Control

MPC1 - Model

$\eta_B = 1.08 \times 10^{-5}$
$\eta_{H_2,e}^{FC} = 8.55 \times 10^{-6}$
$\eta_{e,H_2}^{E} = 2.97 \times 10^{-6}$
$\eta_{Bev1} = 2.3 \times 10^{-3}$
$\eta_{Bev2} = 2.3 \times 10^{-3}$
$\eta_{Bev3} = 2.3 \times 10^{-3}$
$\eta_{Bev4} = 2.3 \times 10^{-3}$

MPC1 - Tuning Parameters

$N_{p1} = 5 \; N_{c1} = 2 \; Q_{u1} = diag\left(\begin{bmatrix} 0 & 3 & 1 & 2 & 0 \\ 0 & 0 & 0 & 0 & 2 \end{bmatrix}\right)$

$Q_{x1} = diag\left(\begin{bmatrix} 5 \times 10^8 & 1 & 0 & 0 & 0 & 0 \end{bmatrix}\right)$

$Q_{\Delta u1} = diag(\begin{bmatrix} 0 & 0 & 0 & 1 & 0 \\ 0 & 0 & 0 & 100 & 1 \end{bmatrix}$

$Q_{Target1} = diag\left(\begin{bmatrix} 0 & 100 & 60 & 1000 & 100 \\ 10000 & 100 & 10000 & 0 & 0 \end{bmatrix}\right)$

$Q_{\Delta \delta 1} = 100$

MPC1 - Constraints

$\underline{x}_1 = diag\left(\begin{bmatrix} 20 & 20 & 0 & 0 & 0 & 0 \end{bmatrix}\right)$
$\overline{x}_1 = diag\left(\begin{bmatrix} 95 & 95 & 100 & 100 & 100 & 100 \end{bmatrix}\right)$

$$\underline{u}_1 = diag\left(\begin{bmatrix} 0 & -1600 & -900 & -900 & -100 \\ -100 & -100 & -100 & 0 & 0 \end{bmatrix}\right)$$

$$\overline{u}_1 = diag\left(\begin{bmatrix} 4650 & 6000 & 900 & 900 & 100 \\ 100 & 100 & 100 & 1 & 900 \end{bmatrix}\right)$$

MPC2 - Model

$\eta_B = 1.1 \times 10^{-3}$

$\eta_{H_2,e}^{FC} = 0.85 \times 10^{-3}$

$\eta_{e,H_2}^{E} = 0.3 \times 10^{-3}$

$\eta_{Bev1} = 2.31 \times 10^{-1}$

$\eta_{Bev2} = 2.31 \times 10^{-1}$

$\eta_{Bev3} = 2.31 \times 10^{-1}$

$\eta_{Bev4} = 2.31 \times 10^{-1}$

MPC2 - Tuning Parameters

$$N_{p2} = 12 \ N_{c2} = 5 \ Q_{u2} = diag\left(\begin{bmatrix} 1\times10^9 & 0 & 0 & 0 & 0 & 0 \\ 0 & 0 & 0 & 0 & 0 & 0 \end{bmatrix}\right)$$

$$Q_{x2} = diag\left(\begin{bmatrix} 10 & 1 & 0 & 0 & 0 & 0 \end{bmatrix}\right)$$

$$Q_{\Delta u2} = diag\left(\begin{bmatrix} 0 & 0 & 0 & 0 & 10 & 10 \\ 10 & 10 & 0 & 0 & 0 & 0 \end{bmatrix}\right)$$

$$Q_{Target2} = diag\left(\begin{bmatrix} 1\times10^9 & 0 & 0 & 0 & 0 & 0 \\ 0 & 0 & 0 & 0 & 0 & 0 \end{bmatrix}\right)$$

$$Q_{\Delta\delta2} = 100$$

MPC2 - Constraints

$$\underline{x}_2 = diag\left(\begin{bmatrix} 20 & 20 & 0 & 0 & 0 & 0 \end{bmatrix}\right)$$

$$\overline{x}_2 = diag\left(\begin{bmatrix} 95 & 95 & 100 & 100 & 100 & 100 \end{bmatrix}\right)$$

$$\underline{u}_2 = diag\left(\begin{bmatrix} 0 & -1600 & -900 & -900 & -100 & -100 \\ -100 & -100 & 0 & 0 & 0 & 0 \end{bmatrix}\right)$$

$$\overline{u}_2 = diag\left(\begin{bmatrix} 4650 & 6000 & 900 & 900 & 100 & 100 \\ 100 & 100 & 1 & 1 & 6000 & 900 \end{bmatrix}\right)$$

A.2 Networked Microgrids

Tuning Parameters

$$N_p = 6 \; N_c = 2 \; Q_{1,2,3,4} = diag\left(\begin{bmatrix} q_{sale} & 1 & 0 & 0 & 0 \\ 0 & 0 & 0 & 0 & 0 \\ 0 & 0 & 0 & 0 & 0 \\ 0 & 0 & 0 & 0 & 0 \\ 0 & 0 & 0 & 0 & 0 \\ 0 & 0 & q_{purchase} - q_{sale} & 1 & 0 \\ 0 & 0 & 0 & 0 & 0 \\ 0 & 0 & 0 & 0 & 0 \\ 0 & 0 & & & \end{bmatrix}\right)$$

$$Q_{x_{1,2,3,4}} = diag\left(\begin{bmatrix} 0.1 & 0 & 0 & 0 & 0 \\ 0 & 0 & 0 & 0 & 0 \end{bmatrix}\right)$$

Constraints

$$\underline{x}_{1,2,3,4} = diag\left(\begin{bmatrix} 20 & 0 & 0 & 0 & 0 \\ 0 & 0 & 0 & 0 & 0 \end{bmatrix}\right)$$

$$\overline{x}_{1,2,3,4} = diag\left(\begin{bmatrix} 95 & 100 & 100 & 100 & 100 \\ 100 & 100 & 100 & 100 & 100 \end{bmatrix}\right)$$

$$\underline{u}_{1,2,3,4} = diag\left(\begin{bmatrix} -50 & -1 & -0.06 & -0.06 & -0.06 \\ -0.06 & -0.06 & -0.06 & -0.06 & -0.06 \\ -0.06 & -0.06 & 0 & 0 & 0 \\ 0 & 0 & 0 & 0 & 0 \\ 0 & 0 & 0 & 0 & 0 \\ 0 & 0 & 0 & 1 & 0 \\ 0 & 0 & 0 & 0 & 0 \\ 0 & 0 & 0 & 0 & 0 \\ 0 & 0 & & & \end{bmatrix}\right)$$

$$\overline{u}_{1,2,3,4} = diag\left(\begin{bmatrix} 50 & 1 & 0.06 & 0.06 & 0.06 \\ 0.06 & 0.06 & 0.06 & 0.06 & 0.06 \\ 0.06 & 0.06 & 10 & 10 & 10 \\ 1 & 1 & 1 & 1 & 1 \\ 1 & 1 & 1 & 1 & 1 \\ 1 & 1 & 50 & 1 & 0.06 \\ 0.06 & 0.06 & 0.06 & 0.06 & 0.06 \\ 0.06 & 0.06 & 0.06 & 0.06 & 10 \\ 10 & 10 & & & \end{bmatrix}\right)$$

A.3   Sugar Cane Industry Case

Tuning Parameters

$$N_p = 12 \; N_c = 5 \; q_u = \begin{bmatrix} 0.3 & 0.6 & 0 & 10 & 0.4 & 5 & 5 \\ 0.01 & 0 & 10 & & & & \\ 0.5 & 0.35 & 2{\times}10^6 & & & & \end{bmatrix}$$

$$Q_x = diag\left(\begin{bmatrix} 0.3 & 0 & 0 & 0 & 0 \end{bmatrix}\right)$$

$$q_\epsilon = 1 \times 10^3$$

$$Q_P = 0.5$$

Constraints

$$\underline{x} = diag\left(\begin{bmatrix} 10 & 10 & 10 & 10 & 10 \end{bmatrix}\right)$$

$$\overline{x} = diag\left(\begin{bmatrix} 100 & 100 & 100 & 100 & 100 \end{bmatrix}\right)$$

$$\underline{u} = diag\left(\begin{bmatrix} 11{\times}10^3 & 3{\times}10^3 & 0 & 0 & 0 \\ 0 & 0 & 800 & 0 & 0 \\ -3{\times}10^3 & 0 & 0 & & \end{bmatrix}\right)$$

$$\overline{u} = diag\left(\begin{bmatrix} 27{\times}10^3 & 2{\times}10^4 & 0 & 1{\times}10^7 & 0 \\ 0 & 0 & 8{\times}10^3 & 0 & 0 \\ 3{\times}10^3 & 0 & 0 & & \end{bmatrix}\right)$$

Bibliography

[1] I. Alvarado, D. Limon, D. Muñoz de la Peña, J.M. Maestre, M.A. Ridao, H. Scheu, W. Marquardt, R.R. Negenborn, B. De Schutter, F. Valencia, and J. Espinosa. A comparative analysis of distributed mpc techniques applied to the hd-mpc four-tank benchmark. *Journal of Process Control*, 21(5):800 – 815, 2011. doi: 10.1016/j.jprocont.2011.03.003. Special Issue on Hierarchical and Distributed Model Predictive Control.

[2] J. M. Alves. Paradigma técnico e co-geração de energia com bagaço de cana de açúcar em goiás / technical paradigm and energy cogeneration from sugarcane bagasse in goiás. *Proceedings of the 6. Encontro de Energia no Meio Rural*, 2006.

[3] D. Anderson and M. Leach. Harvesting and redistributing renewable energy: on the role of gas and electricity grids to overcome intermittency through the generation and storage of hydrogen. *Energy Policy*, 32(14):1603 – 1614, 2004. doi: 10.1016/S0301-4215(03)00131-9.

[4] M. Arnold, R. R. Negenborn, G. Andersson, and B. De Schutter. Model-based predictive control applied to multi-carrier energy systems. In *Power Energy Society General Meeting, 2009. PES '09. IEEE*, pages 1–8, 2009. doi: 10.1109/PES.2009.5275230.

[5] S. Bashash and H. Fathy. Robust demand-side plug-in electric vehicle load control for renewable energy management. *American Control Conference (ACC)*, pages 929–934, 2011. doi: 10.1016/S0005-1098(98)00178-2.

[6] J. Batut and A. Renaud. Daily generation scheduling optimization with transmission constraints: a new class of algorithms. *IEEE Transactions on Power Systems*, 7:982 – 989, 1992.

[7] A. Bemporad and M. Morari. Control of systems integrating logic, dynamics, and constraints. *Automatica*, 35(3):407–427, 1999. doi: 10.1016/S0005-1098(98)00178-2.

[8] D. P. Bertsekas. *Constrained Optimization and Lagrange Multiplier Methods*. Athena Scientific, 1996.

[9] D. P. Bertsekas and J. N. Tsitsiklis. *Distributed Computation: Numerical Methods*. Athena Scientific, New Hampshire, 1997.

[10] A. Bidram and A. Davoudi. Hierarchical structure of microgrids control system. *IEEE Transactions on Smart Grid*, 3(4):1963–1976, 2012. doi: 10.1109/TSG.2012.2197425.

[11] A. M. Borbely and J. F. Kreid. *Distributed Generation: The Power Paradigm for the New Millennium*. CRC Press, Boca Raton, 2001.

[12] C. Bordons, F. Garcia-Torres, and L. Valverde. Optimal energy management for renewable energy microgrids. *Revista Iberoamericana de Automatica e Informatica industrial*, 12(2):117–132, 2015. doi: 10.1016/j.riai.2015.03.001.

[13] R. Bourdais and H. Guéguen. Distributed predictive control for complex hybrid system. the refrigeration system example. *Large Scale Complex Systems Theory and Applications*, 9:388–394, 2010. doi: 10.3182/20100712-3-FR-2020.00065.

[14] Allal M. Bouzid, Josep M. Guerrero, Ahmed Cheriti, Mohamed Bouhamida, Pierre Sicard, and Mustapha Benghanem. A survey on control of electric power distributed generation systems for microgrid applications. *Renewable and Sustainable Energy Reviews*, 44:751 – 766, 2015. doi: 10.1016/j.rser.2015.01.016.

[15] M. C. Bozchalui, S. A. Hashmi, H. Hassen, C. A. Cañizares, and K. Bhattacharya. Optimal operation of residential energy hubs in smart grids. *Smart Grid, IEEE Transactions on*, 3(4):1755–1766, 2012.

[16] K. De Brabandere, K. Vanthournout, J. Driesen, G. Deconinck, and R. Belmans. Control of microgrids. In *Power Engineering Society General Meeting, 2007. IEEE*, pages 1–7, 2007. doi: 10.1109/PES.2007.386042.

[17] E. Camacho and C. Bordons. *Model Predictive Control*. Springer, London, 2007.

[18] E. Camponogara, D. Jia, B. H. Krogh, and S. Talukdar. Distributed model predictive control. *IEEE Control Systems*, 22(1): 44–52, 2002. doi: 10.1109/37.980246.

[19] S. Chakraborty, M. D. Weiss, and M. G. Simoes. Distributed intelligent energy management system for a single-phase high-frequency ac microgrid. *IEEE Transactions on Industrial Electronics*, 54(1):97–109, 2007. doi: 10.1109/TIE.2006.888766.

[20] P. D. Christofides, R. Scattolini, D. M. de la Peña, and J. Liu. Distributed model predictive control: A tutorial review and future research directions. *Computers & Chemical Engineering*, 51:21 – 41, 2013. doi: http://dx.doi.org/10.1016/j.compchemeng.2012.05.011.

[21] S. Cristea, C. de Prada, D. Sarabia, and G. Gutiérrez. Aeration control of a wastewater treatment plant using hybrid nmpc. *Computers & Chemical Engineering*, 35(4):638 – 650, 2011. doi: http://dx.doi.org/10.1016/j.compchemeng.2010.07.021.

[22] D. N. Dantas. *Uso da biomassa de cana-de-açúcar para geração de energia elétrica: análise energética, exergética e ambiental de sistemas de cogeração em sucroalcooleiras do interior paulista / Use of biomass sugarcane to generate electricity: energy analysis, exergetic and environmental cogeneration systems in sugarcane in São Paulo State*. PhD thesis, Universidade de São Paulo, 2010.

[23] Ministério de Minas e Energia. Redes elétricas inteligentes: contexto nacional / smart grids: national context. Technical report, Ministério de Minas e Energia, 2012.

[24] Ministério de Minas e Energia. Plano decenal de expansão de energia 2024. Technical report, Ministério de Minas e Energia, 2014.

[25] Ministério de Minas e Energia. Redes elétricas inteligentes diálogo setorial brasil-união europeia (2014)´/ smart grids dialogue sector brazil-european union (2014). Technical report, Ministério de Minas e Energia, 2014.

[26] Ministério de Minas e Energia. Resenha energética brasileira: Exercício de 2014 / brazilian energy review: Year 2014. Technical report, Ministério de Minas e Energia, 2015.

[27] C. de Prada, I. Grossmann, D. Sarabia, and S. Cristea. A strategy for predictive control of a mixed continuous batch process. *Journal of Process Control*, 19(1):123 – 137, 2009. doi: http://dx.doi.org/10.1016/j.jprocont.2008.01.004.

[28] S. Deilami, A. S. Masoum, P. S. Moses, and M. Masoum. Real-time coordination of plug-in electric vehicle charging in smart grids to minimize power losses and improve voltage profile. *IEEE Trans. on Smart Grid*, 2(3):456–467, 2011. doi: 10.1109/TSG.2011.2159816.

[29] A. J. del Real. *An Integrated Framework for Distributed Model Predictive Control of Large Scale Networks - Applications to Power Networks*. PhD thesis, Universidad de Sevilla, 2011.

[30] A. J. del Real, A. Arce, and C. Bordons. Hybrid model predictive control of a two-generator power plant integrating photovoltaic panels and fuel cell. *IEEE Conference on Decision and Control*, pages 5447–5452, 2007. doi: 10.1109/CDC.2007.4434550.

[31] A. J. del Real, M. D. Galus, C. Bordons, and G. Andersson. Optimal power dispatch of energy networks including external power exchange. *European Control Conference (ECC)*, pages 3616–3621, 2009.

[32] A. J. del Real, A. Arce, and C. Bordons. An integrated framework for distributed model predictive control of large-scale power networks. *IEEE Transactions on Industrial Informatics*, 10(1): 197–209, 2014. doi: 10.1109/TII.2013.2273877.

[33] R. Dell and D. Rand. Energy storage: a key technology for global energy sustainability. *Journal of Power Sources*, 100(1):2–17, 2001. doi: 10.1016/S0378-7753(01)00894-1.

[34] W.B. Dunbar and R.M. Murray. Model predictive control of coordinated multi-vehicle formations. *Proceedings of the 41st IEEE Conference on Decision and Control*, pages 4631 – 4636, 2002.

[35] F. Ekardt and H. Von Bredow. Extended emissions trading versus sustainability criteria: Managing the ecological and social

ambivalences of bioenergy. *Renewable Energy L. & Pol'y Rev.*, page 49, 2012.

[36] Z. Fan. A distributed demand response algorithm and its application to phev charging in smart grids. *IEEE Transactions on Smart Grid*, 3(3):1280–1290, 2012. doi: 10.1109/TSG.2012.2185075.

[37] M. Fathi and H. Bevrani. Adaptive energy consumption scheduling for connected microgrids under demand uncertainty. *IEEE Transactions on Power Delivery*, 28(3):1576–1583, 2013. doi: 10.1109/TPWRD.2013.2257877.

[38] G. Ferrari-Trecate, E. Gallestey, P. Letizia, M. Spedicato, M. Morari, and M. Antonine. Modeling and control of co-generation power plants: a hybrid system approach. *IEEE Transactions on Control Systems Technology*, 12(5):694–705, 2004. doi: 10.1109/TCST.2004.826958.

[39] M. V. A. Costa Filho. *Modelagem, controle e otimização de processos da indústria do etanol / Modeling, control and optimization of processes in the ethanol industry*. PhD thesis, Universidade Federal de Santa Catarina, 2013.

[40] J. R. D. Frejo. *Model Predictive Control for Freeway Traffic Networks*. PhD thesis, University of Seville, 2015.

[41] Q. Fu, A. Hamidi, A. Nasiri, V. Bhavaraju, S. B. Krstic, and P. Theisen. The role of energy storage in a microgrid concept: Examining the opportunities and promise of microgrids. *IEEE Electrification Magazine*, 1(2):21–29, 2013. doi: 10.1109/MELE.2013.2294736.

[42] M. D. Galus and G. Andersson. Power system considerations of plug-in hybrid electric vehicles based on a multi energy carrier model. In *Power Energy Society General Meeting, 2009. PES '09. IEEE*, pages 1–8, July 2009. doi: 10.1109/PES.2009.5275574.

[43] M. D. Galus and G. A. Simon Art. A hierarchical, distributed pev charging control in low voltage distribution grids to ensure network security. *Power and Energy Society General Meeting, 2012 IEEE*, pages 1–8, 2012. doi: 10.1109/PESGM.2012.6345024.

[44] M. D. Galus, R. La Fauci, and G. Andersson. Investigating phev wind balancing capabilities using heuristics and model predictive

control. *Power and Energy Society General Meeting, 2010 IEEE*, pages 1–8, 2010. doi: 10.1109/PES.2010.5589267.

[45] F. Garcia-Torres and C. Bordons. Optimal economical schedule of hydrogen-based microgrids with hybrid storage using model predictive control. *Industrial Electronics, IEEE Transactions on*, 62(8):5195–5207, Aug 2015. ISSN 0278-0046. doi: 10.1109/TIE.2015.2412524.

[46] F. Garcia-Torres, L. Valverde, and C. Bordons. Optimal load sharing of hydrogen-based microgrids with hybrid storage using model predictive control. *IEEE Transactions on Industrial Electronics*, PP(99):1–1, 2016. doi: 10.1109/TIE.2016.2547870.

[47] M. Gautschi, O. Scheuss, and C. Schluchter. Simulation of an agent based vehicle-to-grid (v2g) implementation. *Electric Power Systems Research*, 120:177 – 183, 2009. doi: http://dx.doi.org/10.1016/j.epsr.2014.05.016.

[48] M. Geidl. *Integrated Modeling and Optimization of Multi-Carrier Energy Systems*. PhD thesis, ETH, Zurich, 2007.

[49] M. Geidl, G. Koeppel, P. Favre-Perrod, B. Klockl, G. Andersson, and K. Frohlich. Energy hubs for the future. *EEE Power and Energy Magazine*, 2007.

[50] D. Georges. Decentralized adaptive control for a water distribution system. *3rd IEEE Conference on Control Applications*, pages 1411 – 1416, 1999.

[51] D. Giaouris, A. I. Papadopoulos, C. Ziogou, D. Ipsakis, S. Voutetakis, S. Papadopoulou, P. Seferlis, F. Stergiopoulos, and C. Elmasides. Performance investigation of a hybrid renewable power generation and storage system using systemic power management models. *Energy*, 61:621 – 635, 2013. doi: http://dx.doi.org/10.1016/j.energy.2013.09.016.

[52] A. Di Giorgio, F. Liberati, and S. Canale. Electric vehicle charging control in smartgrids: A model predictive control approach. *Control Engineering Practice*, 22:147–162, 2014. doi: http://dx.doi.org/10.1016/j.conengprac.2013.10.005.

[53] J. R. P. Gonzalez. *Libro Blanco de la Automatización y Control en la Industria de la Caña de Azúcar*, volume 1. Programa Iberoamericano de Ciencia y Tecnologia para el Desarrollo (CYTED), 2011.

[54] W. Greenwell and A. Vahidi. Predictive control of voltage and current in a fuel cell-ultracapacitor hybrid. *IEEE Transactions on Industrial Electronics*, 57(6):1954–1963, 2010. doi: 10.1109/TIE.2009.2031663.

[55] W. Gu, Z. Wu, and X. Yuan. Microgrid economic optimal operation of the combined heat and power system with renewable energy. *IEEE Power and Energy Society General Meeting*, pages 1–6, 2010. doi: 10.1109/PES.2010.5590140.

[56] M. Heidarinejad, J. Liu, and P. D. Christofides. Distributed model predictive control of switched nonlinear systems with scheduled mode transitions. *AIChE Journal*, 59(3):860–871, 2013. doi: 10.1002/aic.14003.

[57] M. Hestenes. Multiplier and gradient methods. *Journal of Optimization Theory and Applications*, 4:303 – 320, 1969.

[58] IBM ILOG. Cplex. 2007.

[59] D. Ipsakis, S. Voutetakis, P. Seferlis, F. Stergiopoulos, S. Papadopoulou, and C. Elmasides. The effect of the hysteresis band on power management strategies in a stand-alone power system. *Energy*, 33(10):1537 – 1550, 2008. doi: http://dx.doi.org/10.1016/j.energy.2008.07.012.

[60] D. Jia and B.H. Krogh. Distributed model predictive control. *American Control Conference*, pages 2767 – 2772, 2001.

[61] D. Jia and B.H. Krogh. Min-max feedback model predictive control for distributed control with communication. *American Control Conference*, pages 4507 – 4512, 2002.

[62] H. Jiayi, J. Chuanwen, and X. Rongi. A review on distributed energy resources and microgrid. *Renewable and Sustainable Energy Reviews*, 12(9):2472 – 2483, 2008. doi: http://dx.doi.org/10.1016/j.rser.2007.06.004.

[63] T. B. Johansson. *Renewable energy: sources for fuels and electricity.* Island press, 1993.

[64] R. A. Romão Junior. Análise da viabilidade do aproveitamento da palha da cana de açúcar para cogeração de energia numa usina sucroalcooleira / feasibility analysis of the use of straw of sugar cane for energy cogeneration in sugar and alcohol plant. Master's thesis, Universidade Estadual Paulista, 2009.

[65] T. Keviczky, F. Borrelli, and G. J. Balas. A study on decentralized receding horizon control for decoupled systems. *American Control Conference*, 6:4921 – 4926, 2004.

[66] B. Kim and R. Baldick. Coarse-grained distributed optimal power flow. *IEEE Transactions on Power Systems*, 12:932 – 939, 1997.

[67] T. Knudsen, K. Trangbk, and C. Kallese. Plug and play process control applied to a district heating system. *IFAC World Congress*, 2008.

[68] R. H. Lasseter. Microgrids. *IEEE Power Engineering Society Winter Meeting*, 1:305–308, 2002. doi: 10.1109/PESW.2002.985003.

[69] J. Lofberg. Yalmip: A toolbox for modeling and optimization in matlab. *IEEE International Symposium on Computer Aided Control Systems Design*, pages 284–289, 2004. doi: 10.1109/CACSD.2004.1393890.

[70] J.A. Peças Lopes, N. Hatziargyriou, J. Mutale, P. Djapic, and N. Jenkins. Integrating distributed generation into electric power systems: A review of drivers, challenges and opportunities. *Electric Power Systems Research*, 77(9):1189 – 1203, 2007. doi: http://dx.doi.org/10.1016/j.epsr.2006.08.016.

[71] J. M. Maestre and R. R. Negenborn. *Distributed Model Predictive Control Made Easy*. Springer-Verlag, London, 2014.

[72] J. M. Maestre, M. A. Ridao, A. Kozma, C. Savorgnan, M. Diehl, M. D. Doan, A. Sadowska, T. Keviczky, B. De Schutter, H. Scheu, W. Marquardt, F. Valencia, and J. Espinosa. A comparison of distributed mpc schemes on a hydro-power plant benchmark. *Optimal Control Applications and Methods*, 36(3):306–332, 2015. ISSN 1099-1514. doi: 10.1002/oca.2154.

[73] G. S. C. Magalhães. *Comercialização de energia elétrica no ambiente de contratação livre: Uma análise regulatório-institucional a partir dos contratos de compra e venda de energia elétrica / Electricity trading in the free market: a regulatory and institutional analysis from the purchase and sale of electricity*. PhD thesis, Universidade de São Paulo, 2009.

[74] Mathworks. Matlab. 2009.

[75] P.R.C. Mendes, J. E. Normey-Rico, and C. Bordons. Economic energy management of a microgrid including electric vehicles. *Innovative Smart Grid Technologies Latin America ISGT-LA*, pages 869–874, 2015. doi: 10.1109/ISGT-LA.2015.7381269.

[76] H. Morais, P. Kádár, P. Faria, Z. A. Vale, and H.M. Khodr. Optimal scheduling of a renewable micro-grid in an isolated load area using mixed-integer linear programming. *Renewable Energy*, 35(1):151 – 156, 2010. doi: http://dx.doi.org/10.1016/j.renene.2009.02.031.

[77] N. Nikmehr and S. N. Ravadanegh. Reliability evaluation of multi-microgrids considering optimal operation of small scale energy zones under load-generation uncertainties. *International Journal of Electrical Power & Energy Systems*, 78:80–87, 2016. doi: doi:10.1016/j.ijepes.2015.11.094.

[78] R. R. Negenborn. *Multi-Agent Model Predictive Control with Applications to Power Networks*. PhD thesis, Delft University of Technology, 2007.

[79] R. R. Negenborn and J. M. Maestre. Distributed model predictive control: An overview and roadmap of future research opportunities. *IEEE Control Systems*, 34(4):87–97, 2014. doi: 10.1109/MCS.2014.2320397.

[80] R. R. Negenborn, B. De Schutter, and J. Hellendoorn. Multi-agent model predictive control: A survey. *Technical Report, Delft Center for Systems and Control*, 2004.

[81] R. R. Negenborn, B. De Schutter, and J. Hellendoorn. Multi-agent model predictive control of transportation networks. *IEEE International Conference on Networking, Sensing and Control*, 2006.

[82] R. R. Negenborn, M. Houwing, B. De Schutter, and J. Hellendoorn. Model predictive control for residential energy resources using a mixed-logical dynamic model. *International Conference on Networking, Sensing and Control*, pages 702–707, 2009. doi: 10.1109/ICNSC.2009.4919363.

[83] N. Nikmehr and S. N. Ravadanegh. Optimal power dispatch of multi-microgrids at future smart distribution grids. *IEEE Transactions on Smart Grid*, 6(4):1648–1657, 2015. doi: 10.1109/TSG.2015.2396992.

[84] J. E. Normey-Rico and E. F. Camacho. *Control of Dead-Time Processes*. Springer, Berlin, 2007.

[85] H.S.V.S.K. Nunna and S. Doolla. Demand response in smart distribution system with multiple microgrids. *IEEE Transactions on Smart Grid*, 3(4):1641–1649, 2012. doi: 10.1109/TSG.2012.2208658.

[86] D. E. Olivares, A. Mehrizi-Sani, A. H. Etemadi, C. A. Canizares, R. Iravani, M. Kazerani, A. H. Hajimiragha, O. Gomis-Bellmunt, A. Saeedifard, R. Palma-Behnke, G. A. Jimenez-Estevez, and N. D. Hatziargyriou. Trends in microgrid control. *IEEE Transactions on Smart Grid*, 5(4):1905–1919, 2014. doi: 10.1109/TSG.2013.2295514.

[87] A. Ouammi, H. Dagdougui, L. Dessaint, and R. Sacile. Coordinated model predictive-based power flows control in a cooperative network of smart microgrids. *IEEE Transactions on Smart Grid*, 6(5):2233–2244, 2015. doi: 10.1109/TSG.2015.2396294.

[88] A. Ouammi, H. Dagdougui, and R. Sacile. Optimal control of power flows and energy local storages in a network of microgrids modeled as a system of systems. *IEEE Transactions on Control Systems Technology*, 23(1):128–138, 2015. doi: 10.1109/TCST.2014.2314474.

[89] O. Palizban and K. Kauhaniemi. Hierarchical control structure in microgrids with distributed generation: Island and grid-connected mode. *Renewable and Sustainable Energy Reviews*, 44:797 – 813, 2015. doi: http://dx.doi.org/10.1016/j.rser.2015.01.008.

[90] O. Palizban, K. Kauhaniemi, and J. M. Guerrero. Microgrids in active network management part i: Hierarchical control, energy storage, virtual power plants, and market participation. *Renewable and Sustainable Energy Reviews*, 36:428 – 439, 2014. doi: http://dx.doi.org/10.1016/j.rser.2014.01.016.

[91] A. Parisio and L. Glielmo. A mixed integer linear formulation for microgrid economic scheduling. In *Smart Grid Communications (SmartGridComm), 2011 IEEE International Conference on*, pages 505–510. IEEE, 2011.

[92] A. Parisio, E. Rikos, and L. Glielmo. A model predictive control approach to microgrid operation optimization. *Control Systems Technology, IEEE Transactions on*, 22(5):1813–1827, 2014. doi: 10.1109/TCST.2013.2295737.

[93] M. Petrollese. *Optimal Generation Scheduling for Renewable Microgrids Using Hydrogen Storage Systems*. PhD thesis, University of Cagliari, 2015.

[94] M. Powell. *Ch. A method for nonlinear constraints inminimization problems*. Academic Press, New York, 1969.

[95] C. Prada, M. Rodriguez, and D. Sarabia. On-line scheduling and control of a mixed continuous batch plant. *Industrial & Engineering Chemistry Research*, 50(9):5041–5049, 2011. doi: 10.1021/ie1014298.

[96] E. E. Rego and F. M. Hernandez. Eletricidade por digestão anaeróbica da vinhaça de cana-de-açúcar: contornos técnicos, econômicos e ambientais de uma opção / electricity through anaerobic digestion of vinasse from sugarcane: technical, economic and environmental contours of an option. *Proceedings of the 6. Encontro de Energia no Meio Rural*, 2006.

[97] P. Richardson, D. Flynn, and A. Keane. Optimal charging of electric vehicles in low-voltage distribution systems. *IEEE Transactions on Power Systems*, 27(1):268–279, 2012. doi: 10.1109/TP-WRS.2011.2158247.

[98] C. Royo. *Generalized Unit Commitment by the Radar Multiplier Method*. PhD thesis, Technical University of Catalonia, 2001.

[99] D. Sarabia, F. Capraro, L. F.S. Larsen, and C. Prada. Hybrid nmpc of supermarket display cases. *Control Engineering Practice*, 17(4):428 – 441, 2009. doi: http://dx.doi.org/10.1016/j.conengprac.2008.09.003.

[100] R. Scattolini. Architectures for distributed and hierarchical model predictive control - a review. *Journal of Process Control*, 19:723 – 731, 2009.

[101] M. Schulze and P. C. Del Granado. Multi-period optimization of cogeneration systems: Considering biomass energy for district heating. In *2nd Power Systems Modeling Conference*, 2009.

[102] B. De Schutter and B. De Moor. Optimal traffic light control for a single intersection. *European Journal of Control*, 4(3):260 – 276, 1998. doi: http://dx.doi.org/10.1016/S0947-3580(98)70119-0.

[103] A. Serna, J. E. Normey-Rico, and F. Tadeo. Model predictive control of hydrogen production by renewable energy. In *Renewable Energy Congress (IREC), 2015 6th International*, pages 1–6, 2015. doi: 10.1109/IREC.2015.7110959.

[104] S. Shafiee and E. Topal. When will fossil fuel reserves be diminished. *Energy policy*, 37(1):181–189, 2009.

[105] W. Shi, X. Xie, C. C. Chu, and R. Gadh. Distributed optimal energy management in microgrids. *IEEE Transactions on Smart Grid*, 6(3):1137–1146, 2015. doi: 10.1109/TSG.2014.2373150.

[106] J. B. M. Sánchez. Optimización de metodologías para la caracterización de biocombustibles sólidos procedentes de la industria del olivar / optimization methods for the characterization of solid biofuels from the olive industry, 2015.

[107] C. Sonntag, A. Devanathan, S. Engell, and O. Stursberg. Hybrid nonlinear model-predictive control of a supermarket refrigeration system. In *Control Applications, 2007. CCA 2007. IEEE International Conference on*, pages 1432–1437, 2007. doi: 10.1109/CCA.2007.4389437.

[108] C. Tiba. *Atlas Solarimerico do Brasil*. Ed. Universitária da UFPE, Recife, Brazil, 2000.

[109] G. Tolentino, H. O. Florentino, and M. M. P. Sartori. Modelagem matemática para o aproveitamento da biomassa residual de colheita da cana-de-açúcar com menor custo / mathematical modeling for the use of residual biomass harvesting of sugarcane at lower cost. *Bragantia*, pages 729–735, 2007.

[110] E. Unamuno and J. A. Barrena. Hybrid ac/dc microgridspart ii: Review and classification of control strategies. *Renewable and Sustainable Energy Reviews*, 52:1123 – 1134, 2015. doi: http://dx.doi.org/10.1016/j.rser.2015.07.186.

[111] T. S. Ustun, C. Ozansoy, and A. Zayegh. Recent developments in microgrids and example cases around the worlda review. *Renewable and Sustainable Energy Reviews*, 15(8):4030 – 4041, 2011. doi: http://dx.doi.org/10.1016/j.rser.2011.07.033.

[112] L. Valverde, C. Bordons, and F. Rosa. Power management using model predictive control in a hydrogen-based microgrid. *Annual Conference on IEEE Industrial Electronics Society*, pages 5669–5676, 2012. doi: 10.1109/IECON.2012.6389059.

[113] L. Valverde, F. Rosa, and C. Bordons. Design, planning and management of a hydrogen-based microgrid. *IEEE Transactions on Industrial Informatics*, 9(3):1398–1404, 2013. doi: 10.1109/TII.2013.2246576.

[114] L. Valverde, F. Rosa, A. Del Real, A. Arce, and C. Bordons. Modeling, simulation and experimental set-up of a renewable hydrogen-based domestic microgrid. *Journal of Hydrogen Energy*, 38(27):11672–11684, 2013. doi: http://dx.doi.org/10.1016/j.ijhydene.2013.06.113.

[115] L. Valverde, C. Bordons, and F. Rosa. Integration of fuel cell technologies in renewable-energy-based microgrids optimizing operational costs and durability. *IEEE Transactions on Industrial Electronics*, 63(1):167–177, 2016. doi: 10.1109/TIE.2015.2465355.

[116] H. van Ekeren, R. R. Negenborn, P. J. van Overloop, and B. De Schutter. Hybrid model predictive control using time-instant optimization for the rhine-meuse delta. In *Networking, Sensing and Control (ICNSC), 2011 IEEE International Conference on*, pages 215–220, 2011.

[117] J. C. Vasquez, J. M. Guerrero, J. Miret, M. Castilla, and L. Garcia de Vicuna. Hierarchical control of intelligent microgrids. *IEEE Industrial Electronics Magazine*, 4(4):23–29, 2010. doi: 10.1109/MIE.2010.938720.

[118] A. Venkat, J. Rawlings, and S. Wright. *ch. Distributed Model Predictive Control of Large-Scale Systems Assessment and Future Directions*. Springer-Verlag, Berlin, 2007.

[119] L. F. Viana. *Potencial energético do bagaço e palhiço de cana-de-açúcar, cv. SP80-1842, em área de alambique artesanal / Energy potential of bagasse and straw of sugarcane cv. SP80-1842 in handmade alembic area*. PhD thesis, Universidade Federal de Lavras, 2014.

[120] L. Wang. *Model Predictive Control System Design and Implementation Using MATLAB*. Springer, London, 2009.

[121] Z. Wang, B. Chen, J. Wang, M.M. Begovic, and C. Chen. Coordinated energy management of networked microgrids in distribution systems. *IEEE Transactions on Smart Grid*, 6(1):45–53, 2015. doi: 10.1109/TSG.2014.2329846.

[122] Z. Wang, B. Chen, J. Wang, and C. Chen. Networked microgrids for self-healing power systems. *IEEE Transactions on Smart Grid*, 7(1):310–319, 2016. doi: 10.1109/TSG.2015.2427513.

[123] C. Wei, Z.M. Fadlullah, N. Kato, and A. Takeuchi. Gtcfs: A game theoretic coalition formulation strategy for reducing power loss in micro grids. *IEEE Transactions on Parallel and Distributed Systems*, 25(9):2307–2317, 2014. doi: 10.1109/TPDS.2013.178.

[124] X. Xu and X. Zha. Overview of the researches on distributed generation and microgrid. In *International Power Engineering Conference (IPEC 2007)*, pages 966–971, 2007.

[125] M. Yazdanian and A. Mehrizi-Sani. Distributed control techniques in microgrids. *IEEE Transactions on Smart Grid*, 5(6): 2901–2909, 2014. doi: 10.1109/TSG.2014.2337838.

[126] C. Ziogou, D. Ipsakis, C. Elmasides, F. Stergiopoulos, S. Papadopoulou, P. Seferlis, and S. Voutetakis. Automation infrastructure and operation control strategy in a stand-alone power system based on renewable energy sources. *Journal of Power Sources*, 196(22):9488 – 9499, 2011. doi: http://dx.doi.org/10.1016/j.jpowsour.2011.07.029.